



OAK RIDGE NATIONAL LABORATORY

operated by
UNION CARBIDE CORPORATION

for the
U.S. ATOMIC ENERGY COMMISSION

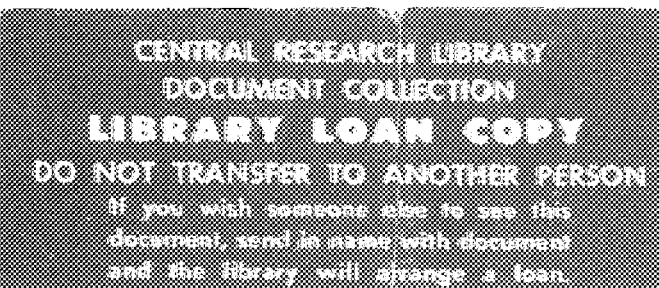


3 4456 0023135 4

CENTRAL RESEARCH LIBRARY
DOCUMENT COLLECTION

A SURVEY OF EMPIRICAL FUNCTIONS USED TO FIT GAMMA-RAY BUILDUP FACTORS

D. K. Trubey



RADIATION SHIELDING INFORMATION CENTER



----- **LEGAL NOTICE** -----

This report was prepared as an account of Government sponsored work. Neither the United States, nor the Commission, nor any person acting on behalf of the Commission:

- A. Makes any warranty or representation, expressed or implied, with respect to the accuracy, completeness, or usefulness of the information contained in this report, or that the use of any information, apparatus, method, or process disclosed in this report may not infringe privately owned rights; or
 - B. Assumes any liabilities with respect to the use of, or for damages resulting from the use of any information, apparatus, method, or process disclosed in this report.
- As used in the above, "person acting on behalf of the Commission" includes any employee or contractor of the Commission, or employee of such contractor, to the extent that such employee or contractor of the Commission, or employee of such contractor prepares, disseminates, or provides access to, any information pursuant to his employment or contract with the Commission, or his employment with such contractor.

Copies of this document are available from

RADIATION SHIELDING INFORMATION CENTER
OAK RIDGE NATIONAL LABORATORY
P.O. Box X
Oak Ridge, Tennessee

ORNL-RSIC-10

Contract No. W-7405-eng-26

Neutron Physics Division

A SURVEY OF EMPIRICAL FUNCTIONS USED TO
FIT GAMMA-RAY BUILDUP FACTORS

D. K. Trubey

FEBRUARY 1966

OAK RIDGE NATIONAL LABORATORY
Oak Ridge, Tennessee
operated by
UNION CARBIDE CORPORATION
for the
U.S. ATOMIC ENERGY COMMISSION



3 4456 0023135 4

TABLE OF CONTENTS

	PAGE
Index to Tables	v
Index to Figures	vii
Abstract	1
PART I - Review of Empirical Buildup Factor Functions	1
Introduction	1
Linear Form	2
Taylor Form	3
Polynomial Form	3
Berger Form	4
Parameters for Linear and Quadratic Forms	5
Other Forms	5
Graphical Comparison	8
Statistical Comparison of Taylor and Berger Forms and Conclusions	9
PART II - Application of Buildup Factors for Distributed Sources in Plane Geometry	84
Plane Isotropic Source Kernel Using Berger Formula	84
Integration of Plane Kernel with Exponential Source Distribu- tion	85
Uncollided Dose Rate	87
Scattered Dose Rate	91
Graphed Functions for Distributed Plane Sources	93
PART III - Application of Buildup Factors in Finite or Laminated Media	103
Acknowledgement	103
References	104

INDEX TO TABLES

	PAGE
1. Buscaglione-Manzini Coefficients for Taylor Dose Buildup Factor Formula	46-49
2. Buscaglione-Manzini Coefficients for Taylor Energy Buildup Factor Formula	50-52
3. Buscaglione-Manzini Coefficients for Taylor Energy Absorption Buildup Factor Formula	53
4. Buscaglione-Manzini Polynomial Coefficients for the Dose Buildup Factor in Various Concretes	54
5. Linear, Quadratic and Berger Coefficients for Dose Buildup Formulas Fitted over the Range (0-7 MFP)	55-64
6. Linear, Quadratic and Berger Coefficients for Energy Absorp- tion Buildup Formulas Fitted over the Range (0-7 MFP) . . .	65-68
7. Linear, Quadratic and Berger Coefficients for Dose Buildup Formulas Fitted over the Range (0-20 MFP)	69-78
8. Linear, Quadratic and Berger Coefficients for Energy Absorp- tion Buildup Formulas Fitted over the Range (0-20 MFP) . . .	79-82
9. Comparison of Average Percentage Deviation Using Berger and Taylor Dose Formulas	83

INDEX TO FIGURES

	PAGE
1. Berger Factor C as a Function of Energy for Various Materials	6
2. Berger Factor D as a Function of Energy for Various Materials	7
3. Comparison of Linear, Quadratic, and Berger Dose Buildup Factors in Water (0.25 MeV, 20 MFP)	10
4. Comparison of Linear, Quadratic, and Berger Dose Buildup Factors in Water (0.25 MeV, 7 MFP)	11
5. Comparison of Polynomial and Berger Dose Buildup Factors in Water (0.25 MeV, 20 MFP)	12
6. Comparison of Polynomial and Berger Dose Buildup Factors in Water (0.25 MeV, 7 MFP)	13
7. Comparison of Linear, Quadratic, and Berger Dose Buildup Factors in Water (0.5 MeV, 20 MFP)	14
8. Comparison of Taylor and Berger Dose Buildup Factors in Water (0.5 MeV, 20 MFP)	15
9. Comparison of Polynomial and Berger Dose Buildup Factors in Water (0.5 MeV, 20 MFP)	16
10. Comparison of Linear, Quadratic, and Berger Dose Buildup Factors in Water (2 MeV, 20 MFP)	17
11. Comparison of Taylor and Berger Dose Buildup Factors in Water (2 MeV, 20 MFP)	18
12. Comparison of Polynomial and Berger Dose Buildup Factors in Water (2 MeV, 20 MFP)	19
13. Comparison of Linear, Quadratic, and Berger Energy Absorption Buildup Factors in Water (6 MeV, 20 MFP)	20
14. Comparison of Taylor and Berger Energy Absorption Buildup Factors in Water (6 MeV, 20 MFP)	21
15. Comparison of Polynomial and Berger Energy Absorption Buildup Factors in Water (6 MeV, 20 MFP)	22
16. Comparison of Linear, Quadratic, and Berger Dose Buildup Factors in Aluminum (6 MeV, 20 MFP)	23
17. Comparison of Taylor and Berger Dose Buildup Factors in Aluminum (6 MeV, 20 MFP)	24

	PAGE
18. Comparison of Polynomial and Berger Dose Buildup Factors in Aluminum (6 MeV, 20 MFP)	25
19. Comparison of Linear, Quadratic, and Berger Dose Buildup Factors in Lead (0.5 MeV, 20 MFP)	26
20. Comparison of Linear, Quadratic, and Berger Dose Buildup Factors in Lead (3 MeV, 20 MFP)	27
21. Comparison of Taylor and Berger Dose Buildup Factors in Lead (3 MeV, 20 MFP)	28
22. Comparison of Polynomial and Berger Dose Buildup Factors in Lead (3 MeV, 20 MFP)	29
23. Comparison of Linear, Quadratic, and Berger Dose Buildup Factors in Lead (6 MeV, 20 MFP)	30
24. Comparison of Taylor and Berger Dose Buildup Factors in Lead (6 MeV, 20 MFP)	31
25. Comparison of Polynomial and Berger Dose Buildup Factors in Lead (6 MeV, 20 MFP)	32
26. Comparison of Linear, Quadratic and Berger Dose Buildup Factors in Lead (10 MeV, 20 MFP)	33
27. Comparison of Taylor and Berger Dose Buildup Factors in Lead (10 MeV, 20 MFP)	34
28. Comparison of Polynomial and Berger Dose Buildup Factors in Lead (10 MeV, 20 MFP)	35
29. Comparison of Linear, Quadratic and Berger Dose Buildup Factors in Lead (6 MeV, 7 MFP)	36
30. Comparison of Linear, Quadratic and Berger Dose Buildup Factors in Lead (10 MeV, 7 MFP)	37
31. Comparison of Linear, Quadratic and Berger Dose Buildup Factors in Ordinary Concrete (1 MeV, 20 MFP)	38
32. Comparison of Taylor and Berger Dose Buildup Factors in Ordinary Concrete (1 MeV, 20 MFP)	39
33. Comparison of Polynomial and Berger Dose Buildup Factors in Ordinary Concrete (1 MeV, 20 MFP)	40
34. Comparison of Linear, Quadratic, and Berger Dose Buildup Factors in Ordinary Concrete (6 MeV, 20 MFP)	41

35. Comparison of Taylor and Berger Dose Buildup Factors in Ordinary Concrete (6 MeV, 20 MFP)	42
36. Comparison of Polynomial Dose Buildup Factors in Ordinary Concrete (6 MeV, 20 MFP)	43
37. Comparison of Linear, Quadratic and Berger Dose Buildup Factor in Lead (6 MeV, 7 MFP)	44
38. Comparison of Linear, Quadratic and Berger Energy Absorption Buildup Factors in Lead (0.5 MeV, 7 MFP)	45
39. Geometry of Integration Over Exponential Source Distribution	86
40. The Slab Function $\Psi_0(x,\alpha)$ for Values of α Between 0 and 3	97
41. The Slab Function $\Psi_1(x,\alpha)$ for Values of α Between 0 and 3	98
42. The Infinite Medium Function $\Psi_0(x,\alpha)$ for Values of α Between 0 and 3	99
43. The Infinite Medium Function $\Psi_1(x,\alpha)$ for Values of α Between 0 and 3	100
44. The Infinite Medium Function $\Psi_2(x,\alpha)$ for Values of α Between 0 and 3	101
45. The Infinite Medium Function $\Psi_3(x,\alpha)$ for Values of α Between 0 and 3	102

A SURVEY OF EMPIRICAL FUNCTIONS USED TO
FIT GAMMA-RAY BUILDUP FACTORS

D. K. Trubey

ABSTRACT

The use of simple functions to estimate gamma-ray buildup factors is reviewed on the basis of simplicity and accuracy. Analysis shows that the best fitting form is the 4 term polynomial fit with coefficients published by Capo. For most purposes, however, a function proposed by Berger is recommended since it is as simple to use as the linear form and is essentially as good as the more complicated forms.

Tables of the coefficients are given for the linear, quadratic, Berger, and Taylor fitting functions. Some typical graphs of the functions are also given.

Use of the Berger and polynomial functions is demonstrated for the case of exponential source distributions in plane geometry and the use of buildup factors in finite geometry is briefly described.

PART I - Review of Empirical Buildup Factor Functions

Introduction

Ever since gamma-ray attenuation results in simple geometry have been available, they have been used in the form of buildup factors. The buildup factors have been, and continue to be, very useful since calculations making use of them are relatively simple and yield relatively quick and, in many cases, accurate results. A simple definition of the buildup factor is the ratio of any desired quantity characteristic of the total gamma ray flux to the same quantity characteristic of the unscattered flux. The two most useful buildup factors are the dose and energy absorption buildup factors. Applying the above definition, the dose buildup factor is the ratio of the total dose (or dose rate) at a given point in a given medium to the dose (or dose rate) at that point due to the unscattered flux which is generally relatively easy to calculate. The energy absorption buildup factor is similarly defined.

Most of the buildup factors in current use are those published by Goldstein and Wilkins¹ in 1954. They give results in infinite media for seven materials and up to nine source energies which cover the range of interest for reactor and weapons shielding. Results for other materials and energies may be obtained by interpolation since the buildup factors are smooth functions of energy and atomic number. They considered plane collimated and point isotropic sources but only the latter are considered in this report.

Linear Form

Probably the earliest used formula for a buildup factor was the linear form. That is, the buildup factor is given by

$$B(E, \mu R) = 1 + A_1(E) \mu R , \quad (1)$$

where

E = source energy,
 μ = linear attenuation coefficient,
 R = distance to source.

Before rigorous results were available, the value of A_1 was assumed to be 1 although Goldstein² pointed out that, in the case of the energy absorption buildup factor, A_1 may be determined by the application of the conservation of energy. That is, the energy of the source is set equal to absorption integrated over all space. Thus

$$E = \int_0^\infty E \mu_a \frac{e^{-\mu R}}{4\pi R^2} B(\mu R) 4\pi R^2 dR , \quad (2)$$

where

$B(\mu R) = 1 + A_1 \mu R ,$
 μ_a = linear energy absorption coefficient,

which yields

$$A_1 = (\mu - \mu_a)/\mu_a . \quad (3)$$

The linear form has the advantage of being simple but (as shown below) is not very good over a significant range.

Taylor Form

The next form to be generally used was probably that of Taylor.³ This form is usually written

$$B(E, \mu R) = A e^{-\alpha_1(E) \mu R} + (1 - A) e^{-\alpha_2(E) \mu R} . \quad (4)$$

The parameters for many materials have been available for a long time (mainly from ref. 3). Additional energy absorption parameters for aluminum, tungsten, and lead and dose parameters for uranium have been published by Strobel.⁴ Recently Buscaglione and Manzini⁵ published a rather complete set of coefficients including values for ordinary, barytes, ferrophosphorous and magnetite concrete. Parameters are given for all point source results reported in ref. 1. The parameters for the dose buildup in concrete are based on data published by Walker and Grotenhuis.⁶ Since the data are so complete, the dose, energy, and energy absorption parameters are reprinted in this report (Tables 1-3). These results are not the same as those published previously^{7,8} but are believed to be better because a more realistic effective atomic number was assumed.

Polynomial Form

The use of a 4-term polynomial, capable of good accuracy, became generally feasible when Capo⁹ published a rather complete set of coefficients for many materials in 1958. That is,

$$B(E, \mu R) = \sum_{n=0}^{\infty} \beta_n(E) (\mu R)^n . \quad (5)$$

Coefficients (β) for several sets of energies are given as well as coefficients for a bivariant fit so one may generate a set of β values for any energy. In fact, for the comparisons described below, this had to be done to obtain coefficients at the same energies used for the other parameter tabulations. Unlike all other formulations considered here, Capo's coefficients result in an expression which does not reduce to exactly one for $\mu R = 0$. The values of β_0 are extremely close to one, however. A set of energy absorption parameters, where $\beta_0 = 1$, for all materials of even atomic number up to $Z = 78$ was published by Vondy.¹⁰ A set of dose parameters for concrete based on data from ref. 6 has recently been published by Buscaglione and Manzini.¹¹ This set is reproduced in Table 4.

Berger Form

A two-parameter formula proposed by Berger¹² and reintroduced by Chilton¹³ has the simplicity of the linear form but fits the buildup factor data well over a long range. This formula is

$$B(E, \mu R) = 1 + C(E) \mu R e^{D(E) \mu R} . \quad (6)$$

In ref. 13, Chilton gave the parameters for aluminum and shows that this formula reproduces the buildup for this material very well. In an effort to investigate the formula for other materials and make it generally useful, the author determined parameters by a least squares procedure for all the dose and energy absorption results given in ref. 1. In addition, dose values were determined for four types of concretes based on data in ref. 6. Two sets of data were obtained. One set is based on data for $\mu R \leq 7$ and the other set is based on data for $\mu R \leq 20$. These values are given in Tables 5-8 for the dose and energy absorption buildup factors. The maximum error encountered over the fitted range is given in the tables in percentage or as a factor indicated by the letter F. Shortly after this was done, it was discovered that extensive data were being

published by Rudloff¹⁴ and by Chilton.¹⁵ The Rudloff values are based on data for $\mu R \leq 15$ and the Chilton values are based on data for $\mu R \leq 10$ and so the parameters determined by the various authors are not the same. Chilton's values are reproduced in Figs. 1 and 2 as functions of energy for various materials. In Fig. 2 it can be seen that for several materials and certain energies the value of D is zero which means that the Berger formula reduces to the linear form.

Parameters for Linear and Quadratic Forms

In addition to deriving the parameters for the Berger formula, the parameters for the linear formula,

$$B(E, \mu R) = 1 + A_1(E) \mu R , \quad (7)$$

and the quadratic formula,

$$B(E, \mu R) = 1 + A_2(E) \mu R + b(E) (\mu R)^2 , \quad (8)$$

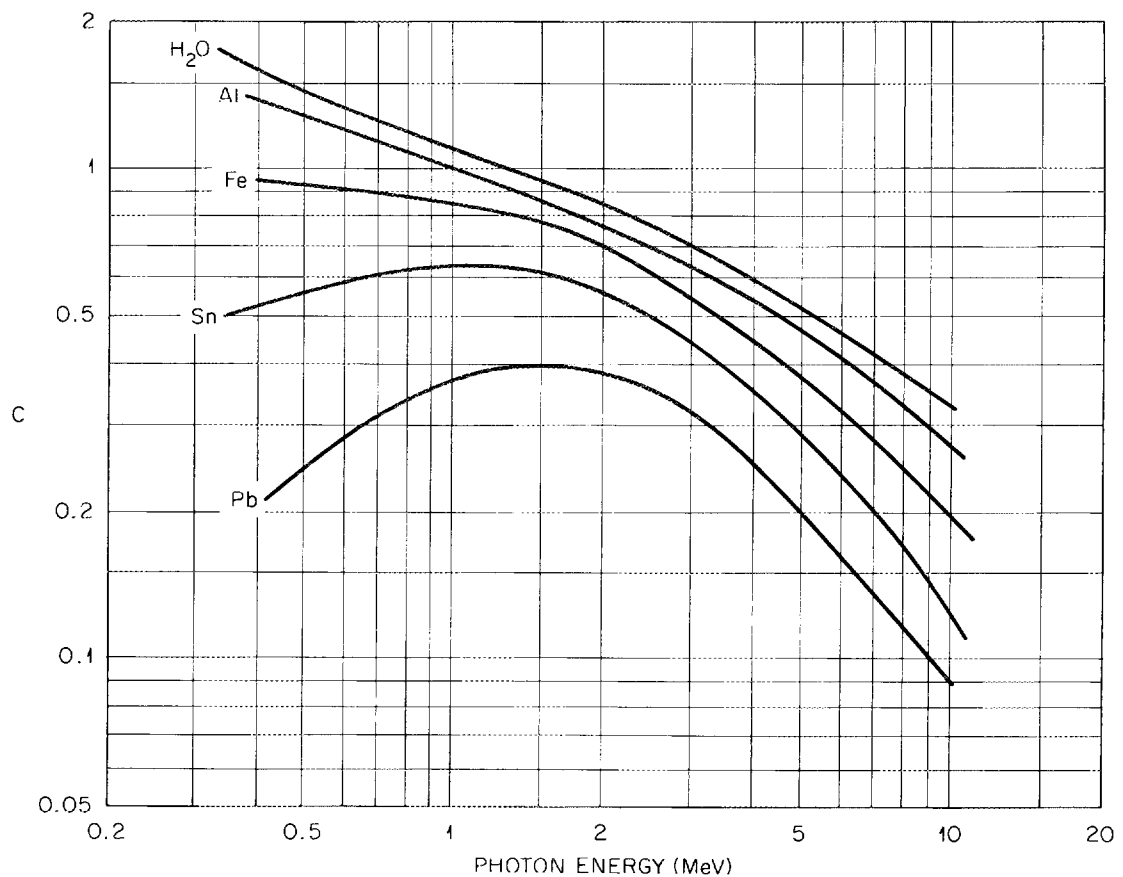
were determined by the author. The fitting procedure used for the latter two formulas minimized the residuals rather than the logarithm of the residuals which resulted in a better fit for large values of the argument rather than for small values. With heavy elements, there is sometimes a large error in the fitting function at small distances such that the value of B, as determined from Eq. 8, goes to zero or is negative. This causes the absurd result of a maximum error ratio of infinity! The parameters for Eq. 7 and Eq. 8 are also given in Tables 5-8.

Other Forms

There are many other possible buildup factor forms such as those cited by Hubbell¹⁶ but they are generally more complicated than the forms cited here. Hubbell's power series form, for example, converges adequately at short distances only and thus usually requires many terms but has the advantage of a separation of the variables dependent on medium properties, geometry, and thickness.

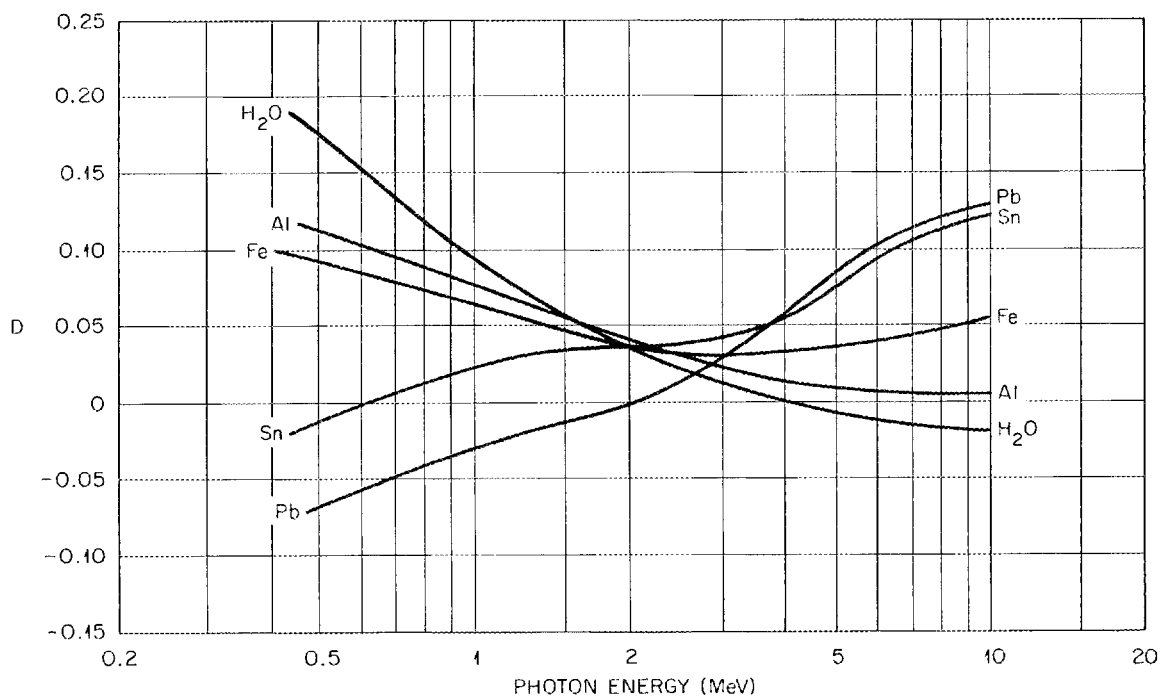
ORNL-DWG 65-11895

Fig. 1.
BERGER FACTOR C AS A FUNCTION OF ENERGY FOR VARIOUS MATERIALS. (FROM REF 15)



ORNL-DWG 65-11896

Fig. 2.
BERGER FACTOR D AS A FUNCTION OF ENERGY FOR VARIOUS MATERIALS. (FROM REF 15)



Graphical Comparison

Typical graphs of the various forms are given in Figs. 3 - 38. Examples of some of the worst fits have been selected to illustrate the problem areas. Some of the better fits are also shown to illustrate how good many of the empirical functions are. Most of the parameters used for the linear, quadratic, and Berger formulas were taken from Table 7. Most of the Taylor parameters were taken from Table 1. However, most of the polynomial parameters were generated from the bivariate coefficients of Capo⁹ since values for β at the generally used energies are not given in ref. 9. Most of the illustrations are for dose buildup factors but the other types behave similarly. The Berger form is given in every graph as a standard of comparison.

One of the most difficult cases to fit is shown in Fig. 3. This is the case of the dose buildup at 0.25 MeV in water. It is obvious that the linear fit is very poor over such a long range and the quadratic fit is also very poor for distances less than 8 mean free paths (mfp). The Berger fit, however is reasonably good with a maximum error of about 30%. Taylor parameters are not available below 0.5 MeV. In Fig. 4 the parameters are based on data for distances less than 7 mfp which results in considerable improvement, especially in the quadratic fit. In Figs. 5 and 6 the very good polynomial fit is demonstrated. In Fig. 7 it is shown that for 0.5 MeV the linear and quadratic fits are better, particularly the quadratic. In Fig. 8 the Berger and Taylor fits are seen to be nearly identical and in Fig. 9 the polynomial form is again seen to be extremely good. Figures 10 - 18 demonstrate that all the fits are quite good for light materials at the higher energies.

In Figs. 19 - 28 it can be seen that the linear and quadratic forms work quite well at low energies in heavy materials but present difficulties at the high energies. Figures 29 - 30 show that the situation improves when the required range is decreased to 7 mfp, with the quadratic becoming quite good.

Figures 31 - 36 show typical results for ordinary concrete. Results for the heavy concretes are similar. The polynomial coefficients were taken from Table 4. Figures 37 - 38 are included to show the danger of using the parameters beyond the fitted range of 7 mfp.

Statistical Comparison of Taylor and Berger Forms and Conclusions

It appeared from graphical comparisons that the 2-parameter Berger form was of comparable accuracy to the 3-parameter Taylor form. In order to examine the two forms further, the average deviation was computed for various materials. The average deviation was taken to be

$$\text{Average Deviation} = \frac{1}{N_E N_R} \sum_{i=1}^{N_E} \sum_{j=1}^{N_R} \frac{|B(E_i, R_j) - B_F(E_i, R_j)|}{B(E_i, R_j)} , \quad (9)$$

where

N_E = number of energies = 8,

N_R = number of distances = 7 (usually),

$B(E_i, R_j)$ = tabulated buildup factor (ref. 1 or 6),

$B_F(E_i, R_j)$ = value given by a formula.

This test was performed by Chilton¹⁵ for certain cases with the result that the Berger formula was found superior. Our results (Table 9) indicate the accuracy is about the same. This leads us to recommend the Berger formula except where the very best fit is desired in which case the polynomial form is recommended. Actually, as Chilton¹⁵ points out, all of the better forms yield results within the uncertainty of the basic data which is given as 5-10%.¹ The Berger formula has several advantages over the Taylor form which are:

1. In the Berger form the two terms are physically meaningful. The first term represents the uncollided flux and the second term represents the scattered flux.
2. The parameters are more slowly varying with energy, especially in the case of water at low energies. As can be seen in Table 1, the Taylor parameter A changes by a factor of 5 between 1 and 0.5 MeV while the Berger parameter C changes by only about 40%.

The Taylor form is easily fitted into the framework of the uncollided flux equations, but this is not a great advantage since the Berger form is easy to integrate, which is illustrated below.

Fig. 3.

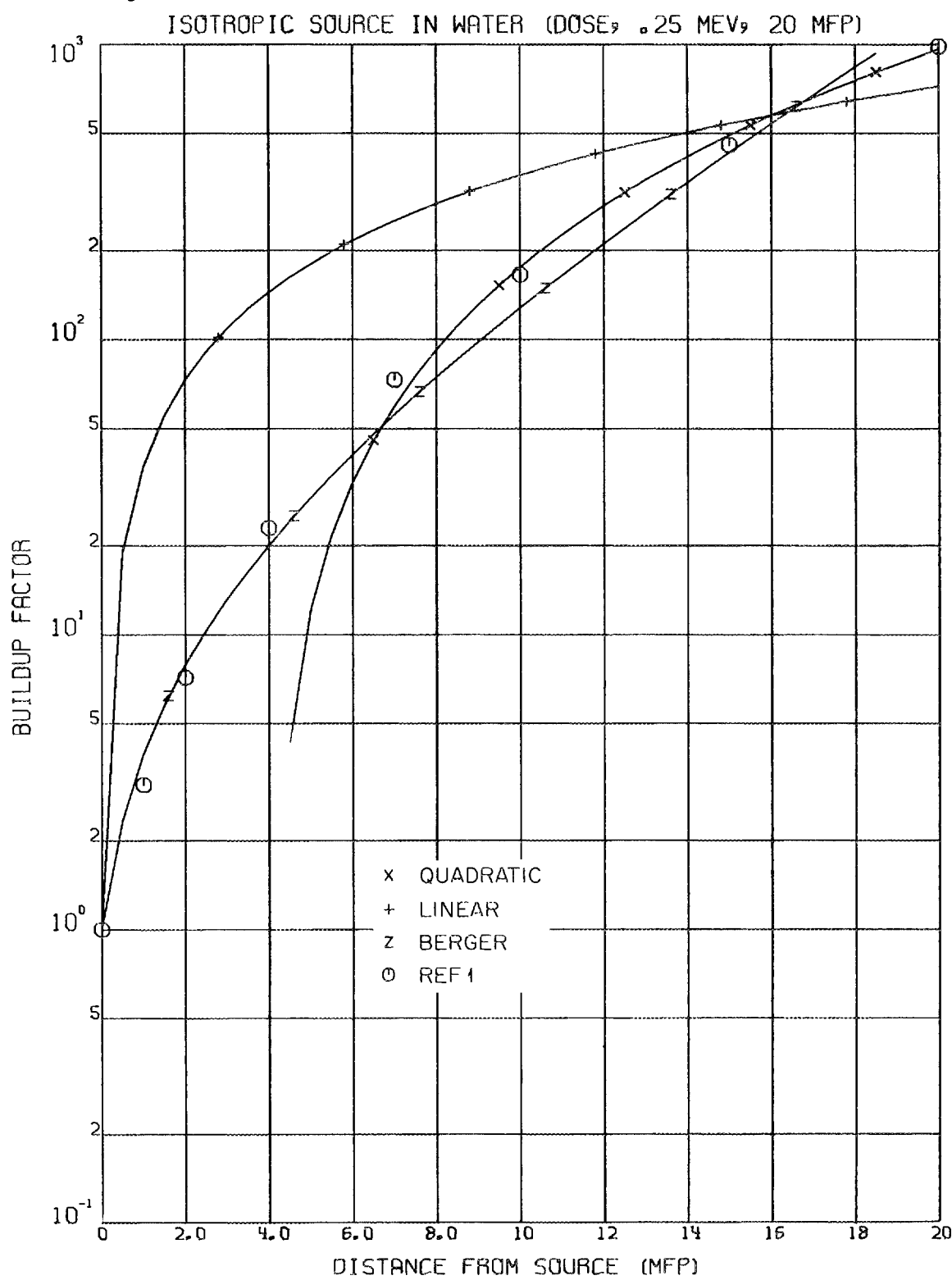


Fig. 4.

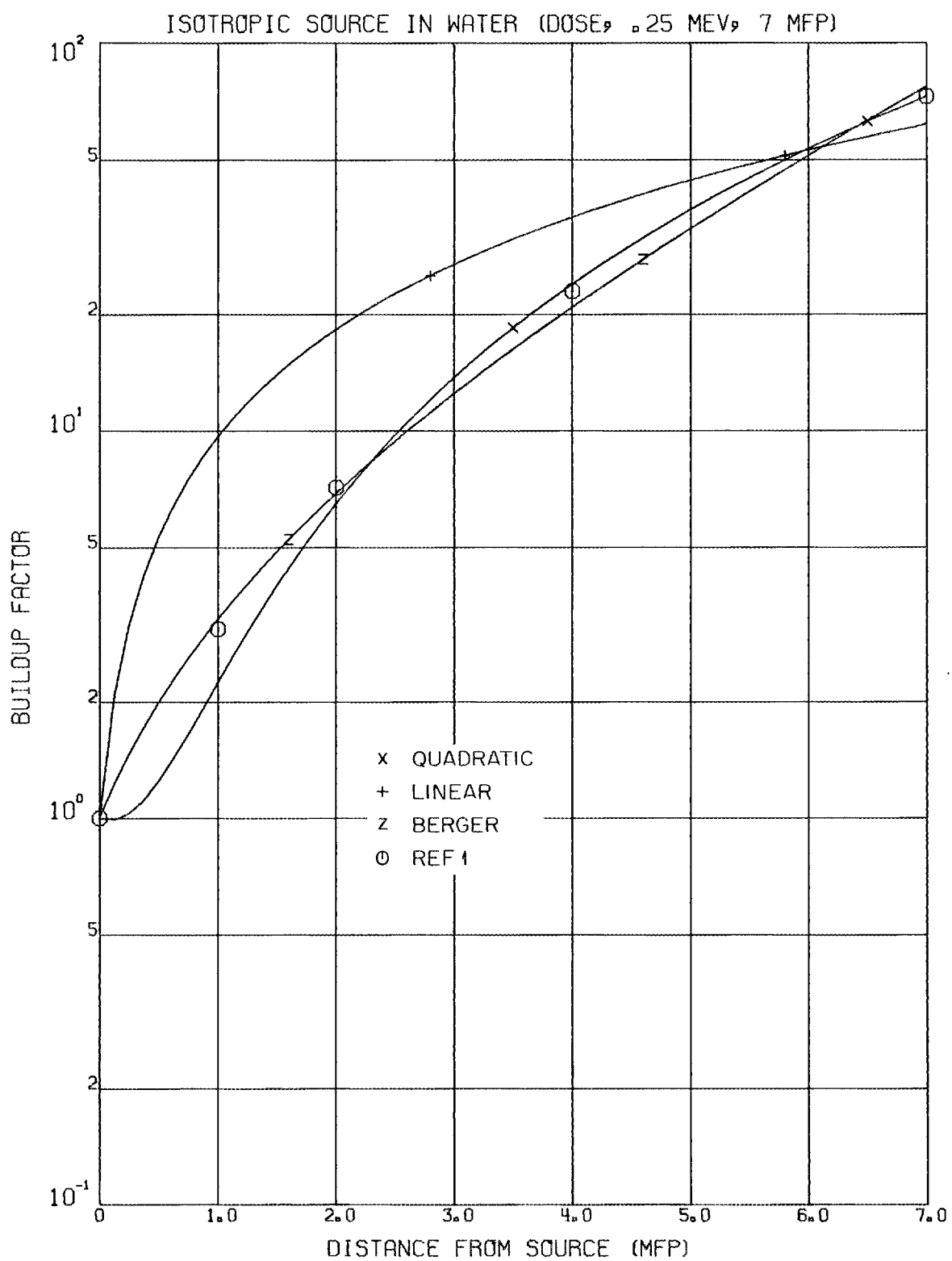


Fig. 5.

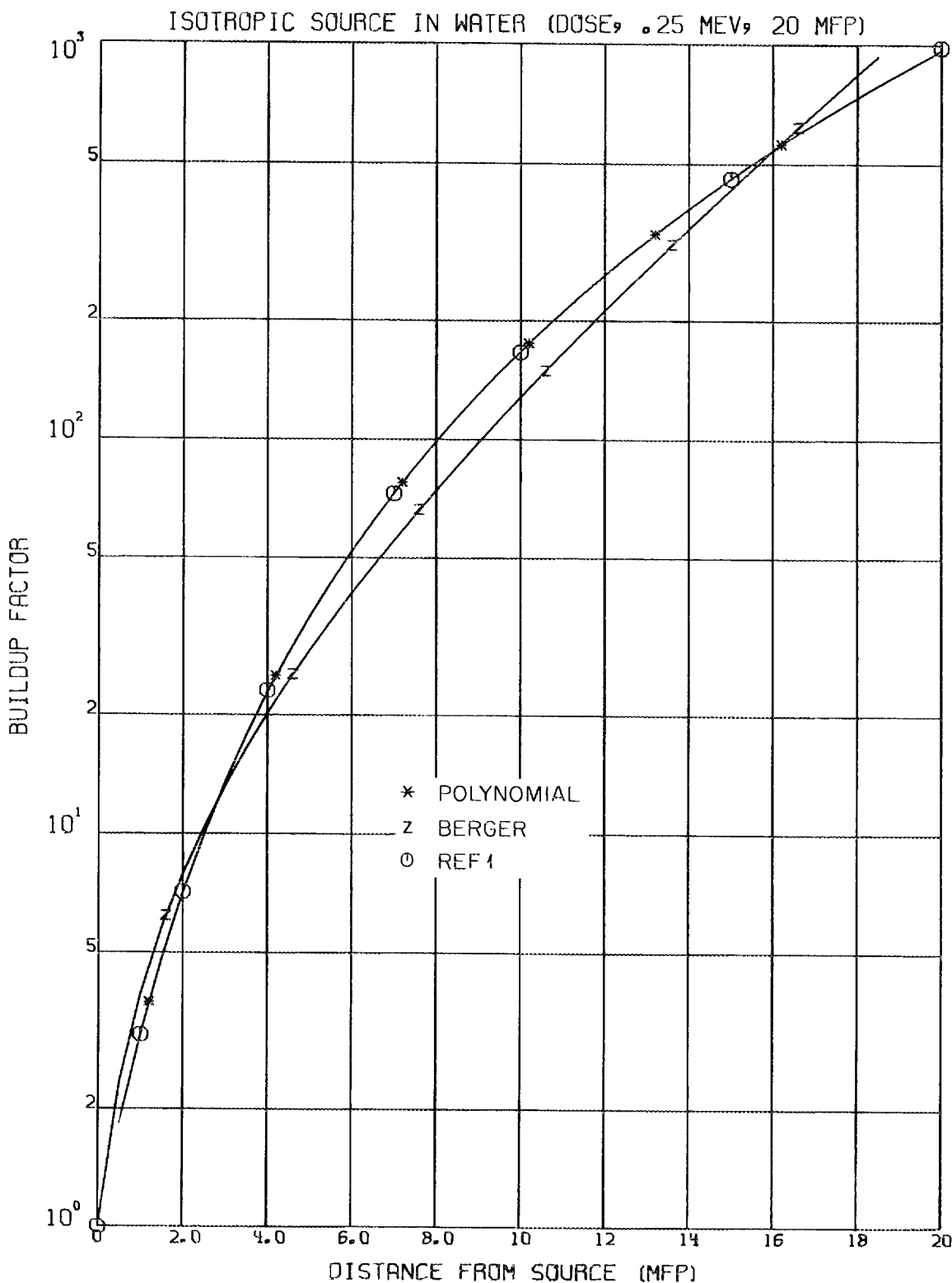


Fig. 6.

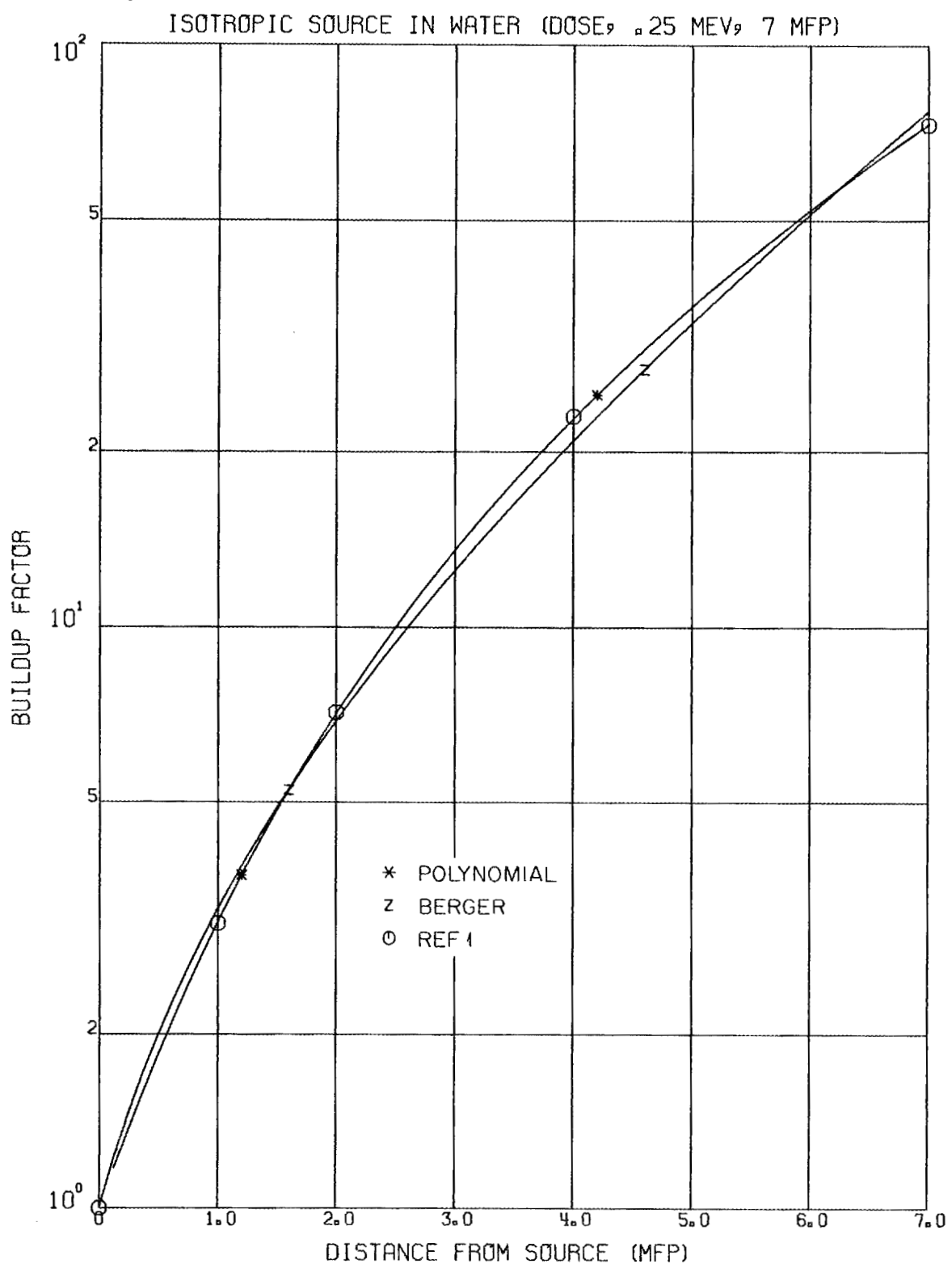


Fig. 7.

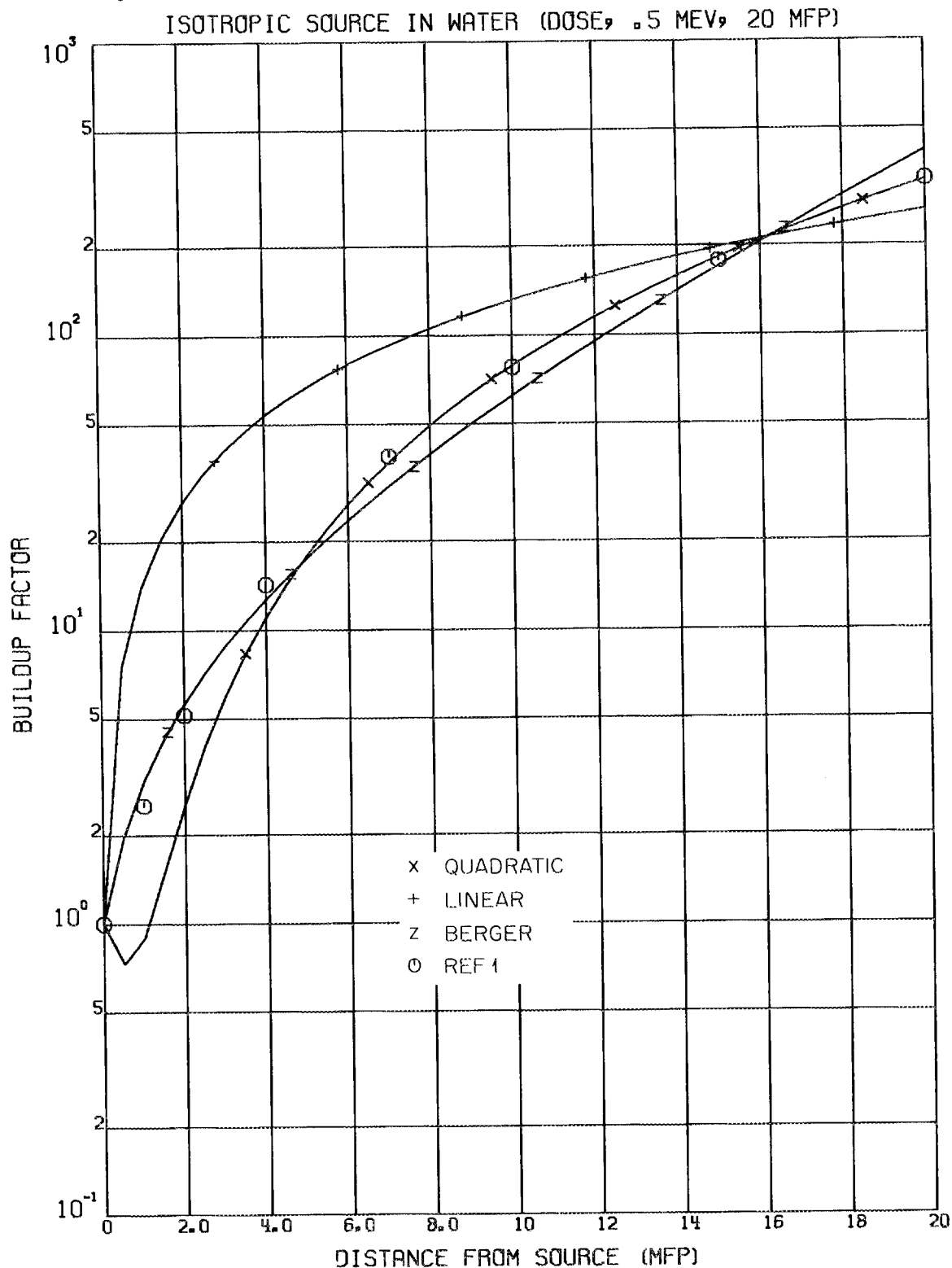


Fig. 8.

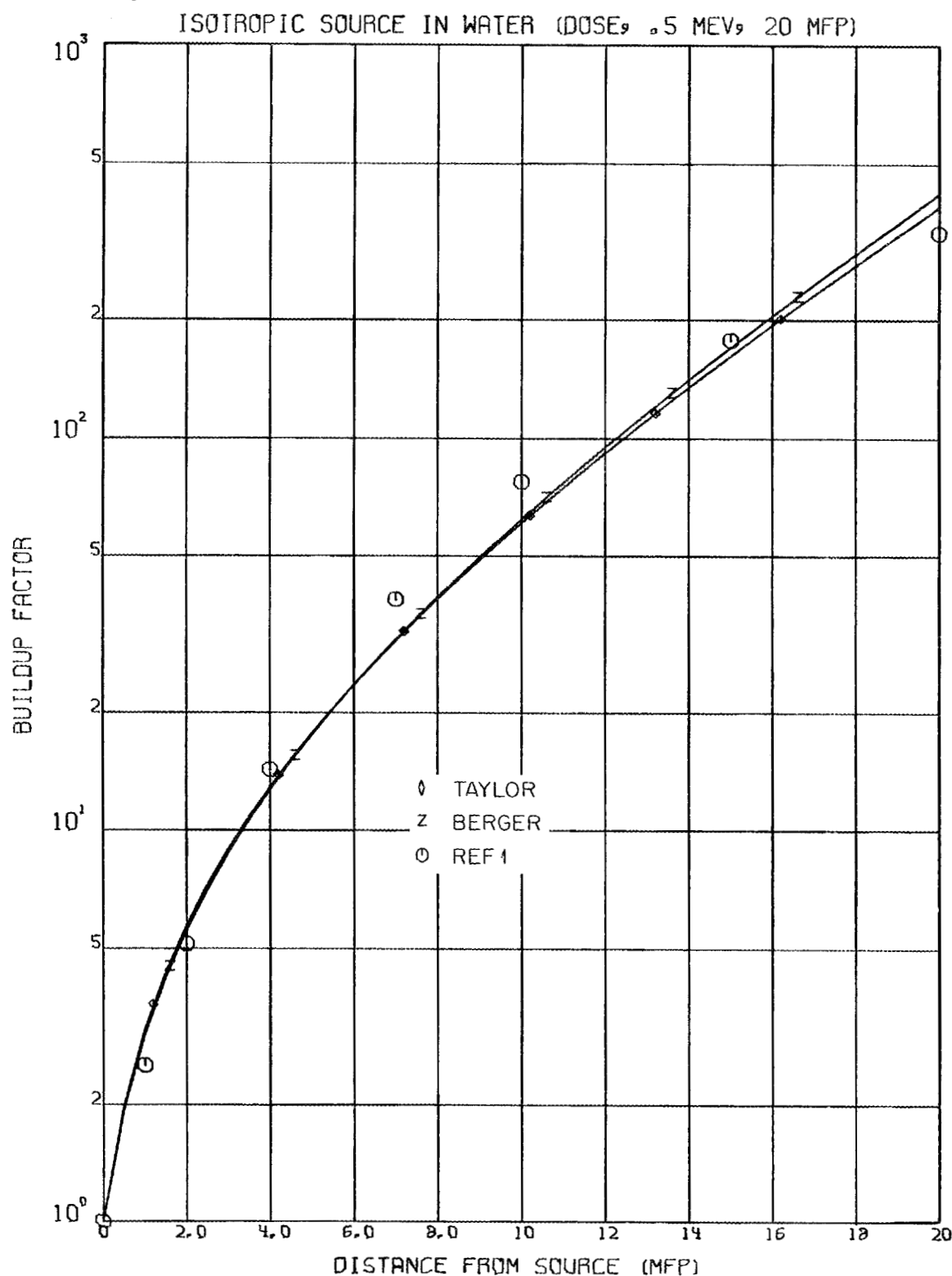


Fig. 9.

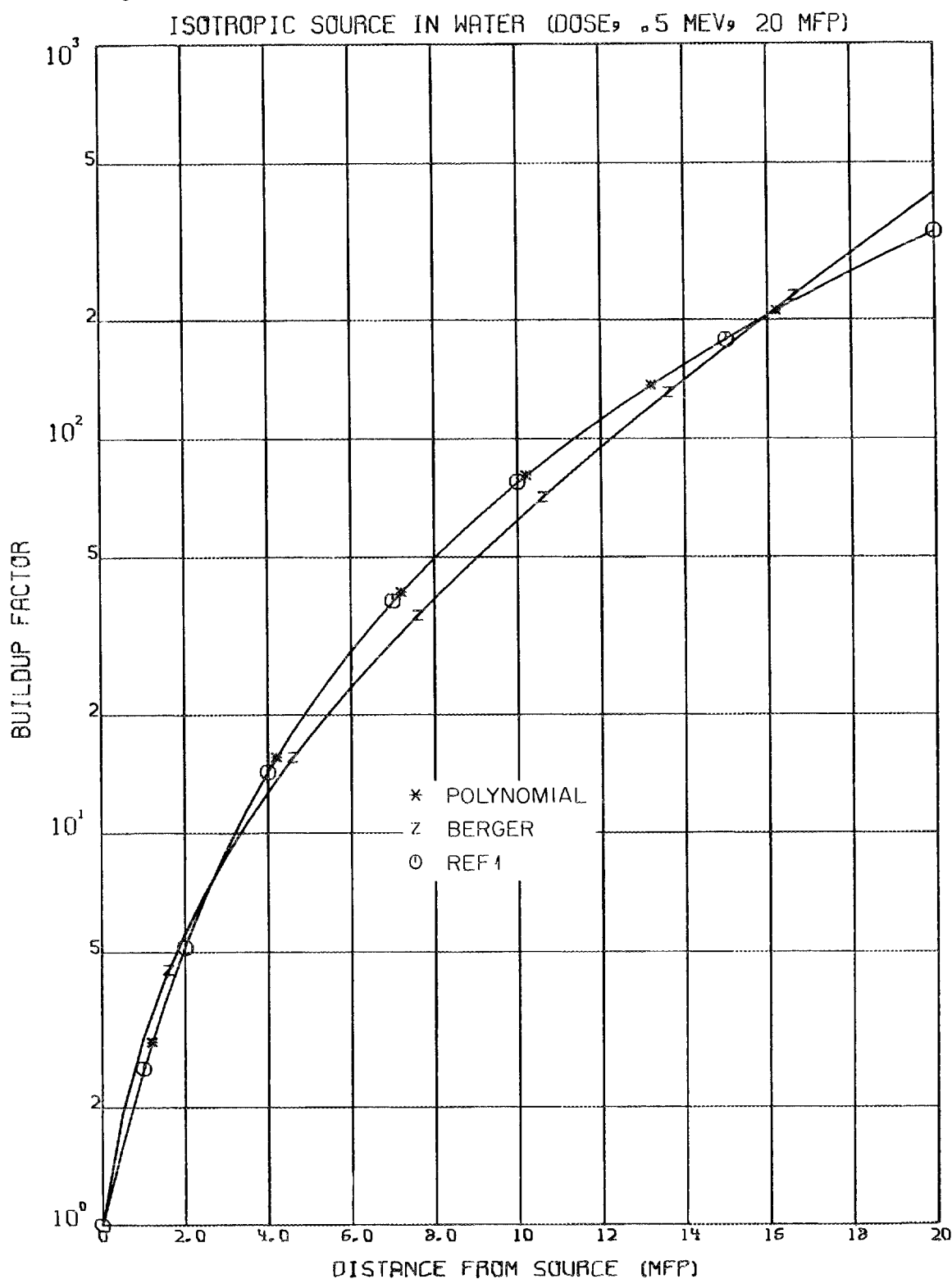


Fig. 10.

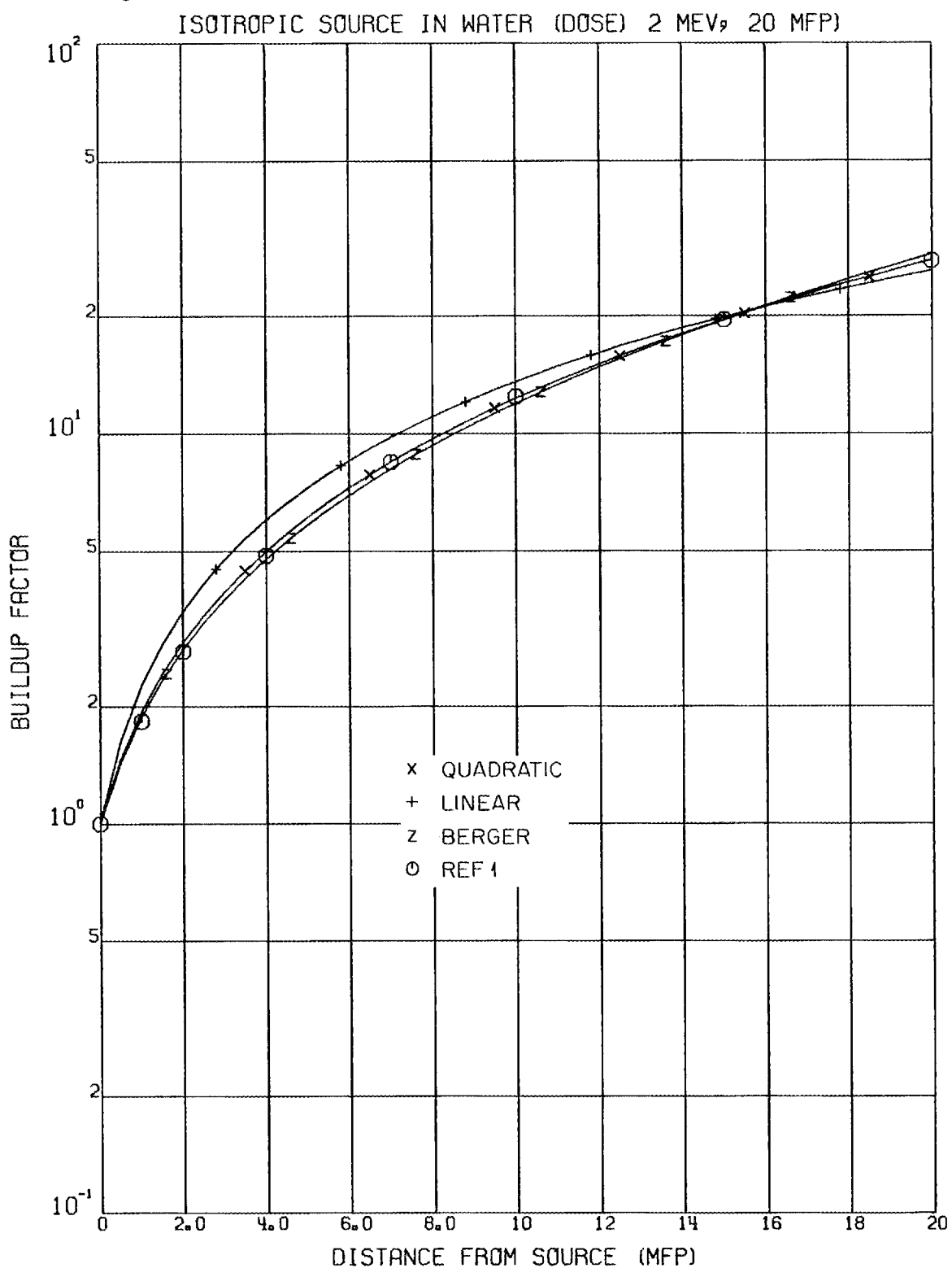


Fig. 11.

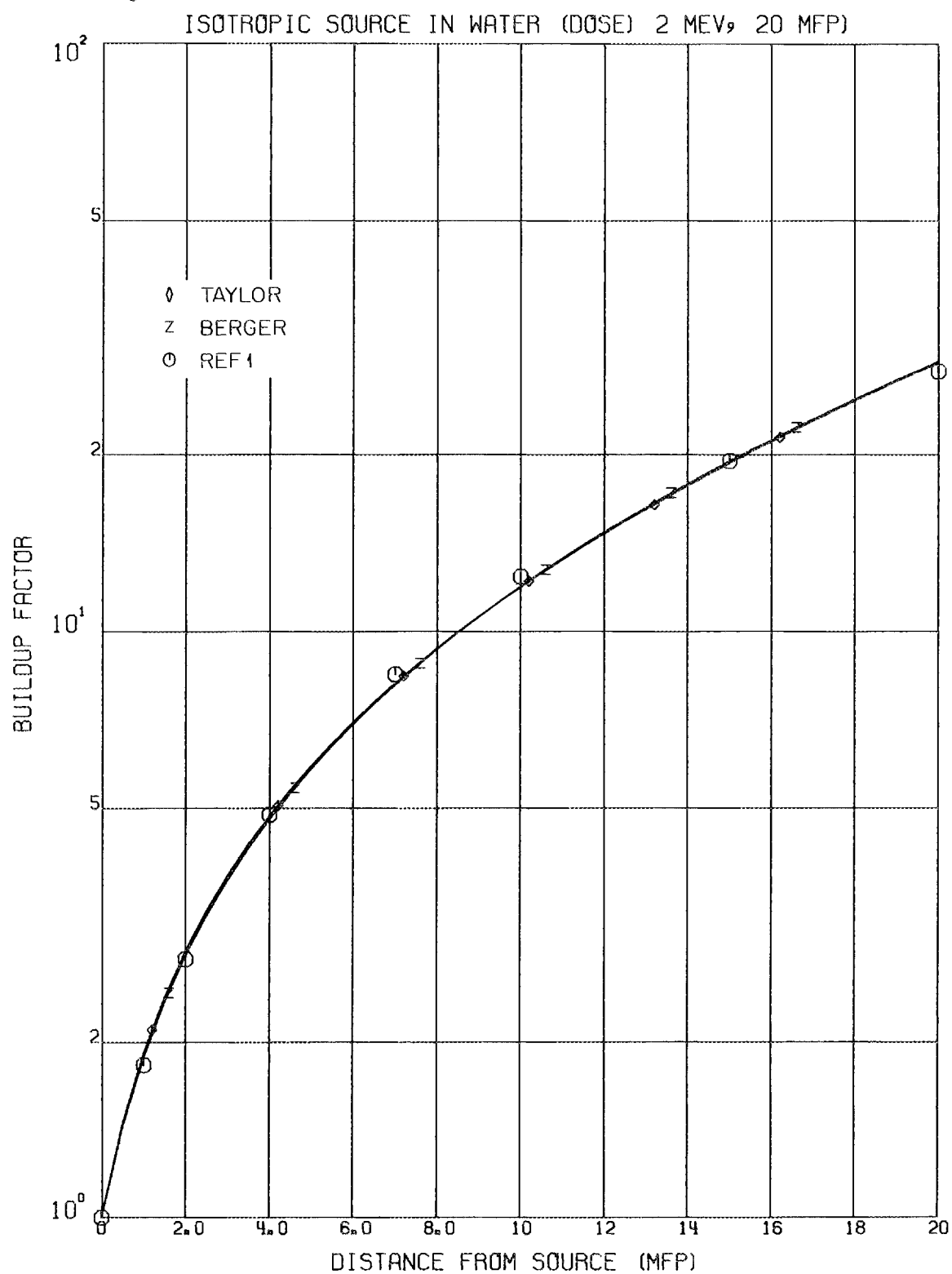


Fig. 12.

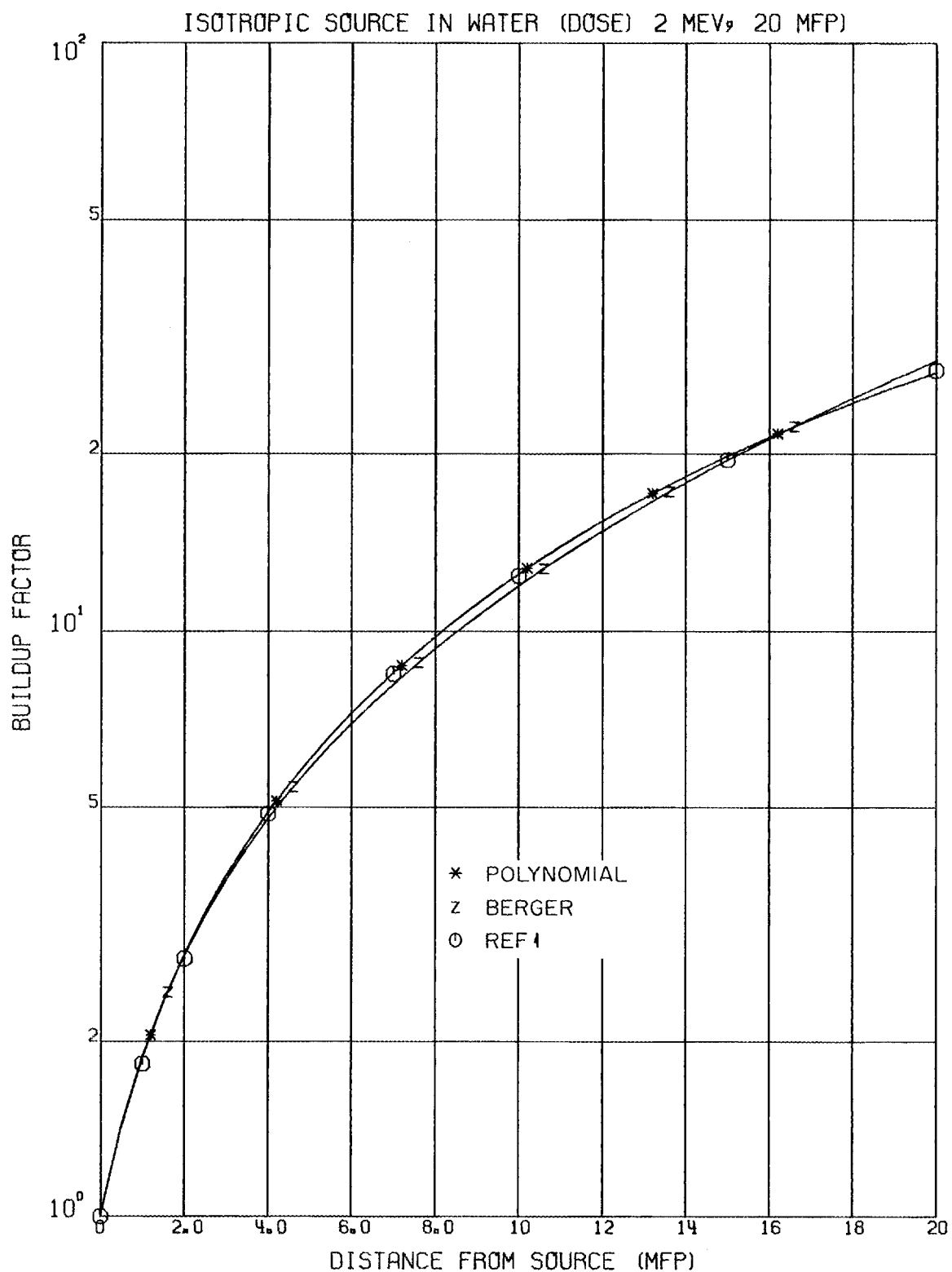


Fig. 13.

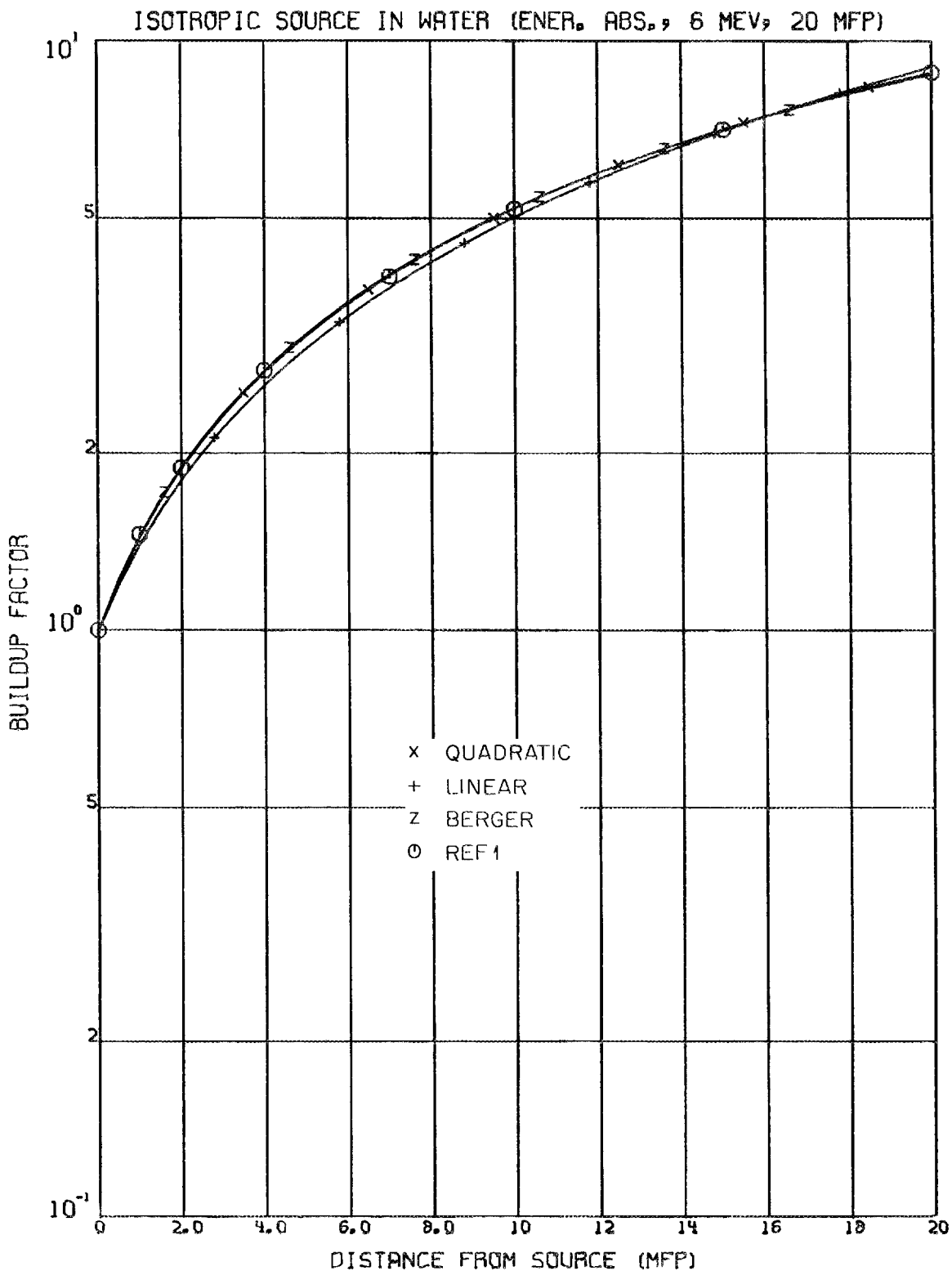


Fig. 14.

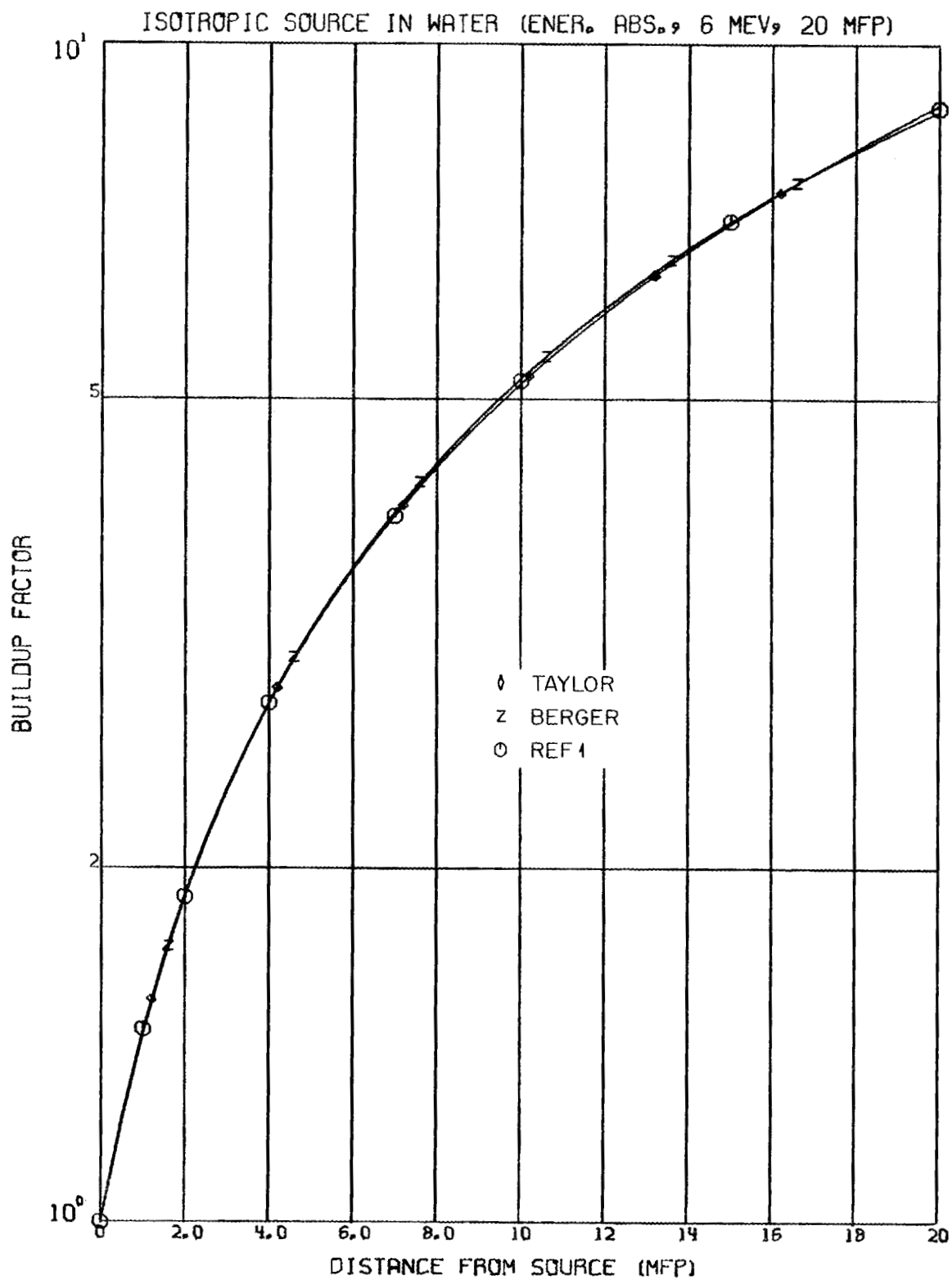


Fig. 15.

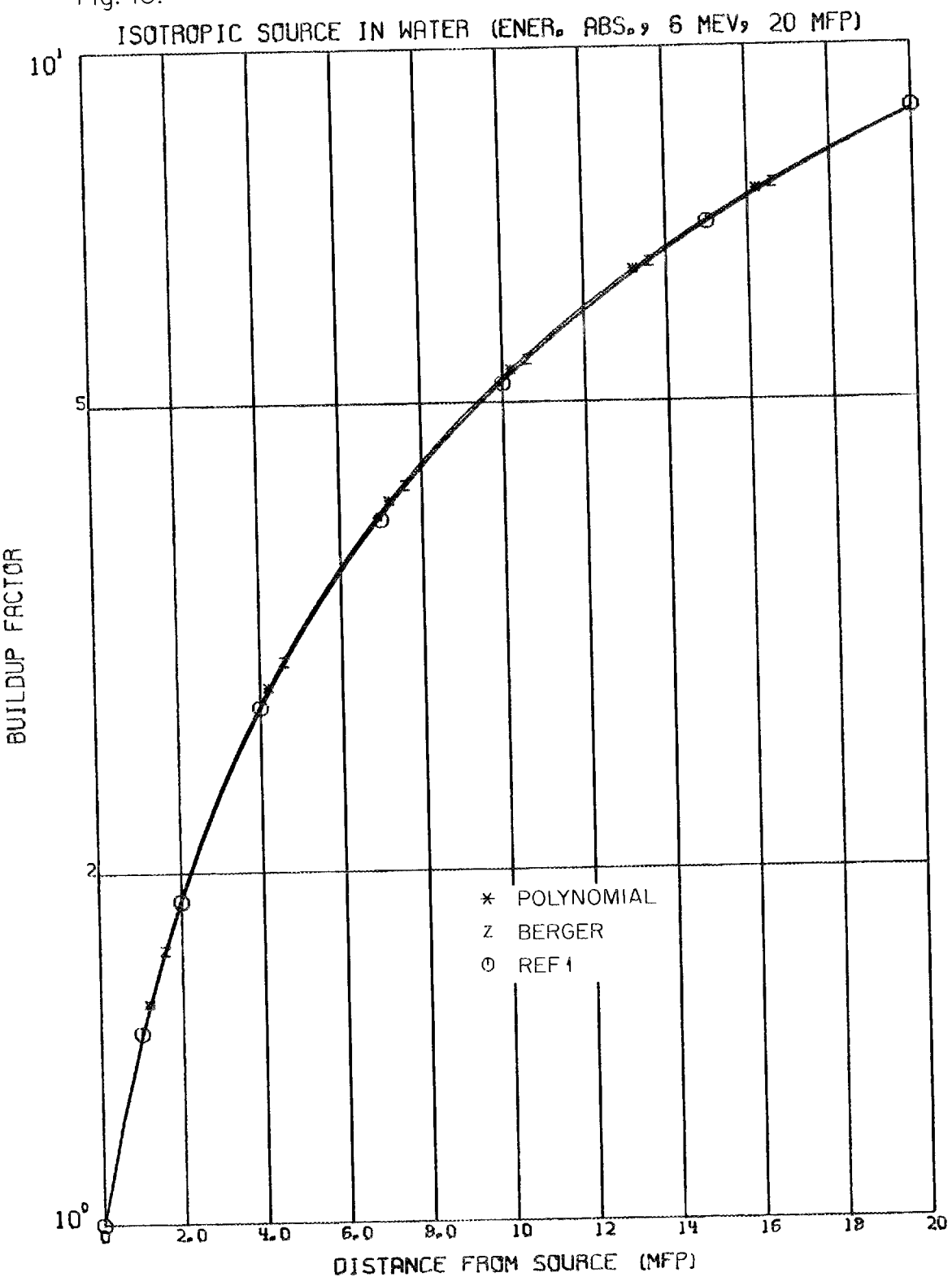


Fig. 16.

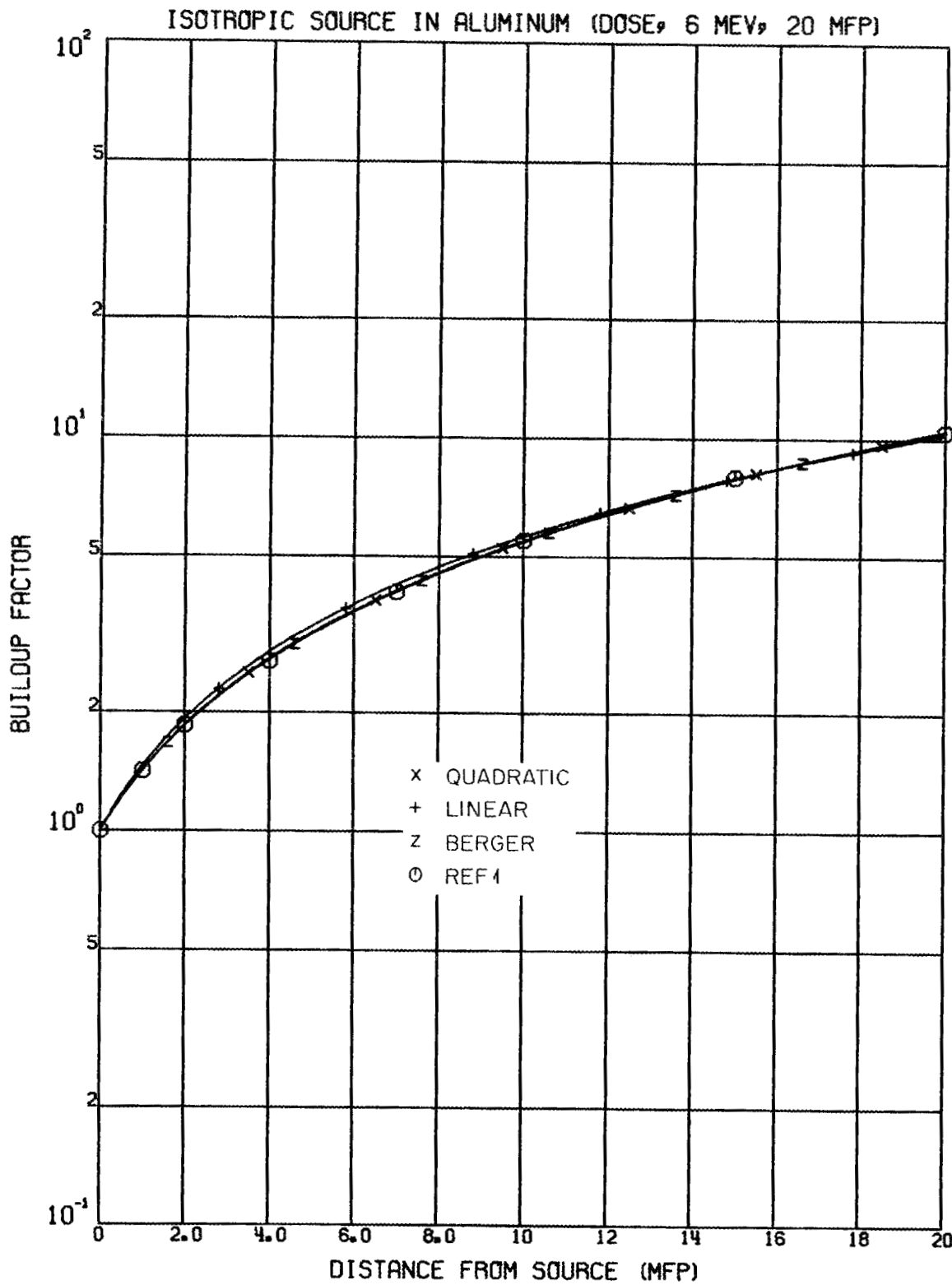


Fig. 17.

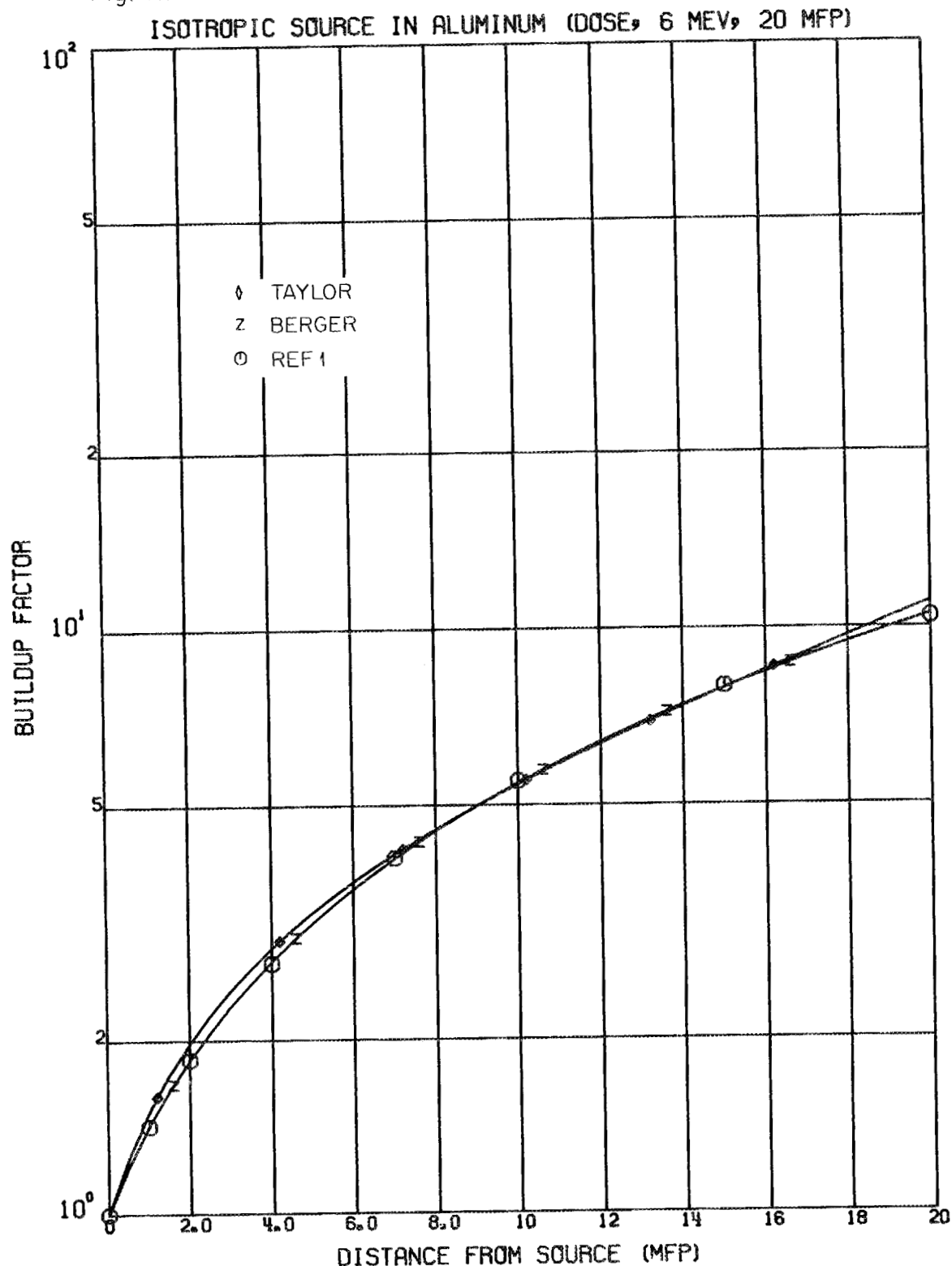


Fig. 18.

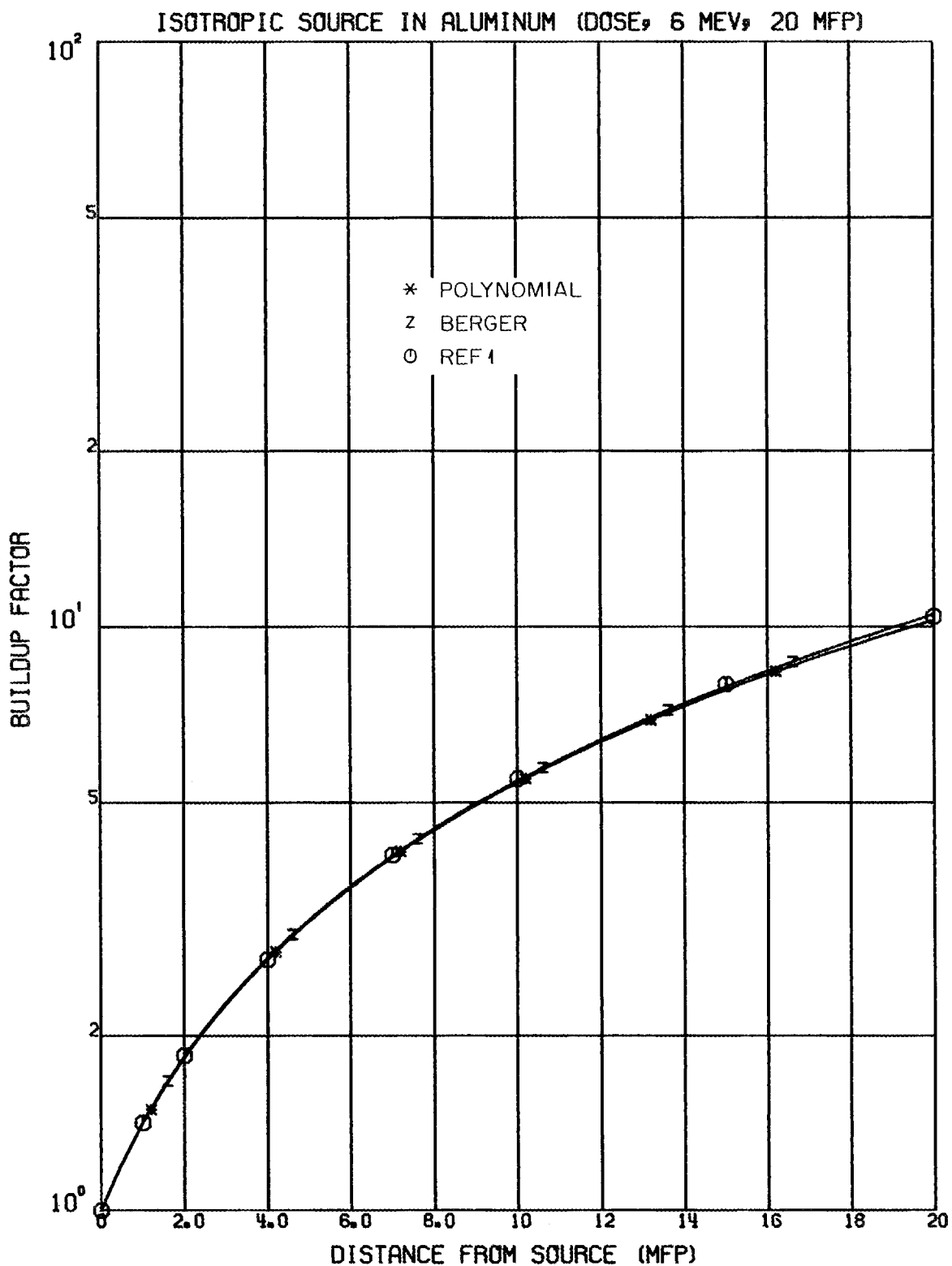


Fig. 19.

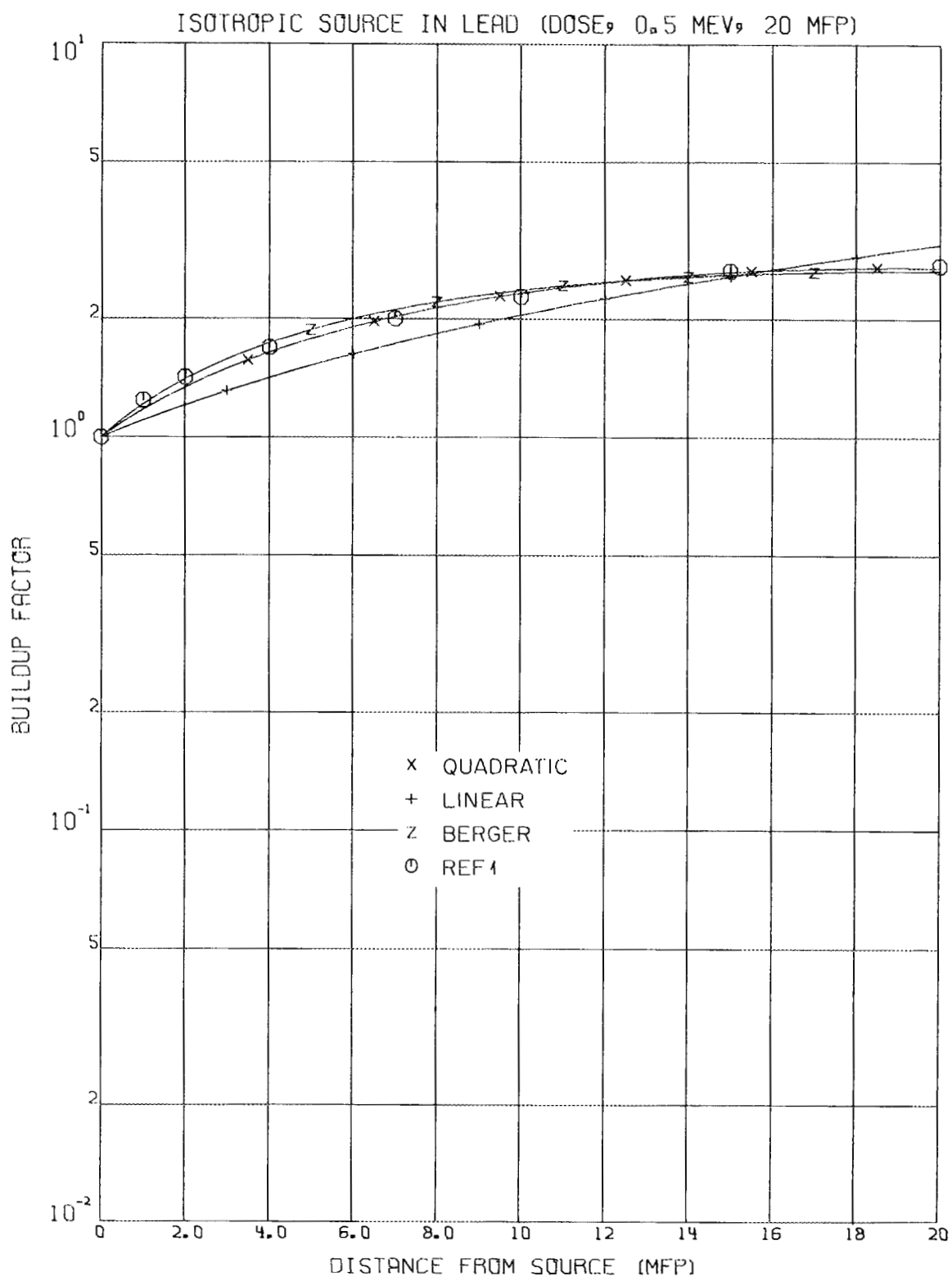


Fig. 20.

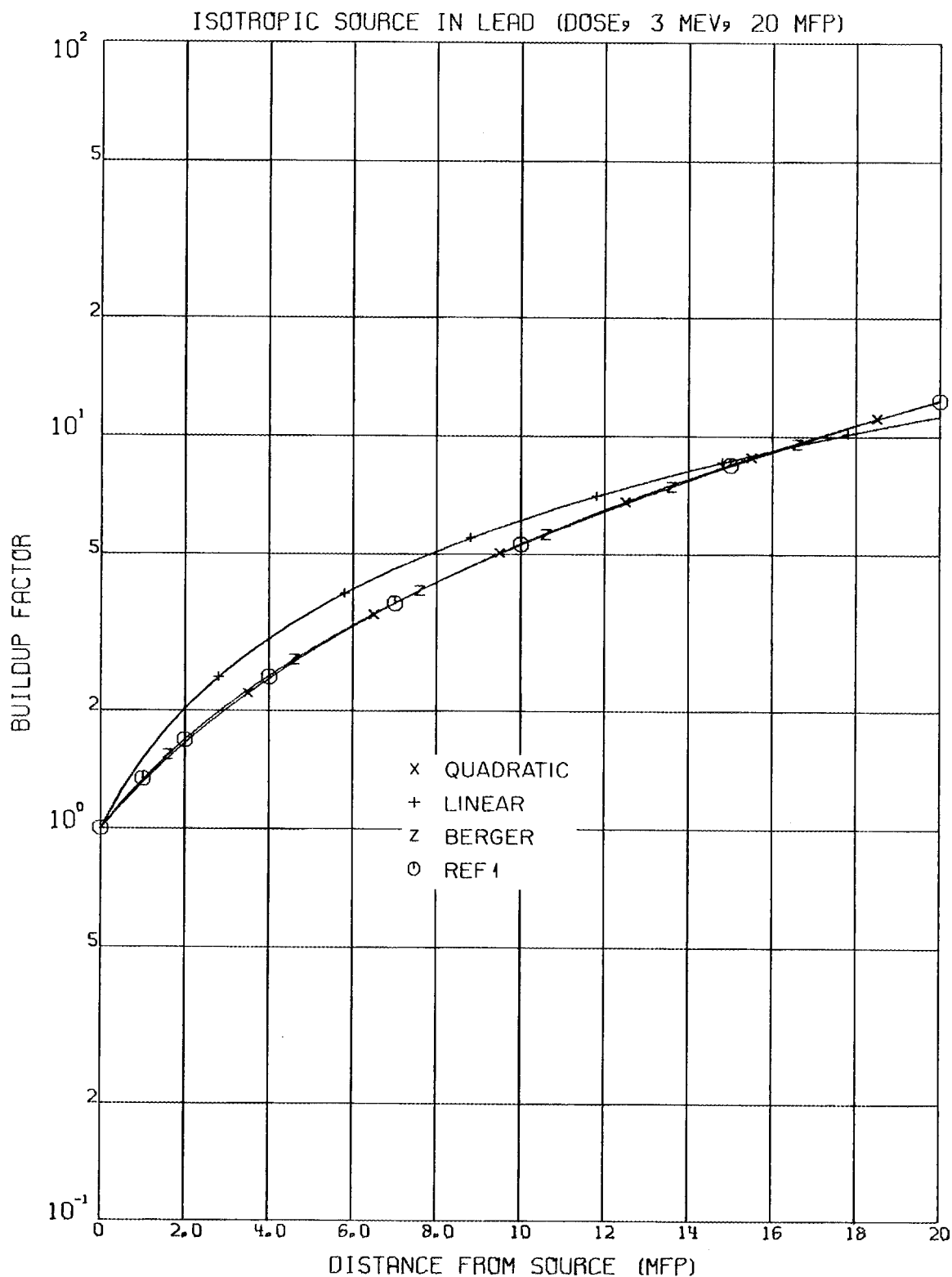


Fig. 21.

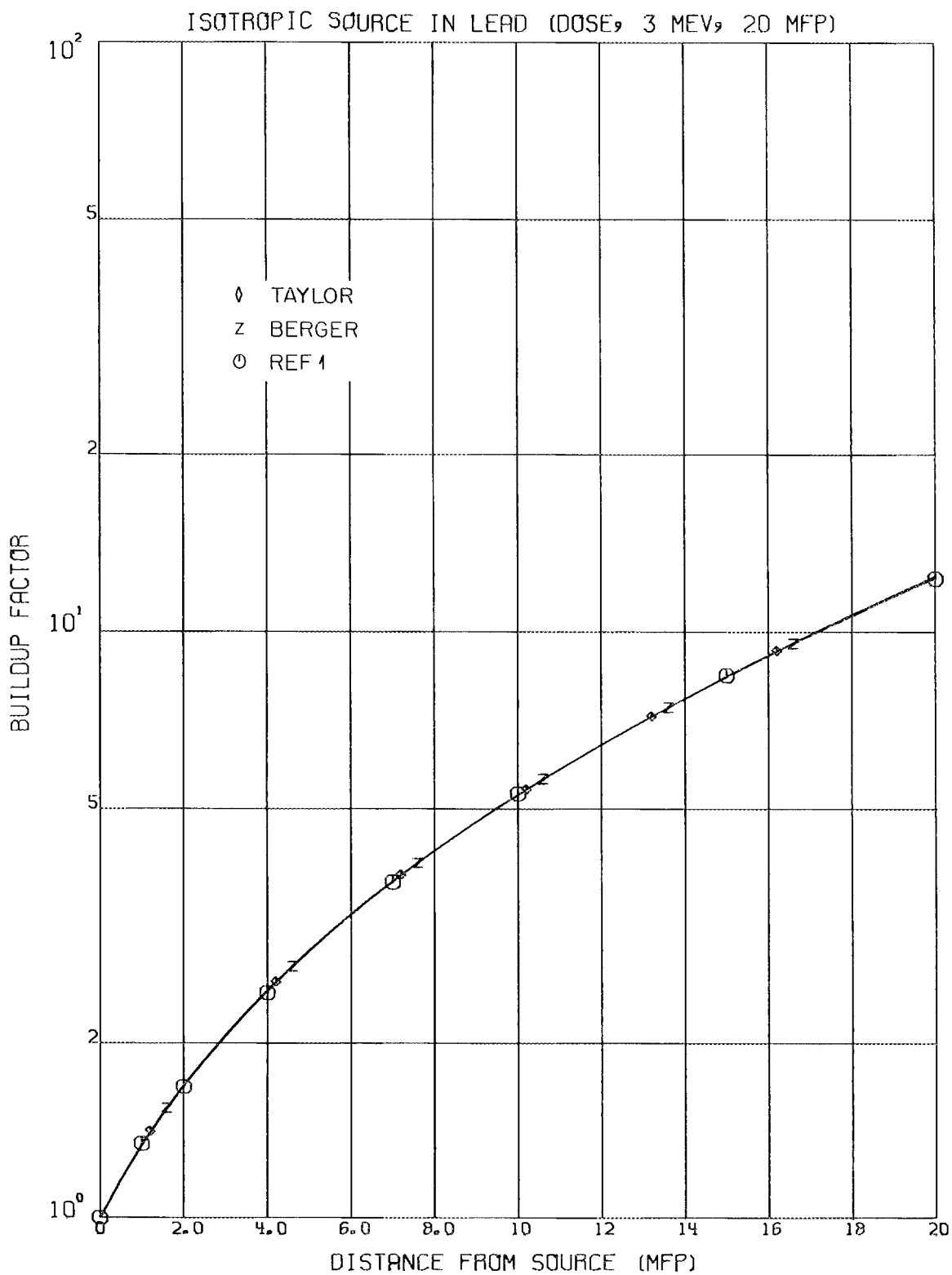


Fig. 22.

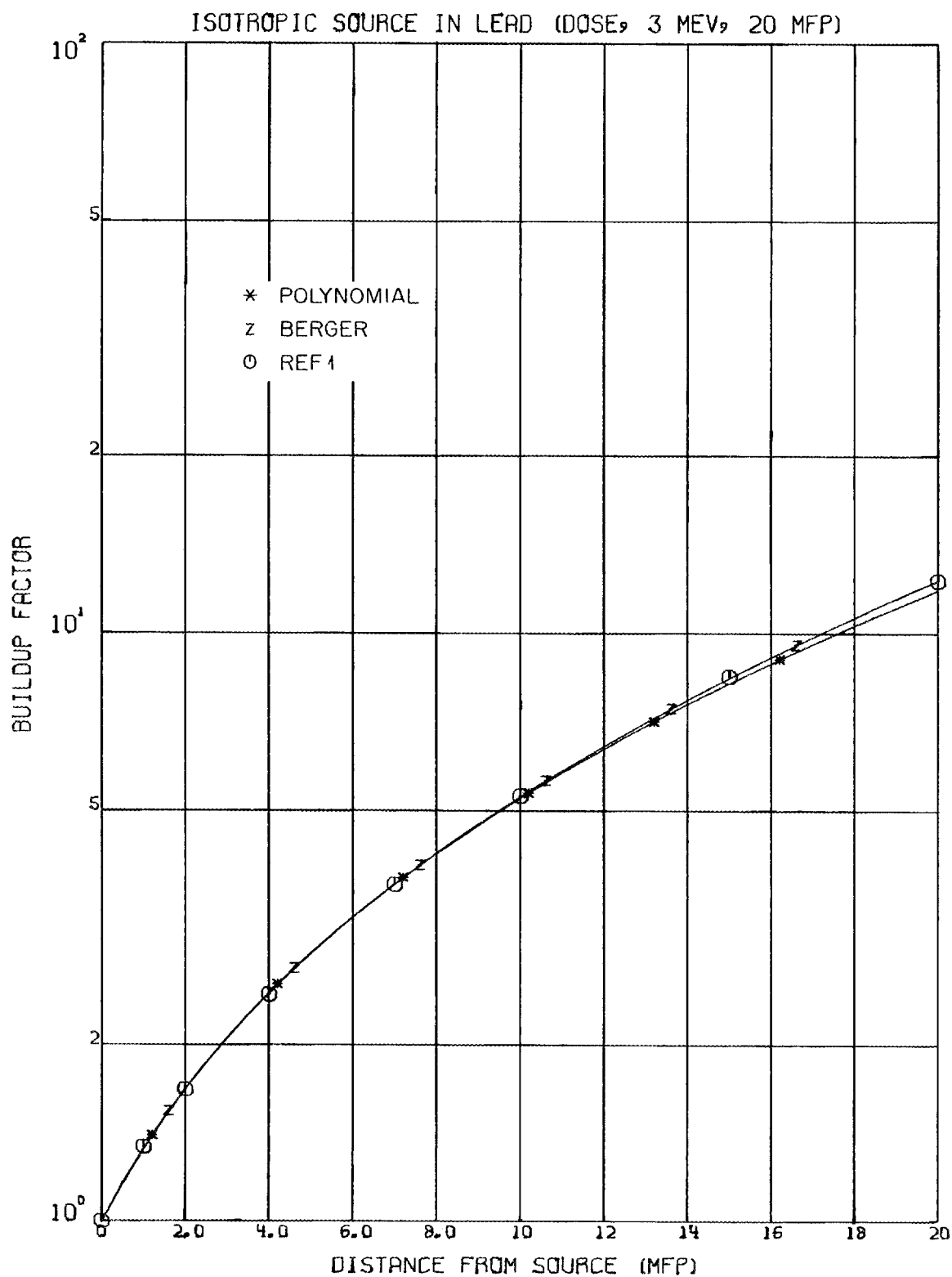


Fig. 23.

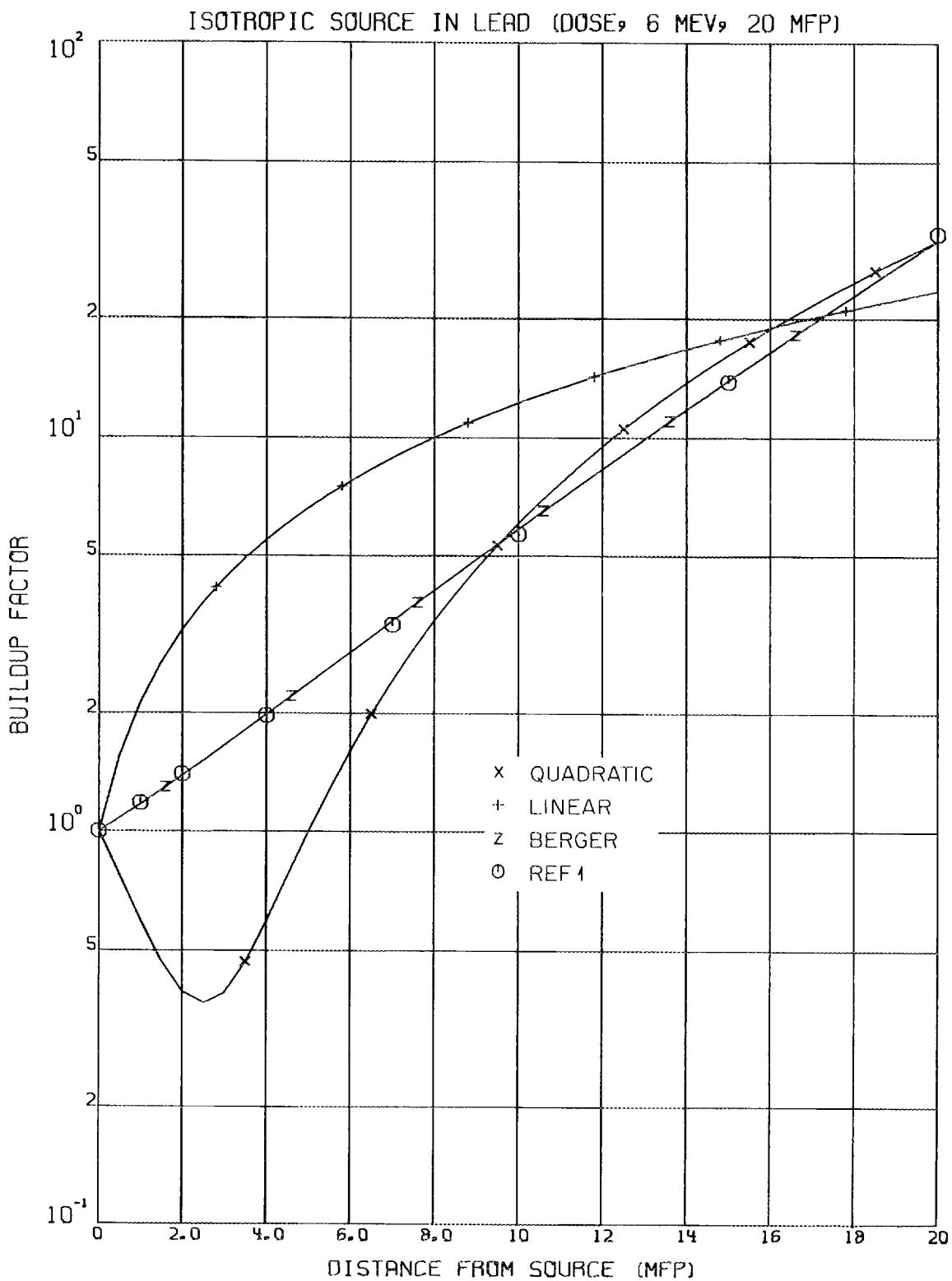


Fig. 24.

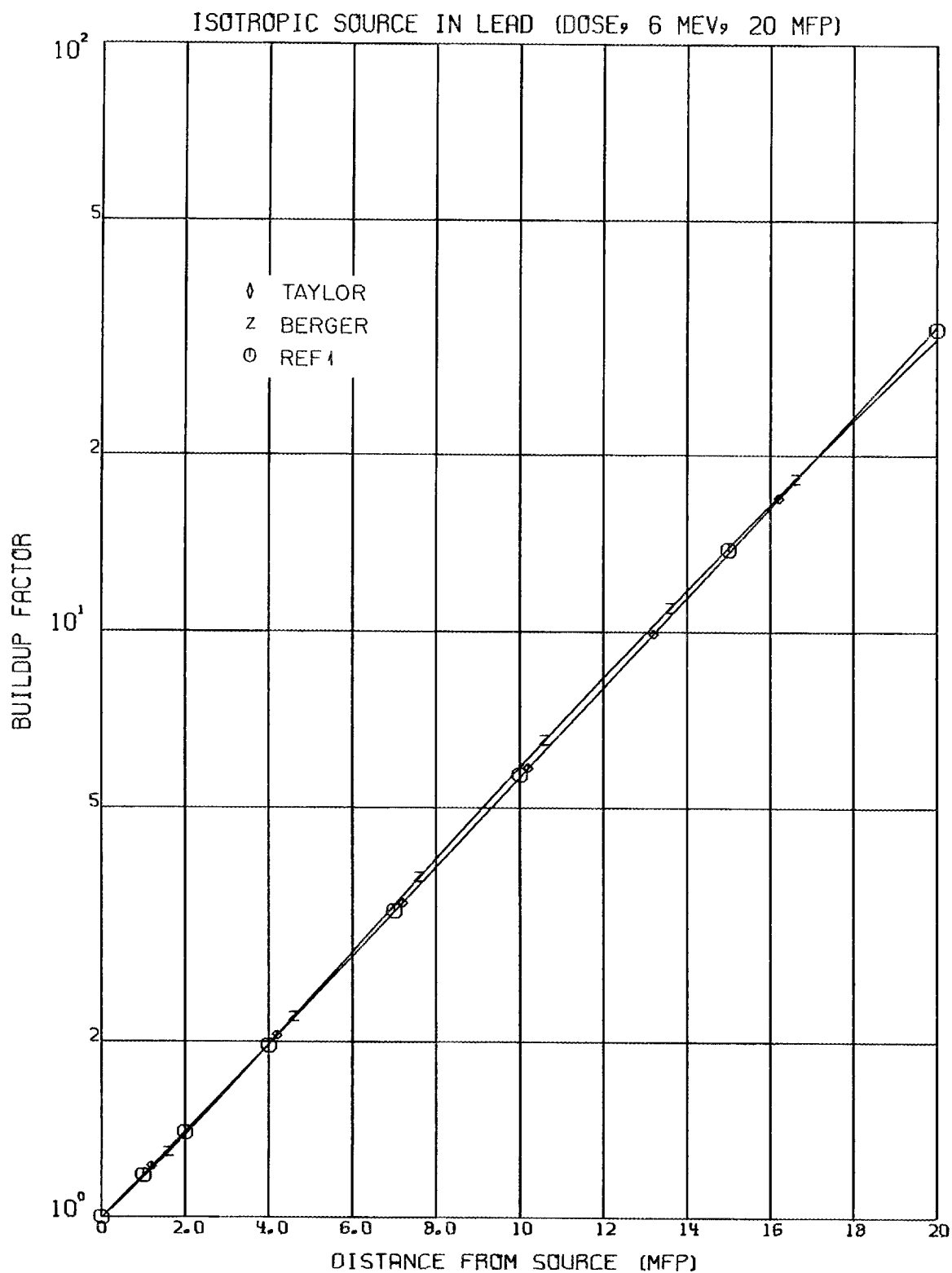


Fig. 25.

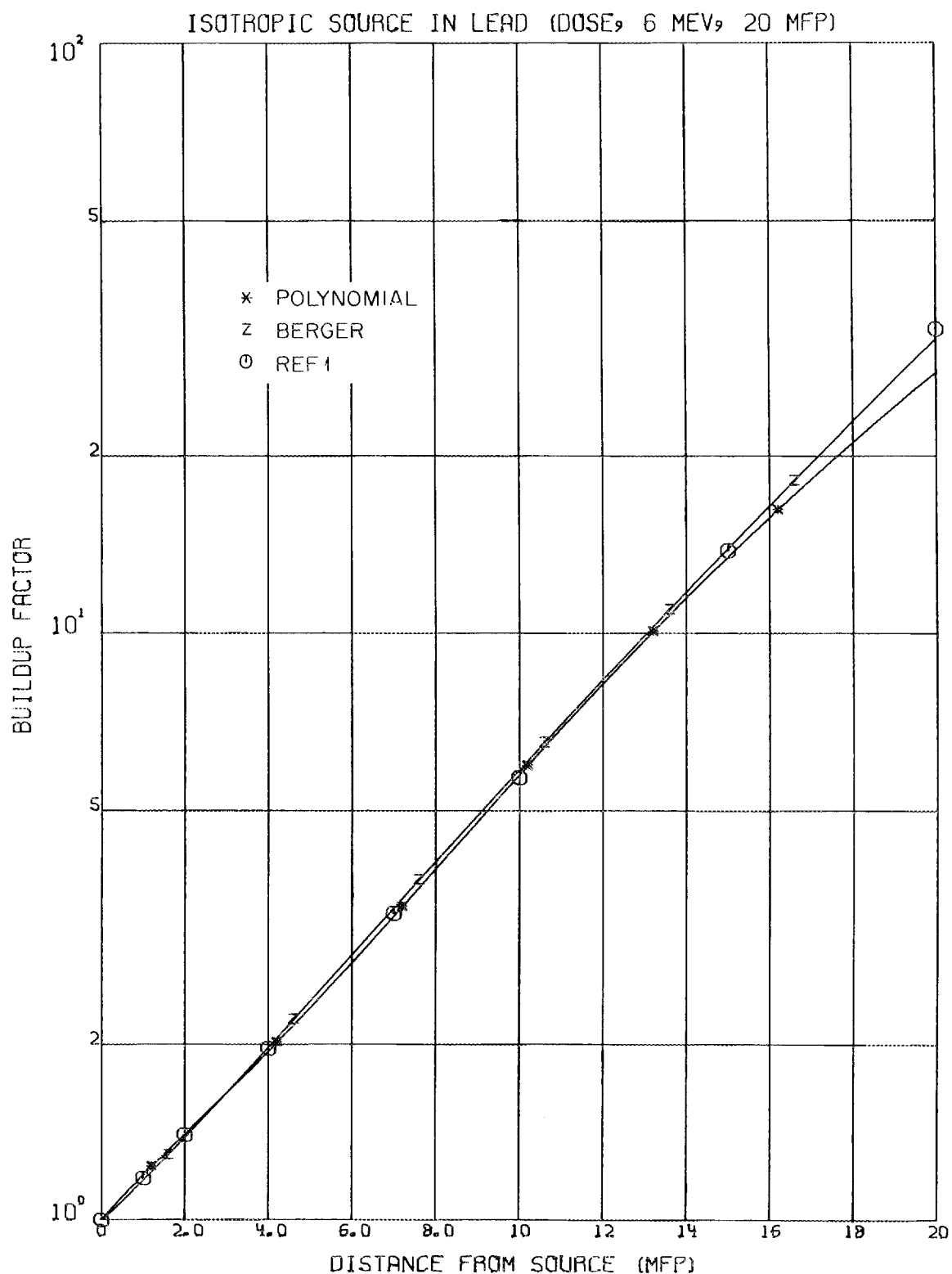


Fig. 26.

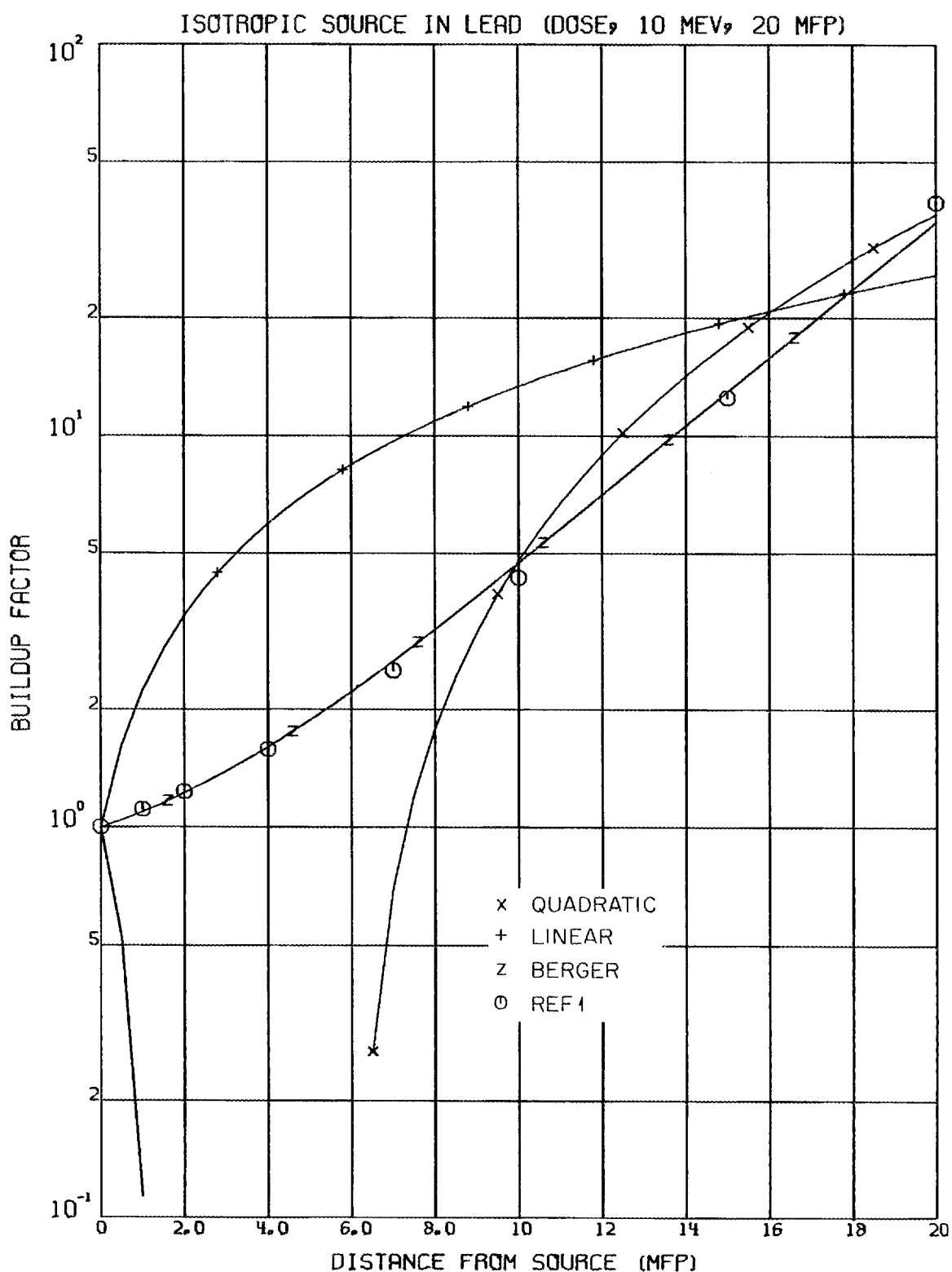


Fig. 27.

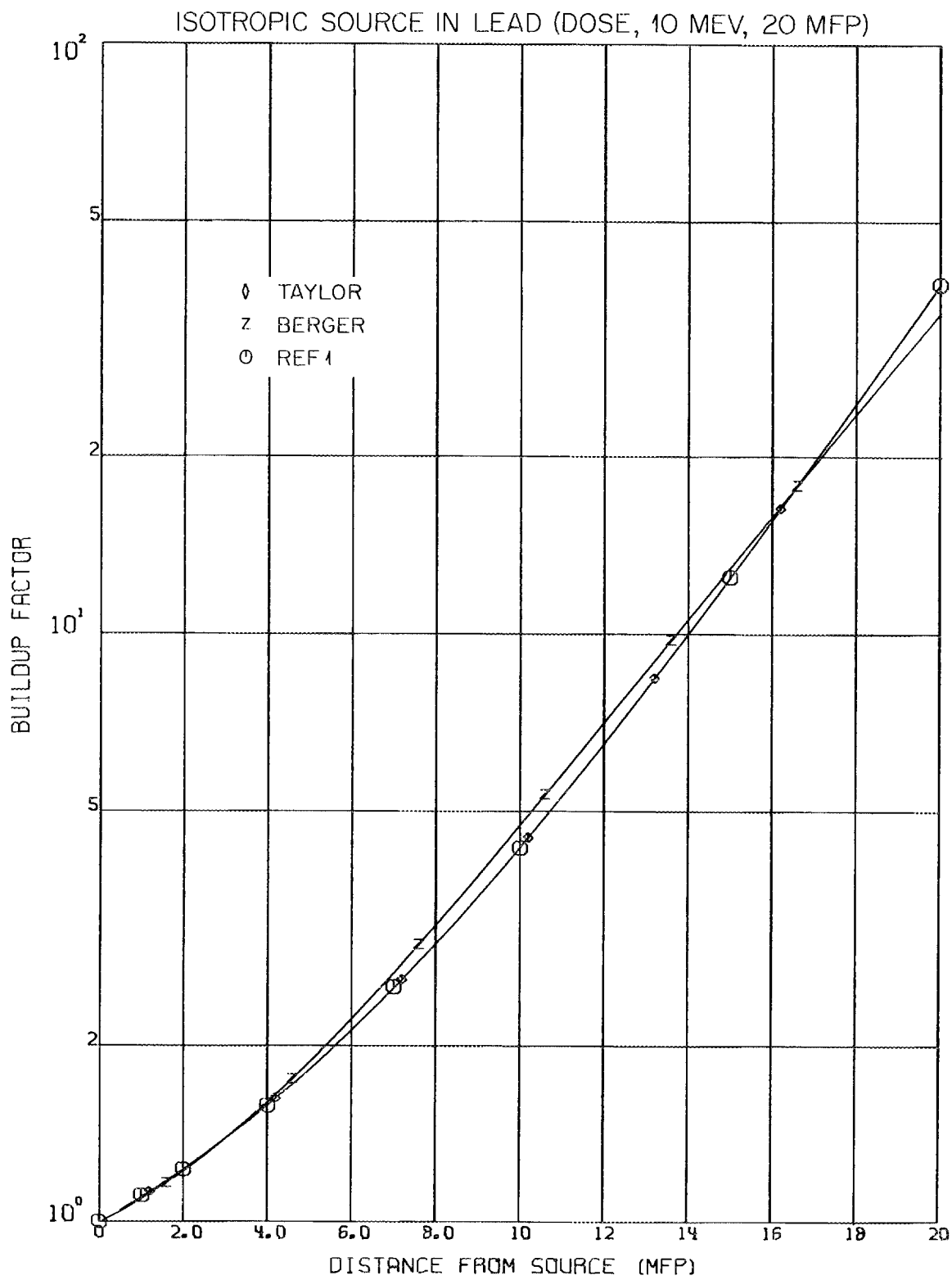


Fig. 28.

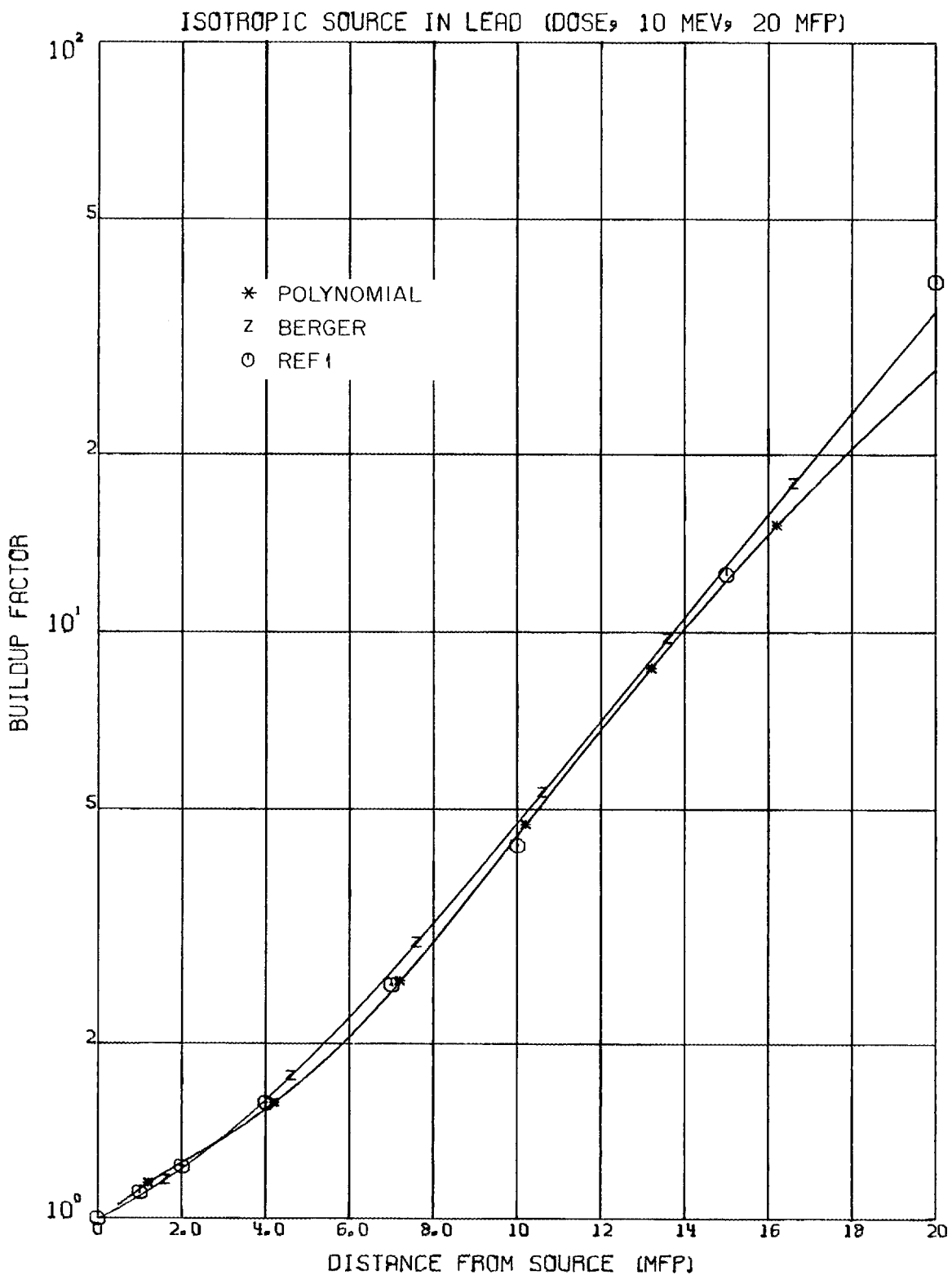


Fig. 29.

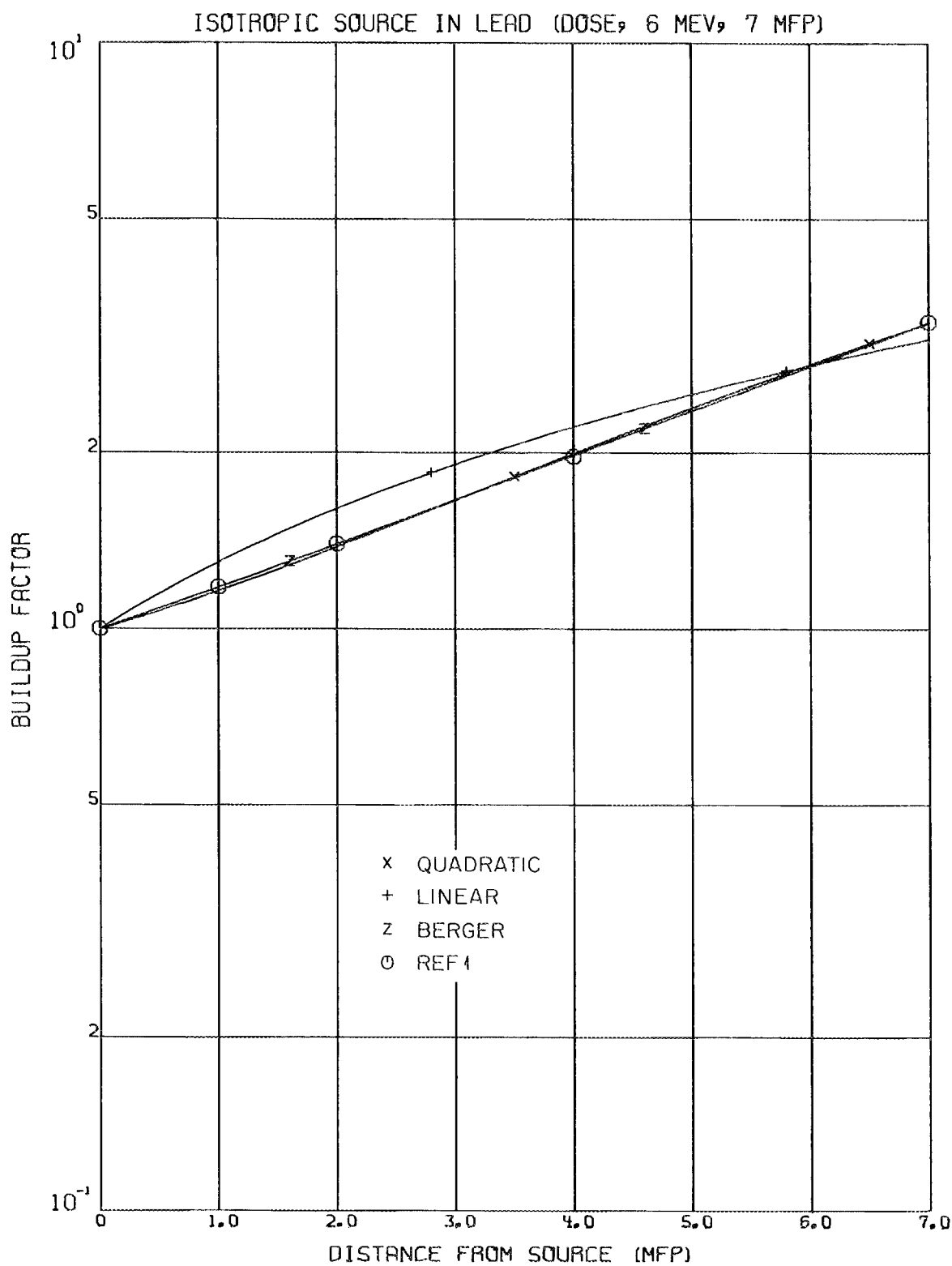


Fig. 30.

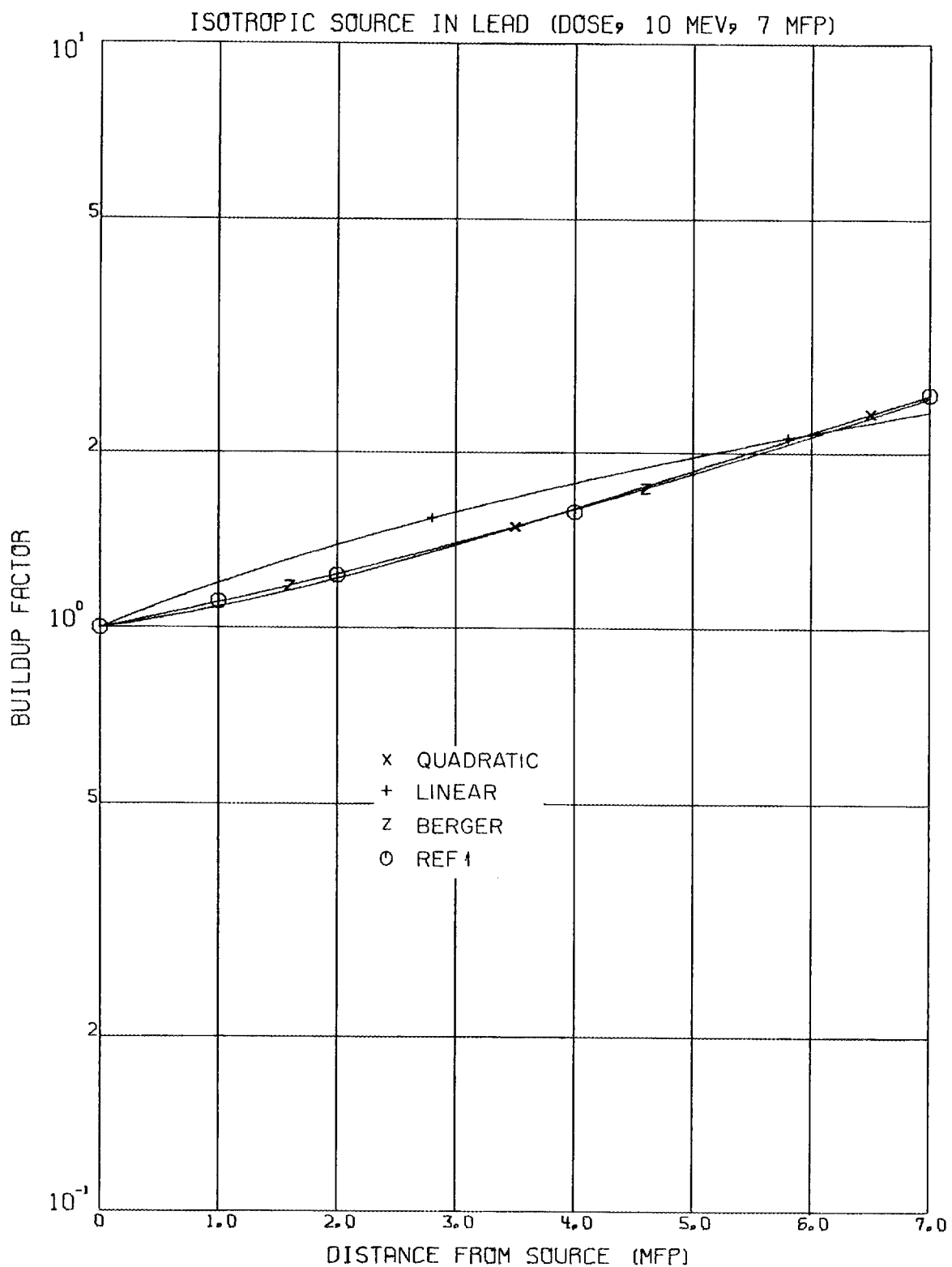


Fig. 31.

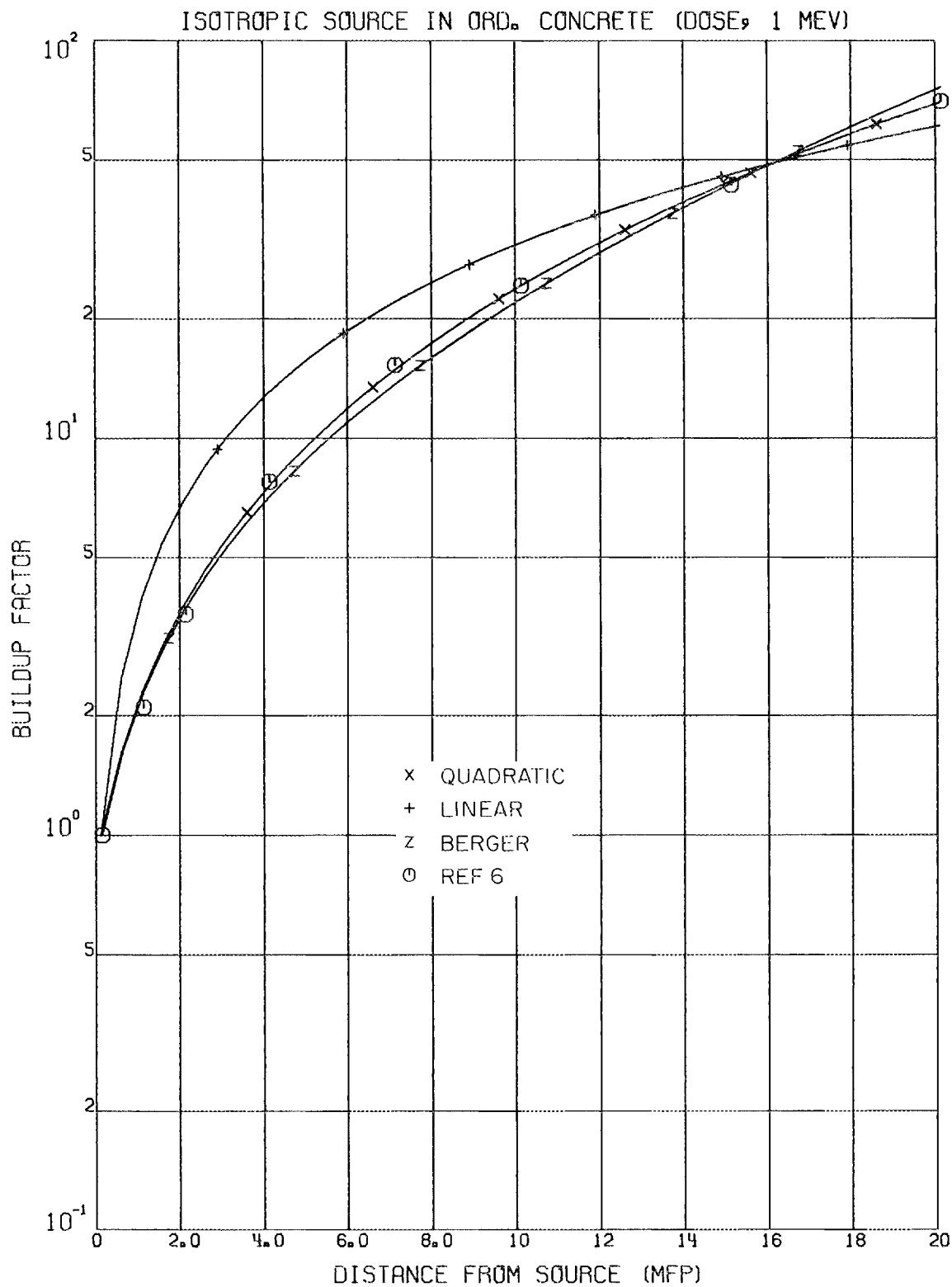


Fig. 32.

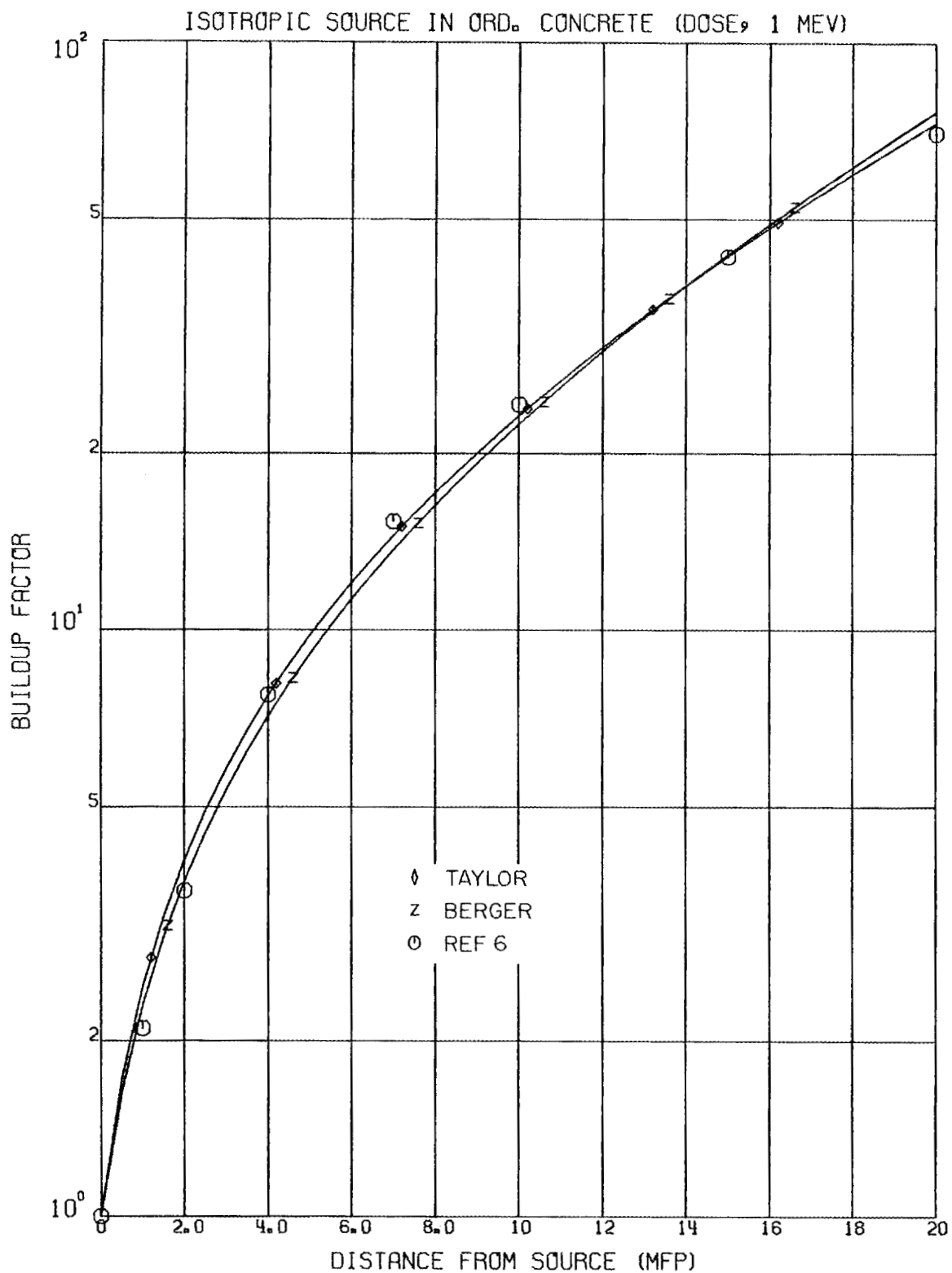


Fig. 33.

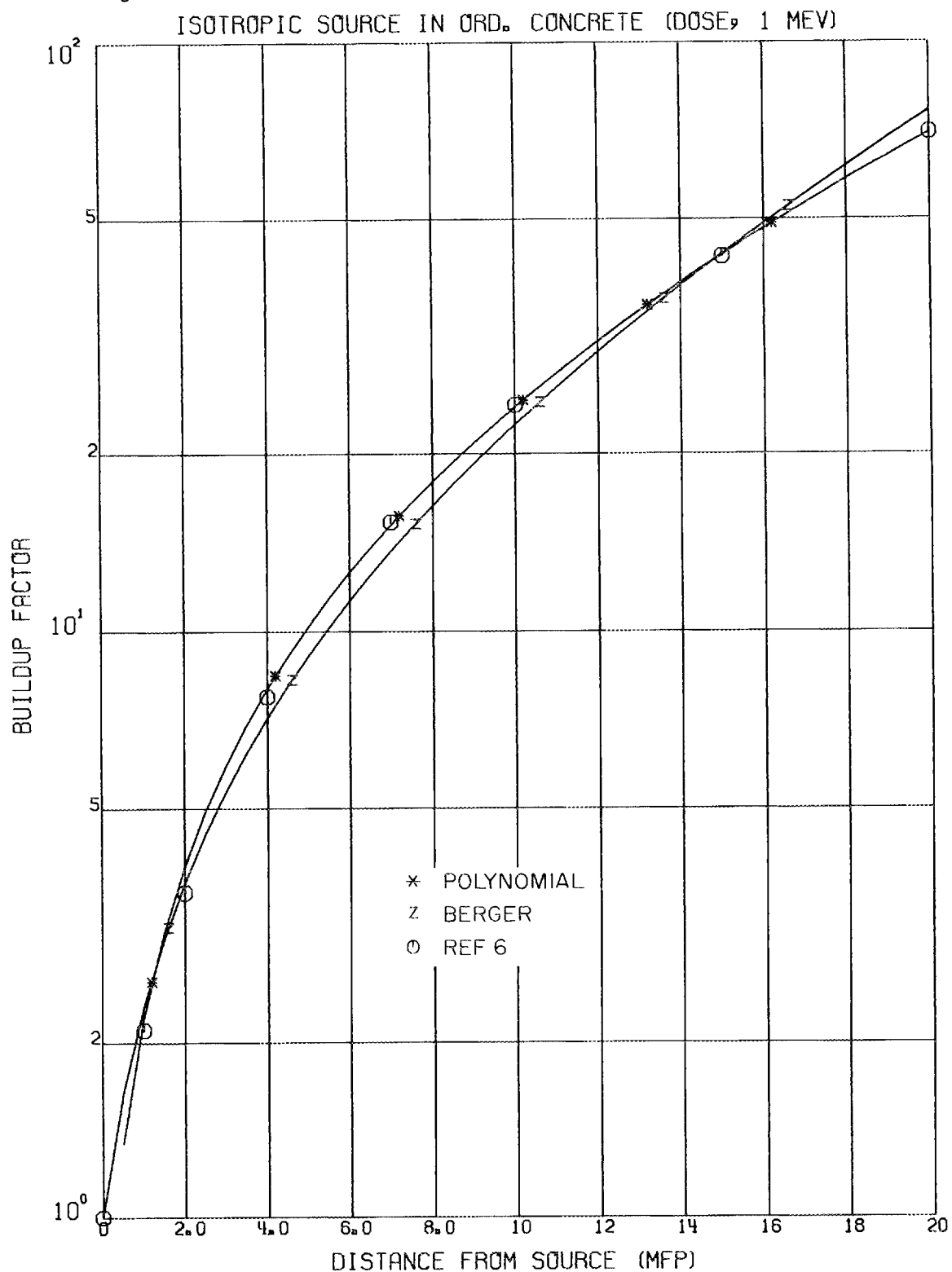


Fig. 34.

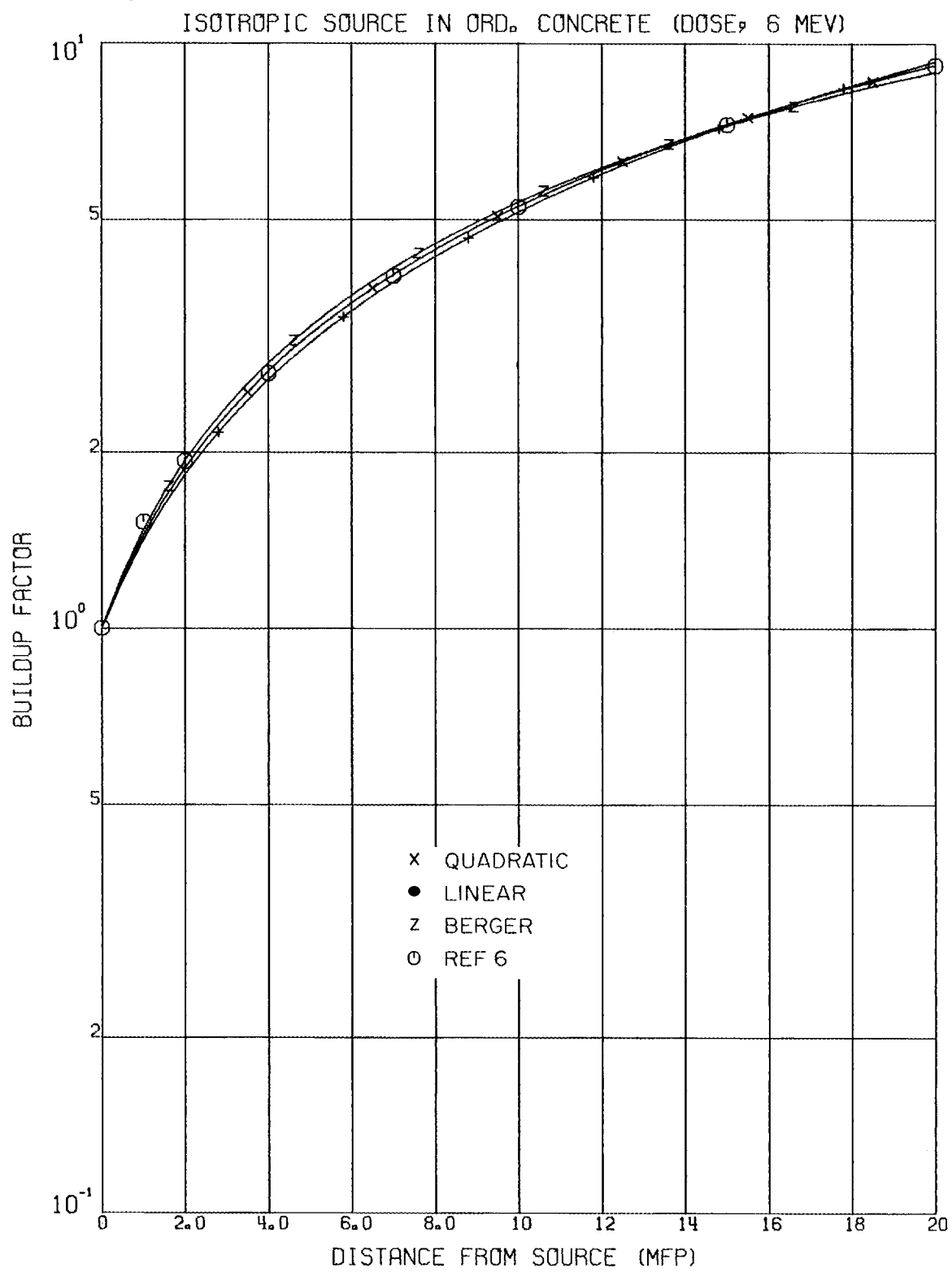


Fig. 35.

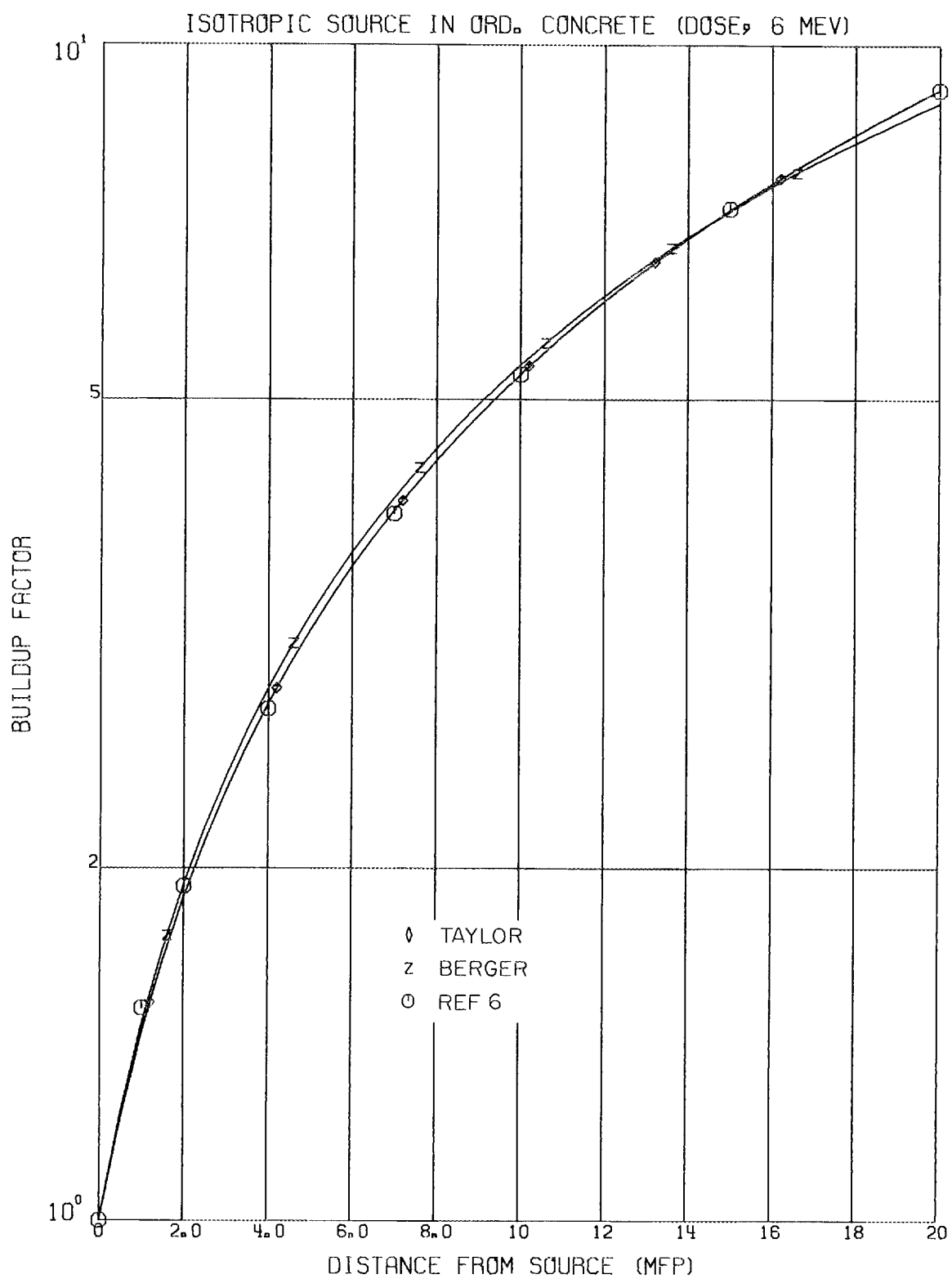


Fig. 36.

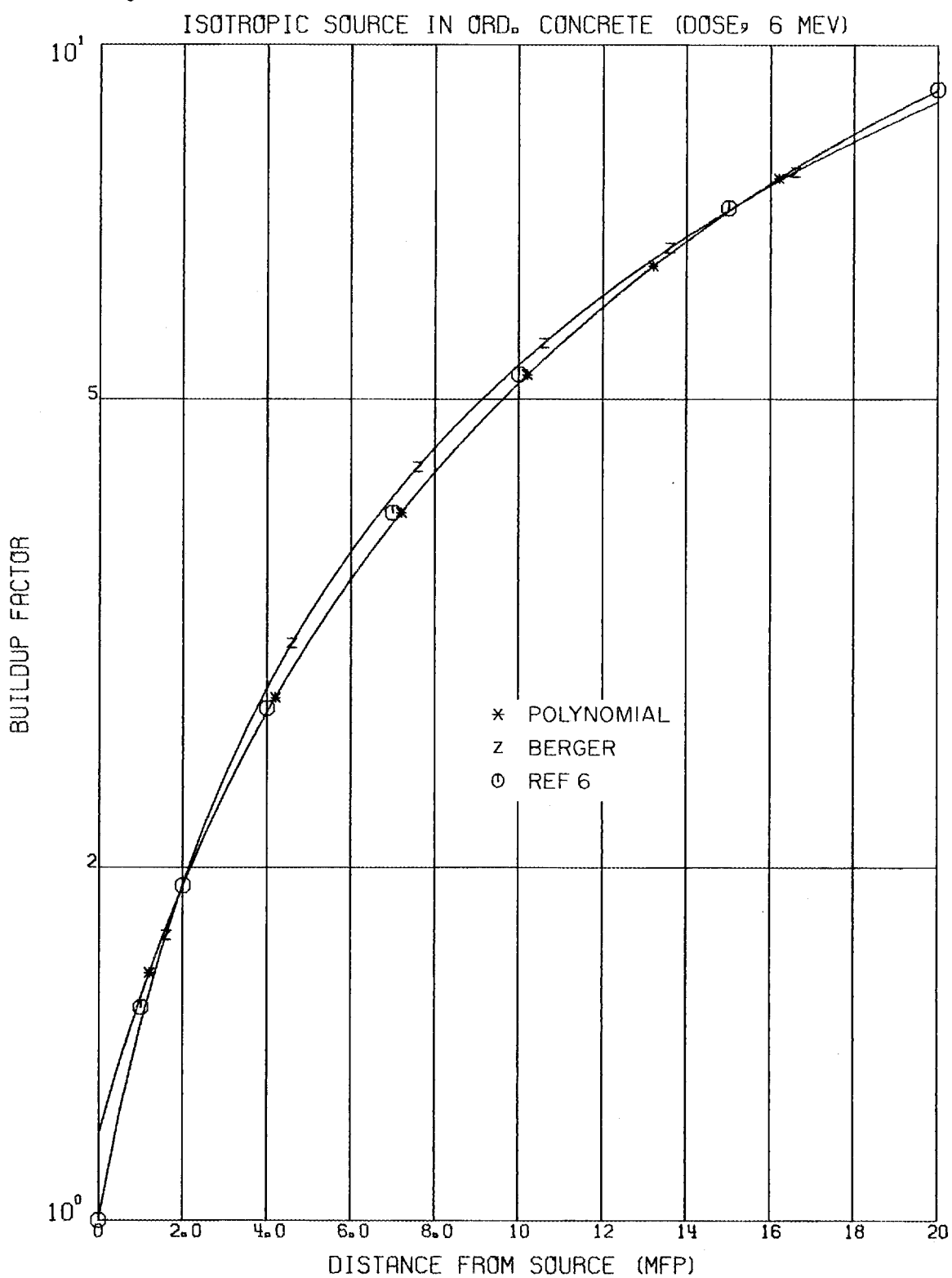


Fig. 37.

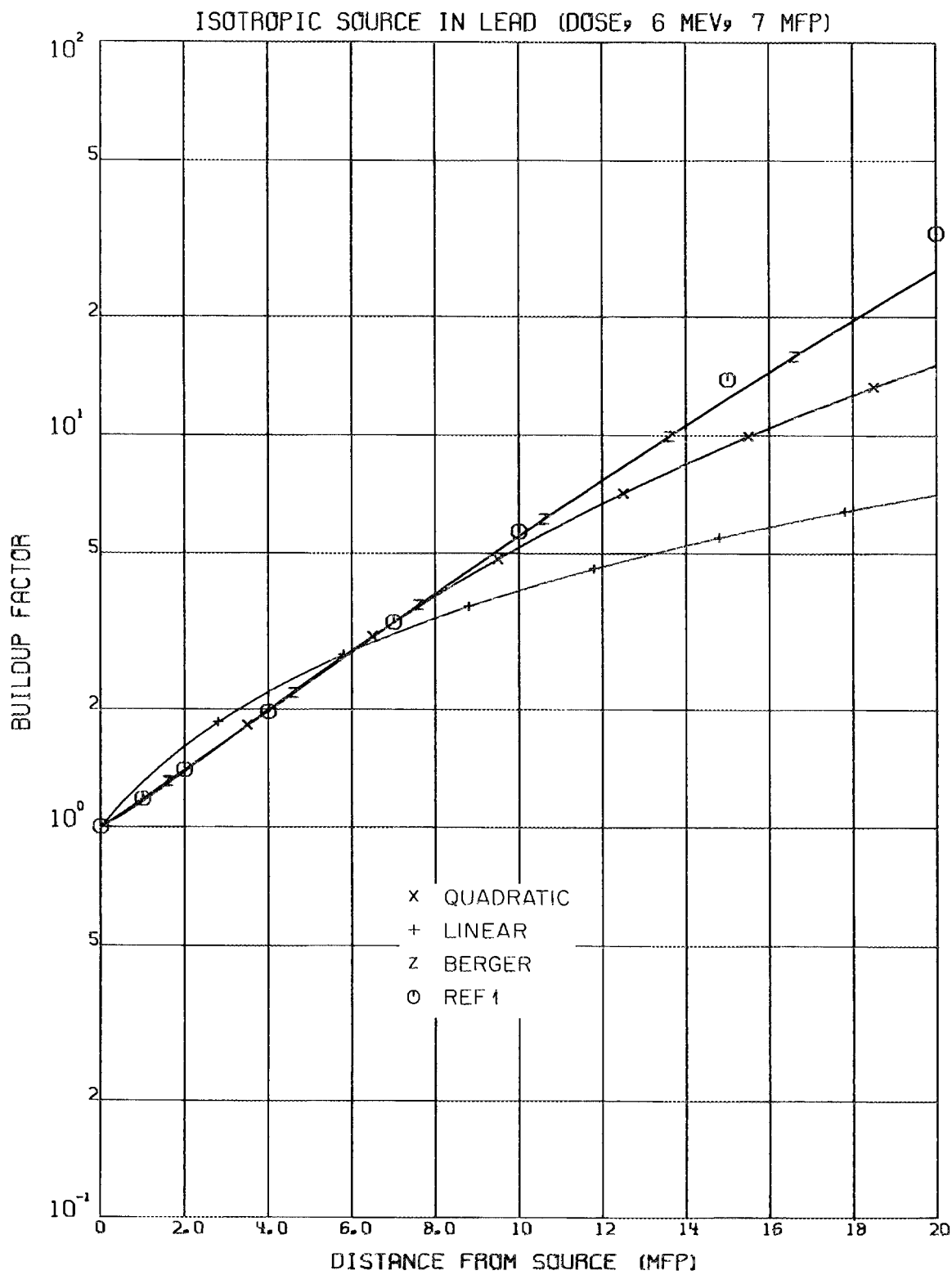


Fig. 38.

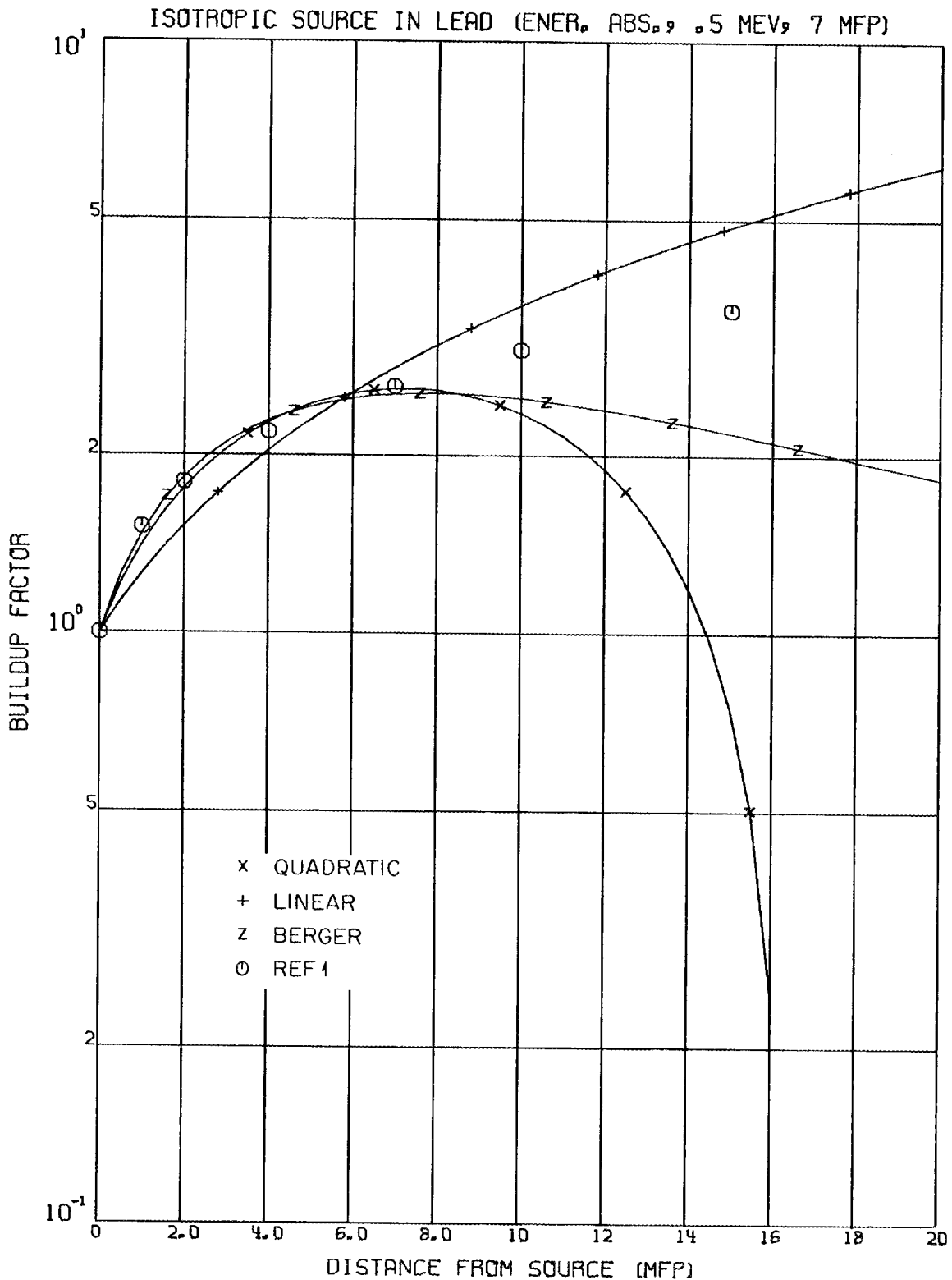


Table 1. Buscaglione-Manzini* Coefficients
for Taylor Dose Buildup Factor Formula

Material	E_0 (MeV)	A	$-\alpha_1$	α_2	Maximum Percent Deviation
Water	0.5	100.845	0.12687	- 0.10925	- 27.4 $\mu\text{x} = 10$
	1	19.601	0.09037	- 0.02522	- 10.8 $\mu\text{x} = 10$
	2	12.612	0.05320	0.01932	+ 4.2 $\mu\text{x} = 1$
	3	11.110	0.03550	0.03206	+ 1.7 $\mu\text{x} = 1$
	4	11.163	0.02543	0.03025	+ 0.8 $\mu\text{x} = 20$
	6	8.385	0.01820	0.04164	- 0.5 $\mu\text{x} = 2$
	8	4.635	0.02633	0.07097	+ 0.6 $\mu\text{x} = 7$
	10	3.545	0.02991	0.08717	- 0.7 $\mu\text{x} = 1$
Aluminum	0.5	38.911	0.10015	- 0.06312	- 12.2 $\mu\text{x} = 10$
	1	28.782	0.06820	- 0.02973	- 8.6 $\mu\text{x} = 10$
	2	16.981	0.04588	0.00271	- 5.2 $\mu\text{x} = 10$
	3	10.583	0.04066	0.02514	- 2.5 $\mu\text{x} = 10$
	4	7.526	0.03973	0.03860	+ 1.8 $\mu\text{x} = 20$
	6	5.713	0.03934	0.04347	+ 1.6 $\mu\text{x} = 20$
	8	4.716	0.03837	0.04431	- 1.3 $\mu\text{x} = 15$
	10	3.999	0.03900	0.04130	+ 1.2 $\mu\text{x} = 20$
Barytes Concrete	0.5	33.026	0.06129	- 0.02883	+ 7.5 $\mu\text{x} = 2$
	1	23.014	0.06255	- 0.02217	+ 8.9 $\mu\text{x} = 20$
	2	9.350	0.05700	0.03850	+ 9.0 $\mu\text{x} = 2$
	3	6.269	0.06064	0.04440	+ 4.8 $\mu\text{x} = 20$
	4	4.730	0.06500	0.05883	+ 4.8 $\mu\text{x} = 2$
	6	3.240	0.08000	0.06407	+ 5.0 $\mu\text{x} = 2$
	8	2.167	0.09514	0.07857	+ 1.3 $\mu\text{x} = 20$
	10	1.433	0.11201	0.13021	+ 3.2 $\mu\text{x} = 20$

*Taken from Ref. 5.

Table 1 (continued)

Material	E_0 (MeV)	A	$-\alpha_1$	α_2	Maximum Percent Deviation
Ferrophos- phorous Concrete	0.5	61.341	0.07292	- 0.05265	+ 11.0 $\mu x = 2$
	1	46.087	0.05202	- 0.02845	+ 10.3 $\mu x = 2$
	2	14.790	0.04720	0.00867	+ 3.0 $\mu x = 2$
	3	10.399	0.04290	0.02211	+ 2.6 $\mu x = 20$
	4	6.240	0.05280	0.03765	+ 1.7 $\mu x = 2$
	6	4.425	0.05880	0.04262	- 1.0 $\mu x = 2$
	8	3.000	0.06750	0.05730	+ 0.8 $\mu x = 4$
Ordinary Concrete	10	2.279	0.07575	0.06438	+ 0.4 $\mu x = 6$
	0.5*	38.225	0.14824	- 0.10579	- 7.5 $\mu x = 4$
	1	25.507	0.07230	- 0.01843	+ 11.1 $\mu x = 2$
	2	18.089	0.04250	0.00849	+ 4.9 $\mu x = 2$
	3	13.640	0.03200	0.02022	+ 4.3 $\mu x = 2$
	4	11.460	0.02600	0.02450	- 5.1 $\mu x = 2$
	6	10.781	0.01520	0.02925	- 2.7 $\mu x = 2$
Magnetite Concrete	8	8.972	0.01300	0.02979	- 3.7 $\mu x = 2$
	10	4.015	0.02880	0.06844	- 2.2 $\mu x = 2$
	0.5	75.471	0.07479	- 0.05534	+ 15.9 $\mu x = 2$
	1	49.916	0.05195	- 0.02796	+ 11.5 $\mu x = 2$
	2	14.260	0.04692	0.01531	+ 4.0 $\mu x = 2$
	3	8.160	0.04700	0.04590	+ 5.0 $\mu x = 2$
	4	5.580	0.05200	0.05728	+ 2.7 $\mu x = 2$
	6	3.437	0.06000	0.11520	+ 4.3 $\mu x = 4$
	8	2.480	0.06645	0.14002	+ 4.0 $\mu x = 20$
	10	1.743	0.08082	0.27209	+ 5.3 $\mu x = 20$

*For some materials, the values of the buildup factor for given energies are known only in the interval of $1 \leq \mu x \leq 15$. In these cases, designated by an asterisk, the parameters are valid up to $\mu x = 15$.

Table 1 (continued)

Material	E_0 (MeV)	A	α_1	α_2	Maximum Percent Deviation
Iron	0.5	31.379	0.06842	- 0.03742	- 6.5 $\mu x = 10$
	1	24.957	0.06086	- 0.02463	- 6.4 $\mu x = 10$
	2	17.622	0.04627	- 0.00526	+ 4.0 $\mu x = 2$
	3	13.218	0.04431	- 0.00087	- 3.0 $\mu x = 10$
	4	9.624	0.04698	0.00175	- 2.7 $\mu x = 10$
	6	5.867	0.06150	- 0.00186	+ 2.1 $\mu x = 20$
	8	3.243	0.07500	0.02123	+ 3.8 $\mu x = 4$
	10	1.747	0.09900	0.06627	+ 3.7 $\mu x = 2$
Lead	0.5*	1.677	0.303084	0.30941	- 0.8 $\mu x = 10$
	1	2.984	0.35503	0.13486	- 1.0 $\mu x = 1$
	2	5.421	0.3482	0.04379	- 0.6 $\mu x = 1$
	3	5.580	0.05422	0.00611	+ 1.3 $\mu x = 4$
	4	3.897	0.08468	- 0.02383	+ 1.4 $\mu x = 20$
	6	0.926	0.17860	- 0.04635	+ 1.3 $\mu x = 20$
	8	0.368	0.23691	- 0.05684	+ 1.8 $\mu x = 15$
	10	0.311	0.24024	- 0.02783	- 0.5 $\mu x = 1$
Tin	0.5*	11.440	0.01800	0.03187	- 1.6 $\mu x = 1$
	1	11.426	0.04266	0.01606	- 2.6 $\mu x = 10$
	2	8.783	0.05349	0.01505	- 2.8 $\mu x = 10$
	3	5.400	0.07440	0.02080	+ 4.3 $\mu x = 20$
	4	3.496	0.09517	0.02598	- 3.9 $\mu x = 10$
	6	2.005	0.13733	- 0.01501	- 2.8 $\mu x = 10$
	8	1.101	0.17288	- 0.01787	- 3.4 $\mu x = 15$
	10	0.708	0.19200	0.01552	+ 2.6 $\mu x = 15$

Table 1 (continued)

Material	E_0 (MeV)	A	$-\alpha_1$	α_2	Maximum Percent Deviation
Tungsten	0.5*	2.655	0.01740	0.11340	- 4.9 $\mu x = 2$
	1*	3.234	0.04754	0.13058	- 0.9 $\mu x = 10$
	2*	3.504	0.06053	0.08862	+ 2.1 $\mu x = 10$
	3	4.722	0.06468	0.01404	- 2.4 $\mu x = 10$
	4	5.520	0.08857	- 0.04570	+ 1.3 $\mu x = 20$
	6	1.273	0.17257	- 0.12178	- 2.9 $\mu x = 15$
	8	0.664	0.20710	0.04692	+ 1.4 $\mu x = 10$
	10	0.509	0.21743	0.05025	- 3.6 $\mu x = 15$
Uranium	0.5*	1.444	0.02459	0.35167	- 0.9 $\mu x = 10$
	1*	2.081	0.03862	0.22639	- 0.7 $\mu x = 10$
	2*	3.287	0.03997	0.08635	- 0.5 $\mu x = 1$
	3	4.883	0.04950	0.00981	- 0.9 $\mu x = 15$
	4	2.800	0.08240	0.00370	+ 1.4 $\mu x = 4$
	6	0.975	0.15886	0.21101	- 2.2 $\mu x = 15$
	8	0.602	0.19189	0.02774	- 2.1 $\mu x = 15$
	10	0.399	0.21314	0.02083	- 2.9 $\mu x = 15$

Table 2. Buscaglione-Manzini* Coefficients
for Taylor Energy Buildup Factor Formula

Material	E_0 (MeV)	A	$-\alpha_1$	α_2	Maximum Percent Deviation
Water	0.5	59.611	0.12428	- 0.09466	- 22.6 $\mu x = 10$
	1	27.060	0.07840	- 0.03349	- 9.8 $\mu x = 10$
	2	17.430	0.04200	0.00288	+ 3.6 $\mu x = 1$
	3	11.954	0.02907	0.02267	- 1.3 $\mu x = 10$
	4	10.661	0.02222	0.02525	- 0.9 $\mu x = 15$
	6	7.171	0.01902	0.03677	- 4.9 $\mu x = 15$
	8	4.155	0.02590	0.05620	- 2.4 $\mu x = 10$
	10	3.509	0.02551	0.06816	- 0.4 $\mu x = 2$
Aluminum	0.5	42.081	0.10038	- 0.06388	- 12.7 $\mu x = 10$
	1	42.465	0.06329	- 0.03789	- 8.2 $\mu x = 10$
	2	26.516	0.03597	- 0.00877	- 4.5 $\mu x = 10$
	3	15.260	0.02925	0.00785	+ 2.2 $\mu x = 1$
	4	8.308	0.03193	0.02497	+ 1.3 $\mu x = 2$
	6	5.776	0.03337	0.03121	+ 1.1 $\mu x = 20$
	8	4.347	0.03483	0.03632	- 1.1 $\mu x = 15$
	10	3.704	0.03592	0.03448	+ 1.0 $\mu x = 20$
Iron	0.5	36.479	0.06602	- 0.03800	- 6.3 $\mu x = 10$
	1	24.481	0.06061	- 0.02470	- 6.6 $\mu x = 10$
	2	16.610	0.04527	- 0.00728	- 4.3 $\mu x = 10$
	3	12.481	0.04205	- 0.00236	- 3.0 $\mu x = 2$
	4	9.929	0.04270	- 0.00256	+ 2.3 $\mu x = 20$
	6	4.893	0.05913	- 0.00100	- 1.7 $\mu x = 10$
	8	3.209	0.06900	- 0.00124	+ 1.8 $\mu x = 20$
	10	2.981	0.07040	- 0.01575	- 4.9 $\mu x = 15$

*Taken from Ref. 5.

Table 2 (continued)

Material	E_0 (MeV)	A	$-\alpha_1$	α_2	Maximum Percent Deviation
Lead	0.5*	2.025	0.01330	0.19040	+ 5.9 $\mu x = 15$
	1	3.568	0.02163	0.10900	- 2.3 $\mu x = 10$
	2	4.709	0.03641	0.04723	+ 0.6 $\mu x = 2$
	3	4.804	0.04389	0.00722	- 1.2 $\mu x = 15$
	4	3.729	0.08084	- 0.02992	+ 0.9 $\mu x = 20$
	6	0.842	0.17000	0.05092	- 0.5 $\mu x = 15$
	8	0.424	0.21074	- 0.01158	+ 0.6 $\mu x = 10$
	10	0.261	0.23120	- 0.01945	+ 1.1 $\mu x = 10$
Tin	0.5*	11.480	0.01840	0.03032	- 2.2 $\mu x = 1$
	1	21.114	0.03087	- 0.00142	- 2.2 $\mu x = 10$
	2	21.746	0.03512	- 0.01200	- 2.0 $\mu x = 10$
	3	11.330	0.05340	- 0.02047	+ 2.7 $\mu x = 4$
	4	3.960	0.08299	- 0.00222	- 2.6 $\mu x = 10$
	6	4.413	0.11038	- 0.08251	- 1.4 $\mu x = 15$
	8	0.897	0.16669	+ 0.01782	- 2.6 $\mu x = 15$
	10	0.560	0.18746	- 0.00962	- 2.8 $\mu x = 15$
Tungsten	0.5*	1.877	0.03373	0.26061	- 0.6 $\mu x = 10$
	1*	4.120	0.03403	0.08757	- 1.1 $\mu x = 1$
	2*	5.986	0.03776	0.03098	- 0.5 $\mu x = 1$
	3	4.400	0.06240	0.01135	+ 1.7 $\mu x = 20$
	4	2.200	0.10700	0.01520	+ 2.6 $\mu x = 2$
	6	0.931	0.17044	0.14967	- 2.4 $\mu x = 15$
	8	0.561	0.19800	0.02843	+ 1.3 $\mu x = 10$
	10	0.386	0.21250	0.01112	- 3.2 $\mu x = 15$

*For some materials, the values of the buildup factor for given energies are known only in the interval of $1 \leq \mu x \leq 15$. In these cases, designated by an asterisk, the parameters are valid up to $\mu x = 15$.

Table 2 (continued)

Material	E_0 (MeV)	A	α_1	α_2	Maximum Percent Deviation	
Uranium	0.5*	1.492	0.02146	0.30891	-	0.7 $\mu x = 10$
	1*	2.052	0.03814	0.22109	-	0.9 $\mu x = 1$
	2*	2.600	0.04760	0.10850	-	1.8 $\mu x = 10$
	3	4.000	0.05110	0.01453	+	1.1 $\mu x = 20$
	4	2.166	0.08506	0.01540	-	1.2 $\mu x = 15$
	6	0.859	0.15319	0.03797	-	1.3 $\mu x = 15$
	8	0.593	0.17773	0.08500	-	2.5 $\mu x = 2$
	10	0.378	0.19927	0.02658	+	2.7 $\mu x = 10$

Table 3. Buscaglione-Manzini* Coefficients for Taylor Energy Absorption Buildup Factor Formula

Material	E_0 (MeV)	A	$-\alpha_1$	α_2	Maximum Percent Deviation
Water	0.5	40.006	0.13587	- 0.09220	- 24.1 $\mu x = 10$
	1	34.852	0.08000	- 0.04377	- 12.2 $\mu x = 10$
	2	23.002	0.04050	- 0.00080	- 4.8 $\mu x = 10$
	3	16.326	0.02728	0.02080	+ 1.5 $\mu x = 1$
	4	11.330	0.02527	0.03027	+ 1.0 $\mu x = 20$
	6	6.280	0.02610	0.05658	+ 0.6 $\mu x = 2$
	8	4.314	0.02914	0.07839	- 0.7 $\mu x = 15$
	10	3.610	0.02790	0.07990	- 0.7 $\mu x = 15$
Aluminum	0.5	74.220	0.09940	- 0.07640	- 13.5 $\mu x = 10$
	1	52.022	0.06395	- 0.04023	- 8.8 $\mu x = 7$
	2	34.530	0.03599	- 0.01068	+ 5.5 $\mu x = 1$
	3	28.581	0.02343	0.00073	+ 2.2 $\mu x = 1$
	4	25.364	0.01800	0.00361	+ 1.4 $\mu x = 20$
	6	19.777	0.01543	0.00516	- 0.9 $\mu x = 15$
	8	17.528	0.01421	0.00366	- 0.9 $\mu x = 15$
	10	12.407	0.01695	0.00351	- 0.8 $\mu x = 15$
Iron	0.5	39.556	0.07500	- 0.02957	- 7.1 $\mu x = 10$
	1	27.213	0.06496	- 0.01828	+ 6.5 $\mu x = 1$
	2	19.705	0.04569	- 0.00509	- 4.0 $\mu x = 10$
	3	13.398	0.04425	0.00092	- 2.9 $\mu x = 10$
	4	9.261	0.04952	0.00027	- 2.0 $\mu x = 10$
	6	5.052	0.06040	0.00135	+ 2.0 $\mu x = 20$
	8	3.875	0.06504	- 0.01237	- 1.4 $\mu x = 10$
	10	3.101	0.07561	- 0.03359	+ 1.0 $\mu x = 1$
Lead	0.5**	2.030	0.03739	0.50644	- 2.2 $\mu x = 10$
	1	4.192	0.04258	0.18642	- 2.0 $\mu x = 1$
	2	6.502	0.03746	0.05634	- 2.0 $\mu x = 1$
	3	7.194	0.04800	0.00000	- 1.2 $\mu x = 1$
	4	2.529	0.09087	0.00000	- 1.2 $\mu x = 15$
	6	0.772	0.16600	0.03822	- 0.8 $\mu x = 1$
	8	0.381	0.20345	0.00000	- 1.6 $\mu x = 2$
	10	0.171	0.23500	- 0.03151	- 0.7 $\mu x = 1$
Tin	0.5	8.405	0.05137	0.11076	- 1.4 $\mu x = 15$
	1	18.518	0.03995	0.02011	- 2.6 $\mu x = 15$
	2	14.587	0.04623	0.00774	- 3.9 $\mu x = 10$
	3	18.534	0.04851	- 0.02219	- 9.2 $\mu x = 15$
	4	11.319	0.06551	- 0.03733	- 8.4 $\mu x = 15$
	6	1.667	0.12900	- 0.01058	- 2.2 $\mu x = 7$
	8	0.841	0.16056	0.00000	- 2.0 $\mu x = 15$
	10	0.637	0.17284	0.04633	- 1.3 $\mu x = 15$

*Taken from Ref. 5.

**For some materials, the values of the buildup factor for given energies are known only in the interval of $1 \leq \mu x \leq 15$. In these cases, designated by an asterisk, the parameters are valid up to $\mu x = 15$.

Table 4. Buscaglione-Manzini** Polynomial Coefficients for the Dose Buildup Factor in Various Concretes

E Mev	β_0	β_1	β_2	β_3	Δ_{\max} %	$\Delta\%$
Ordinary concrete						
1	5.1902(-1)	1.6152(0)	5.4702(-2)	1.8803(-3)	-3.6 $\mu x=4^*$	1.8
2	7.7342(-1)	9.1835(-1)	2.7260(-2)	-3.9911(-4)	1.2 $\mu x=2$	0.4
3	1.0530(0)	6.3743(-1)	1.6185(-2)	-3.8875(-4)	-3.9 $\mu x=2$	1.2
4	1.1506(0)	4.9800(-1)	1.0547(-2)	-2.9613(-4)	-1.9 $\mu x=8$	0.8
5	1.1806(0)	4.1634(-1)	7.2376(-3)	-2.2268(-4)	2.8 $\mu x=2$	1.3
6	1.1846(0)	3.6314(-1)	5.0942(-3)	-1.6888(-4)	2.1 $\mu x=8$	0.9
7	1.1784(0)	3.2590(-1)	3.6051(-1)	-1.2895(-4)	-1.3 $\mu x=4$	0.4
Magnetite concrete						
1	5.2780(-1)	1.1562(0)	9.7936(-2)	-1.4084(-3)	1.8 $\mu x=20$	0.8
2	9.3721(-1)	8.0638(-1)	3.1686(-2)	-4.9503(-4)	1.5 $\mu x=8$	0.6
3	9.5856(-1)	6.5113(-1)	1.3680(-2)	-2.0725(-4)	-1.6 $\mu x=4$	0.6
4	9.7216(-1)	5.3998(-1)	7.8749(-3)	-1.0316(-4)	-2.3 $\mu x=10$	1.7
5	9.8690(-1)	4.5747(-1)	5.8668(-3)	-6.0375(-5)	1.8 $\mu x=10$	1.0
6	1.0010(0)	3.9452(-1)	5.2611(-3)	-4.1859(-5)	3.0 $\mu x=10$	2.3
7	1.0237(0)	3.4521(-1)	5.2272(-3)	-3.4147(-5)	2.6 $\mu x=8$	1.4
Ferrophosphorus concrete						
1	5.2446(-1)	1.1570(0)	6.6197(-2)	-2.6909(-4)	1.4 $\mu x=10$	0.7
2	9.0796(-1)	8.0470(-1)	2.4051(-2)	-1.3747(-4)	1.4 $\mu x=20$	0.5
3	9.7879(-1)	6.3258(-1)	1.3122(-2)	-2.8460(-5)	-3.6 $\mu x=20$	1.1
4	9.9224(-1)	5.2504(-1)	8.2727(-3)	8.2210(-5)	-2.0 $\mu x=12$	1.5
5	9.9175(-1)	4.5156(-1)	5.5458(-3)	1.7478(-4)	2.6 $\mu x=20$	1.0
6	9.8751(-1)	3.9831(-1)	3.7988(-3)	2.4954(-4)	3.3 $\mu x=20$	2.4
7	9.8244(-1)	3.5799(-1)	2.5837(-3)	3.1005(-4)	2.4 $\mu x=6$	1.6
Barytes concrete						
1	1.4863(0)	4.2184(-1)	1.3686(-1)	-2.7616(-3)	2.1 $\mu x=4$	1.0
2	1.0139(0)	6.7003(-1)	3.5826(-2)	-5.2672(-4)	2.2 $\mu x=8$	1.1
3	9.3467(-1)	5.9469(-1)	2.0106(-2)	-2.9295(-4)	-5.4 $\mu x=6$	2.6
4	9.1379(-1)	5.1277(-1)	1.3442(-2)	-5.0691(-5)	-3.8 $\mu x=14$	2.2
5	9.0721(-1)	4.4778(-1)	9.2573(-3)	1.8044(-4)	2.4 $\mu x=8$	1.5
6	9.0525(-1)	3.9750(-1)	6.2307(-3)	3.8250(-4)	5.3 $\mu x=8$	3.8
7	9.0500(-1)	3.5806(-1)	3.8974(-3)	5.5449(-4)	4.0 $\mu x=8$	2.9

*This value of μx is the value for which this error is valid.

**Taken from Ref. 11.

Table 5. Linear, Quadratic and Berger Coefficients
for Dose Buildup Formulas Fitted over the Range
(0-7 MFP)

Table 5 (cont.)

WATER
DOSE BUILDUP
POINT ISOTROPIC SOURCE
7 MFP FIT

E(MEV)	A1	MAXIMUM ERROR	A2	B	MAXIMUM ERROR	C	D	MAXIMUM ERROR
0.255	8.6524	F3.1	-.2525	1.4984	30%	1.7506	0.2609	10%
0.5	4.6800	F2.3	0.6684	0.6750	8%	1.3245	0.2078	5%
1.	1.9953	40%	1.0053	0.1666	2%	1.0622	0.1052	3%
2.	1.0301	10%	0.8242	0.0346	2%	0.8093	0.0408	1%
3.	0.7397	3%	0.6962	0.0073	1%	0.6876	0.0125	1%
4.	0.5884	1%	0.5801	0.0014	1%	0.5800	0.0024	1%
6.	0.4321	3%	0.4616	-.0050	1%	0.4655	-.0126	1%
8.	0.3406	4%	0.3782	-.0063	1%	0.3860	-.0214	1%
10.	0.2877	4%	0.3251	-.0063	1%	0.3342	-.0257	1%

ALUMINUM
DOSE BUILDUP
POINT ISOTROPIC SOURCE
7 MFP FIT

E(MEV)	A1	MAXIMUM ERROR	A2	B	MAXIMUM ERROR	C	D	MAXIMUM ERROR
0.5	2.6461	F1.5	1.0688	0.2654	2%	1.2435	0.1250	3%
1.	1.6089	30%	0.9316	0.1140	2%	0.9589	0.0864	3%
2.	0.9686	13%	0.7437	0.0378	2%	0.7267	0.0486	2%
3.	0.7197	5%	0.6355	0.0142	1%	0.6294	0.0227	1%
4.	0.5663	3%	0.5284	0.0064	1%	0.5253	0.0127	1%
6.	0.4334	2%	0.4142	0.0032	1%	0.4177	0.0061	1%
8.	0.3476	1%	0.3346	0.0022	1%	0.3371	0.0050	1%
10.	0.2847	2%	0.2715	0.0022	1%	0.2752	0.0055	1%

F3.1 MEANS FACTOR OF 3.1

Table 5 (cont.)

IRON
DOSE BUILDUP
POINT ISOTROPIC SOURCE
7 MFP FIT

E(MEV)	MAXIMUM		A2	MAXIMUM		C	D	MAXIMUM
	A1	ERROR		B	ERROR			
0.5	1.4283	25%	0.8642	0.0949	1%	0.9081	0.0752	2%
1.	1.2373	20%	0.8026	0.0731	1%	0.8214	0.0684	2%
2.	0.8556	12%	0.6526	0.0342	5%	0.7020	0.0319	3%
3.	0.6691	9%	0.5338	0.0228	1%	0.5323	0.0384	1%
4.	0.5403	7%	0.4366	0.0175	1%	0.4366	0.0358	1%
6.	0.4297	8%	0.3237	0.0178	1%	0.3271	0.0457	1%
8.	0.3391	8%	0.2473	0.0154	1%	0.2563	0.0464	1%
10.	0.2681	8%	0.1785	0.0151	1%	0.1876	0.0592	1%

TIN
DOSE BUILDUP
POINT ISOTROPIC SOURCE
7 MFP FIT

E(MEV)	MAXIMUM		A2	MAXIMUM		C	D	MAXIMUM
	A1	ERROR		B	ERROR			
0.5	0.5153	3%	0.5479	-0.0055	2%	0.5608	-0.0146	1%
1.	0.7199	6%	0.6153	0.0176	1%	0.6219	0.0244	1%
2.	0.6731	8%	0.5455	0.0215	1%	0.5498	0.0338	1%
3.	0.5837	11%	0.4284	0.0261	1%	0.4379	0.0479	1%
4.	0.5146	12%	0.3420	0.0290	1%	0.3583	0.0601	1%
6.	0.4153	17%	0.2082	0.0348	2%	0.2369	0.0925	1%
8.	0.3317	17%	0.1371	0.0327	2%	0.1692	0.1103	1%
10.	0.2550	16%	0.0945	0.0270	2%	0.1232	0.1190	1%

F3.1 MEANS FACTOR OF 3.1

Table 5 (cont.)

TUNGSTEN
DOSE BUILDUP
POINT ISOTROPIC SOURCE
7 MFP FIT

E(MEV)	A1	MAXIMUM ERROR	A2	B	MAXIMUM ERROR	C	D	MAXIMUM ERROR
0.5	0.1903	8%	0.2692	-.0133	2%	0.2938	-.0751	2%
1.	0.3817	5%	0.4269	-.0076	2%	0.4425	-.0255	1%
2.	0.4376	2%	0.4164	0.0036	1%	0.4172	0.0080	1%
3.	0.4171	5%	0.3515	0.0110	1%	0.3501	0.0295	1%
4.	0.4054	12%	0.2540	0.0255	1%	0.2710	0.0666	1%
6.	0.3363	17%	0.1435	0.0324	2%	0.1771	0.1049	1%
8.	0.2624	16%	0.0957	0.0281	2%	0.1245	0.1223	1%
10.	0.2073	14%	0.0748	0.0223	2%	0.0974	0.1238	1%

LEAD
DOSE BUILDUP
POINT ISOTROPIC SOURCE
7 MFP FIT

E(MEV)	A1	MAXIMUM ERROR	A2	B	MAXIMUM ERROR	C	D	MAXIMUM ERROR
0.5	0.1549	8%	0.2273	-.0122	3%	0.2526	-.0848	2%
1.	0.2990	6%	0.3613	-.0105	2%	0.3779	-.0403	1%
2.	0.3796	1%	0.3787	0.0001	1%	0.3862	0.0032	1%
3.	0.3810	5%	0.3164	0.0109	1%	0.3267	0.0253	1%
4.	0.3523	10%	0.2389	0.0191	1%	0.2530	0.0547	1%
5.1	0.3219	13%	0.1747	0.0248	1%	0.1936	0.0839	1%
6.	0.3034	15%	0.1346	0.0284	2%	0.1622	0.1027	1%
8.	0.2419	15%	0.0894	0.0257	3%	0.1220	0.1112	2%
10.	0.1933	13%	0.0642	0.0217	3%	0.0939	0.1167	2%

F3.1 MEANS FACTOR OF 3.1

Table 5 (cont.)

URANIUM
DOSE BUILDUP
POINT ISOTROPIC SOURCE
7 MFP FIT

E(MEV)	A1	MAXIMUM ERROR	A2	B	MAXIMUM ERROR	C	D	MAXIMUM ERROR
0.5	0.1054	7%	0.1637	-0.0098	2%	0.1825	-0.0951	2%
1.	0.2264	7%	0.2990	-0.0122	2%	0.3204	-0.0599	2%
2.	0.3023	3%	0.3250	-0.0038	1%	0.3321	-0.0162	1%
3.	0.3169	4%	0.2760	0.0069	1%	0.2814	0.0196	1%
4.	0.3010	7%	0.2199	0.0136	1%	0.2283	0.0458	1%
6.	0.2571	12%	0.1314	0.0212	1%	0.1476	0.0916	1%
8.	0.2081	12%	0.0885	0.0201	1%	0.1081	0.1076	1%
10.	0.1621	11%	0.0638	0.0165	1%	0.0798	0.1163	1%

F3.1 MEANS FACTOR OF 3.1

Table 5 (cont.)

ORDINARY CONCRETE
DOSE BUILDUP
POINT ISOTROPIC SOURCE
7 MFP FIT

E(MEV)	A1	MAXIMUM ERROR	A2	B	MAXIMUM ERROR	C	D	MAXIMUM ERROR
0.5	3.7443	30%	1.3563	0.4018	7%	1.4489	0.1586	10%
1.	1.9057	40%	1.0980	0.1359	7%	1.0448	0.1014	7%
2.	1.0226	12%	0.8238	0.0335	2%	0.8062	0.0403	2%
3.	0.7303	7%	0.6189	0.0187	1%	0.6267	0.0254	1%
4.	0.5736	5%	0.6106	-.0062	3%	0.6451	-.0207	3%
6.	0.4329	6%	0.4667	-.0057	4%	0.5086	-.0286	3%
8.	0.3376	6%	0.3794	-.0070	3%	0.4085	-.0334	2%
10.	0.2923	5%	0.3344	-.0071	3%	0.3584	-.0356	2%

FERROPHOSPHOROUS CONCRETE
DOSE BUILDUP
POINT ISOTROPIC SOURCE
7 MFP FIT

E(MEV)	A1	MAXIMUM ERROR	A2	B	MAXIMUM ERROR	C	D	MAXIMUM ERROR
0.5	1.9407	1.5	0.9330	0.1696	8%	0.9059	0.1283	8%
1.	1.4657	30%	0.8542	0.1029	3%	0.8467	0.0921	5%
2.	0.9264	10%	0.7481	0.0300	2%	0.7327	0.0397	2%
3.	0.6996	4%	0.6198	0.0134	1%	0.6331	0.0164	1%
4.	0.5611	6%	0.4980	0.0106	2%	0.4879	0.0237	2%
6.	0.4399	2%	0.4119	0.0047	2%	0.4346	0.0011	2%
8.	0.3493	2%	0.3243	0.0042	2%	0.3390	0.0043	2%
10.	0.2827	3%	0.2574	0.0043	1%	0.2563	0.0165	1%

F3.1 MEANS FACTOR OF 3.1

Table 5 (cont.)

MAGNETITE CONCRETE
DOSE BUILDUP
POINT ISOTROPIC SOURCE
7 MFP FIT

E(MEV)	A1	MAXIMUM ERROR	A2	B	MAXIMUM ERROR	C	D	MAXIMUM ERROR
0.5	2.3150	F1.5	0.9510	0.2295	3%	1.1049	0.1221	4%
1.	1.6021	33%	0.8847	0.1207	3%	0.9006	0.0965	4%
2.	0.9757	10%	0.7636	0.0357	2%	0.7770	0.0380	1%
3.	0.7110	5%	0.6163	0.0159	2%	0.6321	0.0194	1%
4.	0.5634	4%	0.5177	0.0077	1%	0.5241	0.0119	2%
6.	0.4410	2%	0.4200	0.0035	2%	0.4401	-0.0004	2%
8.	0.3391	2%	0.3127	0.0044	1%	0.3225	0.0080	1%
10.	0.2840	2%	0.2670	0.0029	1%	0.2682	0.0096	1%

BARYTES CONCRETE
DOSE BUILDUP
POINT ISOTROPIC SOURCE
7 MFP FIT

E(MEV)	A1	MAXIMUM ERROR	A2	B	MAXIMUM ERROR	C	D	MAXIMUM ERROR
0.5	1.4414	23%	0.8769	0.0950	2%	0.9313	0.0724	1%
1.	1.2066	21%	0.7599	0.0752	1%	0.7764	0.0737	2%
2.	0.8740	10%	0.6886	0.0312	1%	0.7006	0.0368	1%
3.	0.6556	6%	0.5345	0.0204	3%	0.5508	0.0289	2%
4.	0.5634	9%	0.4682	0.0160	3%	0.4413	0.0418	3%
6.	0.4571	10%	0.3344	0.0207	1%	0.3342	0.0525	2%
8.	0.3519	5%	0.2836	0.0115	1%	0.2901	0.0321	1%
10.	0.2684	7%	0.1894	0.0133	1%	0.1990	0.0495	1%

F3.1 MEANS FACTOR OF 3.1

Table 5 (cont.)

WATER
DOSE BUILDUP
PLANE COLLIMATED SOURCE
7 MFP FIT

E(MEV)	MAXIMUM ERROR		A2	MAXIMUM ERROR		C	D	MAXIMUM ERROR
	A1			B				
0.5	2.4773	40%	1.1802	0.2183	10%	1.4309	0.0894	3%
1.	1.4374	15%	1.0937	0.0578	5%	1.1664	0.0339	3%
2.	0.8420	3%	0.7946	0.0080	2%	0.8204	0.0038	2%
3.	0.6451	3%	0.6551	-.0017	2%	0.6797	-.0094	2%
4.	0.5239	4%	0.5579	-.0057	2%	0.5775	-.0170	2%
6.	0.4001	4%	0.4369	-.0062	2%	0.4522	-.0211	2%
8.	0.3151	4%	0.3546	-.0066	1%	0.3647	-.0251	1%

IRON
DOSE BUILDUP
PLANE COLLIMATED SOURCE
7 MFP FIT

E(MEV)	MAXIMUM ERROR		A2	MAXIMUM ERROR		C	D	MAXIMUM ERROR
	A1			B				
0.5	1.0229	4%	0.9218	0.0170	4%	1.0100	0.0006	4%
1.	0.9479	6%	0.8188	0.0217	5%	0.8737	0.0126	2%
2.	0.7171	4%	0.6491	0.0114	2%	0.6698	0.0110	1%
3.	0.5991	4%	0.5486	0.0085	2%	0.5633	0.0099	1%
4.	0.5050	6%	0.4434	0.0104	2%	0.4549	0.0169	2%
6.	0.3909	4%	0.3330	0.0097	1%	0.3399	0.0232	1%
8.	0.3134	5%	0.2535	0.0101	1%	0.2598	0.0311	1%
10.	0.2590	6%	0.1987	0.0101	1%	0.2081	0.0360	1%

F3.1 MEANS FACTOR OF 3.1

Table 5 (cont.)

TIN
DOSE BUILDUP
PLANE COLLIMATED SOURCE
7 MFP FIT

E(MEV)	A1	MAXIMUM ERROR	A2	B	MAXIMUM ERROR	C	D	MAXIMUM ERROR
1.	0.5999	4%	0.6208	-.0035	2%	0.6444	-.0127	2%
2.	0.5823	2%	0.5508	0.0053	2%	0.5676	0.0038	2%
4.	0.4560	7%	0.3640	0.0155	1%	0.3754	0.0322	1%
6.	0.3647	10%	0.2343	0.0219	1%	0.2524	0.0607	1%
10.	0.2367	11%	0.1184	0.0199	2%	0.1428	0.0822	1%

LEAD
DOSE BUILDUP
PLANE COLLIMATED SOURCE
7 MFP FIT

E(MEV)	A1	MAXIMUM ERROR	A2	B	MAXIMUM ERROR	C	D	MAXIMUM ERROR
0.5	0.1376	10%	0.2177	-.0135	3%	0.2511	-.1049	2%
1.	0.2723	10%	0.3633	-.0153	3%	0.3925	-.0632	2%
2.	0.3440	4%	0.3871	-.0073	2%	0.4041	-.0278	2%
3.	0.3616	2%	0.3481	0.0023	1%	0.3553	0.0026	1%
4.	0.3164	5%	0.2582	0.0098	1%	0.2682	0.0272	1%
6.	0.2609	10%	0.1512	0.0185	2%	0.1749	0.0650	2%
8.	0.2110	10%	0.1081	0.0173	2%	0.1272	0.0828	2%
10.	0.1663	10%	0.0848	0.0137	2%	0.1006	0.0821	2%

F3.1 MEANS FACTOR OF 3.1

Table 5 (cont.)

URANIUM
DOSE BUILDUP
PLANE COLLIMATED SOURCE
7 MFP FIT

E(MEV)	A1	MAXIMUM ERROR	A2	B	MAXIMUM ERROR	C	D	MAXIMUM ERROR
0.5	0.0961	7%	0.1582	-.0104	2%	0.1809	-.1101	2%
1.	0.2029	9%	0.2879	-.0143	3%	0.3137	-.0754	2%
2.	0.2751	5%	0.3228	-.0080	2%	0.3354	-.0340	1%
3.	0.2870	1%	0.2800	0.0012	1%	0.2867	-.0002	1%
4.	0.2699	4%	0.2307	0.0066	1%	0.2399	0.0191	1%
6.	0.2340	8%	0.1546	0.0134	1%	0.1675	0.0549	1%
8.	0.1834	8%	0.1017	0.0137	2%	0.1181	0.0717	2%
10.	0.1469	8%	0.0760	0.0119	2%	0.0903	0.0792	2%

F3.1 MEANS FACTOR OF 3.1

Table 6. Linear, Quadratic and Berger Coefficients
for Energy Absorption Buildup Formulas
Fitted over the Range (0-7 MFP)

Table 6 (cont.)

WATER
ENERGY ABSORPTION BUILDUP
POINT ISOTROPIC SOURCE
7 MFP FIT

E(MEV)	A1	MAXIMUM ERROR	A2	B	MAXIMUM ERROR	C	D	MAXIMUM ERROR
0.255	8.0956	F3	-1.1070	1.3802	25%	1.7033	0.2546	6%
0.5	4.3517	F2.2	0.6651	0.6203	8%	1.2727	0.2024	5%
1.	2.0650	44%	0.9832	0.1820	2%	1.0530	0.1122	4%
2.	1.0591	11%	0.8472	0.0357	2%	0.8300	0.0413	2%
3.	0.7881	3%	0.7445	0.0073	1%	0.7377	0.0113	1%
4.	0.5956	1%	0.5870	0.0014	1%	0.5881	0.0021	1%
6.	0.4306	2%	0.4576	-0.0045	1%	0.4608	-0.0116	1%
8.	0.3437	3%	0.3816	-0.0064	1%	0.3858	-0.0197	1%
10.	0.2741	3%	0.3075	-0.0056	1%	0.3150	-0.0238	1%

ALUMINUM
ENERGY ABSORPTION BUILDUP
POINT ISOTROPIC SOURCE
7 MFP FIT

E(MEV)	A1	MAXIMUM ERROR	A2	B	MAXIMUM ERROR	C	D	MAXIMUM ERROR
0.5	3.3193	F1.7	1.1996	0.3567	2%	1.4581	0.1360	4%
1.	1.8576	F1.4	1.0517	0.1356	2%	1.0825	0.0902	3%
2.	1.0487	14%	0.8059	0.0409	3%	0.7788	0.0505	3%
3.	0.7481	6%	0.6556	0.0156	1%	0.6496	0.0239	1%
4.	0.5719	3%	0.5336	0.0064	1%	0.5334	0.0117	1%
6.	0.4140	1%	0.3970	0.0029	1%	0.3981	0.0065	1%
8.	0.3191	1%	0.3063	0.0022	1%	0.3071	0.0064	1%
10.	0.2594	1%	0.2489	0.0018	1%	0.2496	0.0065	1%

F3.1 MEANS FACTOR OF 3.1

Table 6 (cont.)

IRON
ENERGY ABSORPTION BUILDUP
POINT ISOTROPIC SOURCE
7 MFP FIT

E(MEV)	A1	MAXIMUM ERROR			MAXIMUM ERROR	C	D	MAXIMUM ERROR
			A2	B				
0.5	2.5880	30%	1.5668	0.1718	3%	1.6700	0.0726	1%
1.	1.6936	23%	1.0932	0.1010	1%	1.1218	0.0687	2%
2.	0.9497	10%	0.7483	0.0339	1%	0.7551	0.0384	1%
3.	0.6970	9%	0.5592	0.0232	1%	0.5617	0.0362	1%
4.	0.5396	7%	0.4404	0.0167	1%	0.4393	0.0346	1%
6.	0.3741	7%	0.2850	0.0150	1%	0.2883	0.0436	1%
8.	0.2714	7%	0.1994	0.0121	1%	0.2020	0.0495	1%
10.	0.2179	7%	0.1501	0.0114	1%	0.1532	0.0588	1%

TIN
ENERGY ABSORPTION BUILDUP
POINT ISOTROPIC SOURCE
7 MFP FIT

E(MEV)	A1	MAXIMUM ERROR			MAXIMUM ERROR	C	D	MAXIMUM ERROR
			A2	B				
0.5	1.1016	7%	1.2165	-.0193	3%	1.2576	-.0229	2%
1.	1.1647	5%	1.0461	0.0200	3%	1.0833	0.0116	2%
2.	0.8939	10%	0.7123	0.0306	1%	0.7087	0.0390	1%
3.	0.6299	12%	0.4599	0.0286	1%	0.4672	0.0499	1%
4.	0.4684	12%	0.3158	0.0257	1%	0.3237	0.0617	1%
6.	0.3234	14%	0.1628	0.0270	2%	0.1901	0.0871	1%
8.	0.2261	11%	0.1108	0.0194	1%	0.1277	0.0941	1%
10.	0.1796	10%	0.0833	0.0162	1%	0.0990	0.0976	1%

F3.1 MEANS FACTOR OF 3.1

Table 6 (cont.)

LEAD
ENERGY ABSORPTION BUILDUP
POINT ISOTROPIC SOURCE
7 MFP FIT

E(MEV)	A1	MAXIMUM ERROR	A2	B	MAXIMUM ERROR	C	D	MAXIMUM ERROR
0.5	0.2591	20%	0.4407	-0.0305	7%	0.5384	-0.1282	4%
1.	0.5606	12%	0.7213	-0.0270	4%	0.7796	-0.0570	3%
2.	0.5320	4%	0.5553	-0.0039	2%	0.5748	-0.0136	2%
3.	0.3969	4%	0.3424	0.0092	1%	0.3568	0.0172	2%
4.	0.3047	8%	0.2126	0.0155	1%	0.2247	0.0502	1%
5.1	0.2607	10%	0.1555	0.0177	2%	0.1737	0.0665	1%
6.	0.2133	11%	0.1060	0.0181	2%	0.1248	0.0876	1%
8.	0.1570	9%	0.0711	0.0145	2%	0.0886	0.0930	1%
10.	0.1194	8%	0.0547	0.0109	2%	0.0698	0.0868	2%

F3.1 MEANS FACTOR OF 3.1

Table 7. Linear, Quadratic and Berger Coefficients
for Dose Buildup Formulas Fitted over the Range
(0-20 MFP)

Table 7 (cont.)

WATER
DOSE BUILDUP
POINT ISOTROPIC SOURCE
20 MFP FIT

E(MEV)	A1	MAXIMUM ERROR	A2	B	MAXIMUM ERROR	C	D	MAXIMUM ERROR
0.255	36.1015	F12	-12.9947	3.0515	F ∞	2.5048	0.1623	30%
0.5	13.0926	F5.6	-0.9744	0.8743	F3	1.8035	0.1224	25%
1.	3.4788	F2	1.1152	0.1469	6%	1.2282	0.0649	11%
2.	1.2549	25%	0.9173	0.0210	6%	0.8594	0.0240	5%
3.	0.7863	6%	0.7218	0.0040	2%	0.7004	0.0074	2%
4.	0.5951	1%	0.5907	0.0003	1%	0.5826	0.0014	1%
6.	0.4030	5%	0.4471	-0.0027	2%	0.4853	-0.0082	1%
8.	0.3085	7%	0.3561	-0.0038	2%	0.3741	-0.0124	2%
10.	0.2584	7%	0.3002	-0.0026	3%	0.3206	-0.0139	2%

ALUMINUM
DOSE BUILDUP
POINT ISOTROPIC SOURCE
20 MFP FIT

E(MEV)	A1	MAXIMUM ERROR	A2	B	MAXIMUM ERROR	C	D	MAXIMUM ERROR
0.5	5.7374	F3	0.6696	0.3150	20%	1.4412	0.0850	12%
1.	2.5385	F1.9	1.1185	0.0883	10%	1.0831	0.0535	9%
2.	1.1928	30%	0.8751	0.0197	8%	0.7869	0.0266	6%
3.	0.8061	12%	0.6812	0.0078	3%	0.6504	0.0137	3%
4.	0.6075	6%	0.5503	0.0036	2%	0.5343	0.0082	2%
6.	0.4626	6%	0.4252	0.0023	2%	0.4182	0.0063	1%
8.	0.3697	5%	0.3395	0.0019	1%	0.3366	0.0058	1%
10.	0.3087	5%	0.2750	0.0021	1%	0.2738	0.0074	1%

F3.1 MEANS FACTOR OF 3.1

Table 7 (cont.)

IRON
DOSE BUILDUP
POINT ISOTROPIC SOURCE
20 MFP FIT

E(MEV)	A1	MAXIMUM ERROR	A2	B	MAXIMUM ERROR	C	D	MAXIMUM ERROR
0.5	2.3773 F1.9		0.9019	0.0917	3%	0.9814	0.0548	7%
1.	1.8643 F1.6		0.9212	0.0586	7%	0.8932	0.0460	7%
2.	1.1194 33%		0.7423	0.0234	6%	0.7173	0.0277	4%
3.	0.8446 25%		0.5840	0.0162	4%	0.5571	0.0261	4%
4.	0.6942 25%		0.4605	0.0145	2%	0.4518	0.0268	3%
6.	0.6134 34%		0.3201	0.0182	1%	0.3381	0.0368	3%
8.	0.5245 40%		0.2207	0.0189	3%	0.2603	0.0428	2%
10.	0.4759 50%		0.1143	0.0225	6%	0.1902	0.0553	1%

TIN
DOSE BUILDUP
POINT ISOTROPIC SOURCE
20 MFP FIT

E(MEV)	A1	MAXIMUM ERROR	A2	B	MAXIMUM ERROR	C	D	MAXIMUM ERROR
0.5	0.5090 4%		0.5150	-.0005	3%	0.5457	-.0063	3%
1.	0.8495 18%		0.6666	0.0114	3%	0.6378	0.0180	3%
2.	0.8521 25%		0.5826	0.0168	3%	0.5678	0.0254	3%
3.	0.8509 40%		0.4254	0.0264	1%	0.4533	0.0388	3%
4.	0.8643 F1.58		0.2845	0.0360	5%	0.3700	0.0518	3%
6.	1.0786 F2.2		-.1374	0.0756	40%	0.2401	0.0891	2%
8.	1.1907 F2.8		-.4693	0.1032	F3	0.1669	0.1145	1%
10.	1.1075 F3.0		-.6523	0.1094	F12	0.1190	0.1278	5%

F3.1 MEANS FACTOR OF 3.1

Table 7 (cont.)

TUNGSTEN
DOSE BUILDUP
POINT ISOTROPIC SOURCE
20 MFP FIT

E(MEV)	A1	MAXIMUM ERROR	A2	B	MAXIMUM ERROR	C	D	MAXIMUM ERROR
0.5	0.1550	13%	0.2206	-.0054	5%	0.2692	-.0477	5%
1.	0.3382	9%	0.4149	-.0048	2%	0.4279	-.0150	2%
2.	0.4671	8%	0.4072	0.0037	3%	0.4163	0.0070	4%
3.	0.5919	30%	0.3255	0.0165	2%	0.3484	0.0324	2%
4.	0.8102 F1.8		0.0995	0.0442	15%	0.2727	0.0653	1%
6.	1.2616 F3		-.5462	0.1124	F4	0.1704	0.1160	2%
8.	1.3753 F3.5		-.9399	0.1439	F ∞	0.1161	0.1405	6%
10.	1.2730 F3.8		-.9502	0.1382	F ∞	0.0882	0.1510	7%

LEAD
DOSE BUILDUP
POINT ISOTROPIC SOURCE
20 MFP FIT

E(MEV)	A1	MAXIMUM ERROR	A2	B	MAXIMUM ERROR	C	D	MAXIMUM ERROR
0.5	0.1043	15%	0.1791	-.0047	5%	0.2243	-.0500	5%
1.	0.2549	11%	0.3133	-.0036	5%	0.3530	-.0211	4%
2.	0.3947	3%	0.3695	0.0015	2%	0.3791	0.0021	1%
3.	0.5123	30%	0.2990	0.0133	2%	0.3244	0.0279	1%
4.	0.6378 F1.6		0.1449	0.0306	10%	0.2526	0.0557	1%
5.1	0.8560 F2.1		-.1480	0.0624	40%	0.1904	0.0883	2%
6.	1.1247 F2.8		-.5070	0.1014	F4	0.1554	0.1143	4%
8.	1.4165 F4		-.1408	0.1589	F ∞	0.1075	0.1440	12%
10.	1.2370 F4		-.0279	0.1408	F ∞	0.0824	0.1513	12%

F3.1 MEANS FACTOR OF 3.1

Table 7 (cont.)

URANIUM
DOSE BUILDUP
POINT ISOTROPIC SOURCE
20 MFP FIT

E(MEV)	A1	MAXIMUM ERROR	MAXIMUM ERROR			C	D	MAXIMUM ERROR
			A2	B	C			
.5	0.0812	11%	0.1262	-.0037	5%	0.1635	-.0606	5%
1.	0.1914	11%	0.2556	-.0053	5%	0.2991	-.0385	5%
2.	0.2838	5%	0.3185	-.0022	2%	0.3240	-.0084	2%
3.	0.4081	20%	0.2614	0.0091	2%	0.2781	0.0234	1%
4.	0.4991	43%	0.1621	0.0210	6%	0.2273	0.0475	1%
6.	0.8088	F2.3	-.2492	0.0658	F2	0.1426	0.1011	2%
8.	0.9323	F2.9	-.5357	0.0912	F5	0.1004	0.1274	5%
10.	0.9203	F3.3	-.6560	0.0980	F ∞	0.0721	0.1442	7%

F3.1 MEANS FACTOR OF 3.1

Table 7 (cont.)

**ORDINARY CONCRETE
DOSE BUILDUP
POINT ISOTROPIC SOURCE
20 MFP FIT**

E(MEV)	MAXIMUM ERROR		A2	B	MAXIMUM ERROR		C	D	MAXIMUM ERROR	
	A1	F								
0.5	5.0124	F2.3	0.8341	0.5016	10%	1.5177	0.1413	12%		
1.	2.9917	F2	1.1821	0.1125	10%	1.2208	0.0562	11%		
2.	1.2334	25%	0.9344	0.0186	7%	0.8579	0.0231	5%		
3.	0.7857	12%	0.7141	0.0044	6%	0.6589	0.0115	5%		
4.	0.5942	4%	0.5662	0.0017	5%	0.6056	-0.0018	4%		
6.	0.4145	5%	0.4440	-0.0018	5%	0.4769	-0.0093	4%		
8.	0.3200	4%	0.3445	-0.0015	5%	0.3789	-0.0113	4%		
10.	0.2737	5%	0.3015	-0.0017	5%	0.3318	-0.0128	4%		

**FERROPHOSPHOROUS CONCRETE
DOSE BUILDUP
POINT ISOTROPIC SOURCE
20 MFP FIT**

E(MEV)	MAXIMUM ERROR		A2	B	MAXIMUM ERROR		C	D	MAXIMUM ERROR	
	A1	F								
0.5	3.4067	F2.2	1.1051	0.1431	15%	1.1098	0.0704	15%		
1.	2.1096	F1.7	1.1170	0.0617	15%	0.9892	0.0481	10%		
2.	1.1583	30%	0.7992	0.0223	4%	0.7703	0.0256	3%		
3.	0.8138	16%	0.6488	0.0103	2%	0.6373	0.0152	2%		
4.	0.6702	16%	0.4923	0.0111	2%	0.4966	0.0186	2%		
6.	0.5469	18%	0.3622	0.0115	5%	0.4118	0.0167	3%		
8.	0.4477	19%	0.2692	0.0111	5%	0.3207	0.0196	4%		
10.	0.3972	25%	0.1971	0.0124	5%	0.2456	0.0287	3%		

F3.1 MEANS FACTOR OF 3.1

Table 7 (cont.)

MAGNETITE CONCRETE
DOSE BUILDUP
POINT ISOTROPIC SOURCE
20 MFP FIT

E(MEV)	A1	MAXIMUM ERROR	A2	B	MAXIMUM ERROR	C	D	MAXIMUM ERROR
0.5	4.2793	F2.5	1.4544	0.1756	23%	1.3246	0.0736	18%
1.	2.3058	F1.7	1.2562	0.0652	20%	1.0651	0.0492	12%
2.	1.1752	25%	0.8756	0.0186	5%	0.8208	0.0227	5%
3.	0.8098	15%	0.6616	0.0092	3%	0.6445	0.0143	2%
4.	0.6263	10%	0.5280	0.0061	2%	0.5265	0.0108	1%
6.	0.4781	7%	0.4257	0.0033	2%	0.4312	0.0062	2%
8.	0.3805	9%	0.3195	0.0038	2%	0.3204	0.0106	2%
10.	0.3399	12%	0.2428	0.0060	3%	0.2623	0.0156	2%

BARYTES CONCRETE
DOSE BUILDUP
POINT ISOTROPIC SOURCE
20 MFP FIT

E(MEV)	A1	MAXIMUM ERROR	A2	B	MAXIMUM ERROR	C	D	MAXIMUM ERROR
0.5	2.2489	F1.8	1.1064	0.0710	11%	1.0183	0.0496	10%
1.	1.8761	F1.7	1.0022	0.0543	14%	0.8555	0.0495	12%
2.	1.1122	30%	0.7591	0.0219	4%	0.7291	0.0265	4%
3.	0.8068	24%	0.6047	0.0126	6%	0.5673	0.0222	4%
4.	0.6873	21%	0.4913	0.0122	4%	0.4689	0.0242	4%
6.	0.6277	30%	0.3420	0.0178	2%	0.3542	0.0355	4%
8.	0.5574	40%	0.1882	0.0229	10%	0.2806	0.0409	3%
10.	0.4943	50%	0.0936	0.0249	10%	0.1949	0.0555	2%

F3.1 MEANS FACTOR OF 3.1

Table 7 (cont.)

WATER
DOSE BUILDUP
PLANE COLLIMATED SOURCE
20 MFP FIT

E(MEV)	MAXIMUM		A2	B	MAXIMUM		D	MAXIMUM
	A1	ERROR			C	ERROR		
0.5	4.1289	F2.2	0.8313	0.2719	20%	1.4646	0.0831	4%
1.	1.8168	36%	1.0908	0.0599	5%	1.1605	0.0363	3%
2.	0.8826	6%	0.8238	0.0049	2%	0.8155	0.0065	2%
3.	0.6505	3%	0.6404	0.0008	3%	0.6646	-.0022	2%
4.	0.5106	5%	0.5428	-.0027	3%	0.5629	-.0085	2%
6.	0.3881	5%	0.4064	-.0015	3%	0.4367	-.0104	3%
8.	0.3015	5%	0.3230	-.0018	3%	0.3509	-.0132	3%

IRON
DOSE BUILDUP
PLANE COLLIMATED SOURCE
20 MFP FIT

E(MEV)	MAXIMUM		A2	B	MAXIMUM		D	MAXIMUM
	A1	ERROR			C	ERROR		
0.5	1.2142	20%	0.8359	0.0312	10%	0.9558	0.0184	5%
1.	1.1161	20%	0.7910	0.0268	5%	0.8503	0.0216	3%
2.	0.8063	12%	0.6356	0.0141	3%	0.6595	0.0162	2%
3.	0.6634	10%	0.5380	0.0103	2%	0.5560	0.0142	1%
4.	0.5665	12%	0.4466	0.0099	2%	0.4536	0.0181	2%
6.	0.4600	15%	0.3237	0.0112	1%	0.3381	0.0250	1%
8.	0.3866	17%	0.2400	0.0121	2%	0.2587	0.0325	1%
10.	0.3401	21%	0.1765	0.0135	3%	0.2053	0.0404	1%

F3.1 MEANS FACTOR OF 3.1

Table 7 (cont.)

TIN
DOSE BUILDUP
PLANE COLLIMATED SOURCE
20 MFP FIT

E(MEV)	A1	MAXIMUM ERROR	A2	B	MAXIMUM ERROR	C	D	MAXIMUM ERROR
1.	0.6238	4%	0.5844	0.0032	4%	0.6203	-.0002	3%
2.	0.6381	9%	0.5235	0.0095	3%	0.5547	0.0110	2%
4.	0.4995	11%	0.3529	0.0176	2%	0.3732	0.0344	1%
6.	0.5651	43%	0.1547	0.0338	8%	0.2490	0.0651	1%
10.	0.4609 F1.6		-.0069	0.0386	15%	0.1376	0.0942	2%

LEAD
DOSE BUILDUP
PLANE COLLIMATED SOURCE
20 MFP FIT

E(MEV)	A1	MAXIMUM ERROR	A2	B	MAXIMUM ERROR	C	D	MAXIMUM ERROR
0.5	0.1202	10%	0.1927	-.0087	5%	0.2383	-.0854	4%
1.	0.2305	12%	0.3107	-.0066	6%	0.3642	-.0394	5%
2.	0.3334	5%	0.3545	-.0017	4%	0.3855	-.0128	3%
3.	0.3955	7%	0.3284	0.0055	2%	0.3468	0.0103	2%
4.	0.4039	20%	0.2288	0.0144	3%	0.2622	0.0345	2%
6.	0.4636	50%	0.0439	0.0346	13%	0.1672	0.0796	3%
8.	0.4247 F1.6		-.0250	0.0371	16%	0.1216	0.0971	3%
10.	0.3482 F1.6		-.0380	0.0318	16%	0.0950	0.1003	4%

F3.1 MEANS FACTOR OF 3.1

Table 7 (cont.)

URANIUM
DOSE BUILDUP
PLANE COLLIMATED SOURCE
2D MFP FIT

E(MEV)	A1	MAXIMUM		B	MAXIMUM		C	D	MAXIMUM	
		ERROR			ERROR				ERROR	
0.5	0.0825	10%		0.1391	-.0068	4%	0.1722	-.0918	3%	
1.	0.1777	12%		0.2127	-.0029	8%	0.2784	-.0396	7%	
2.	0.2613	5%		0.2794	-.0015	5%	0.3170	-.0171	5%	
3.	0.3142	6%		0.2556	0.0048	3%	0.2778	0.0094	3%	
4.	0.3330	15%		0.2047	0.0106	3%	0.2330	0.0283	2%	
6.	0.3783	38%		0.0806	0.0245	8%	0.1613	0.0670	3%	
8.	0.3411	47%		0.0120	0.0271	11%	0.1130	0.0861	3%	
10.	0.2939	47%		-.0148	0.0255	12%	0.0859	0.0954	3%	

F3.1 MEANS FACTOR OF 3.1

Table 8. Linear, Quadratic and Berger Coefficients
for Energy Absorption Buildup Formulas
Fitted over the Range (0-20 MFP)

Table 8 (cont.)

WATER
ENERGY ABSORPTION BUILDUP
POINT ISOTROPIC SOURCE
20 MFP FIT

E(MEV)	A1	MAXIMUM ERROR	A2	B	MAXIMUM ERROR	C	D	MAXIMUM ERROR
0.255	33.3292	F11	-11.8413	2.8075	F ∞	2.4039	0.1598	30%
0.5	11.9995	F5.3	-8251	0.7971	F3	1.7128	0.1201	24%
1.	3.5674	F2.2	1.2155	0.1462	11%	1.2443	0.0660	12%
2.	1.2958	27%	0.9477	0.0216	7%	0.8829	0.0243	5%
3.	0.8307	6%	0.7696	0.0038	2%	0.7506	0.0065	2%
4.	0.6016	1%	0.6005	0.0001	1%	0.5905	0.0012	1%
6.	0.4020	5%	0.4462	-0.0027	1%	0.4550	-0.0079	1%
8.	0.3111	8%	0.3595	-0.0030	2%	0.3757	-0.0121	2%
10.	0.2470	7%	0.2863	-0.0024	3%	0.3036	-0.0133	2%

ALUMINUM
ENERGY ABSORPTION BUILDUP
POINT ISOTROPIC SOURCE
20 MFP FIT

E(MEV)	A1	MAXIMUM ERROR	A2	B	MAXIMUM ERROR	C	D	MAXIMUM ERROR
0.5	7.4709	F3.2	0.5870	0.4279	13%	1.7237	0.0902	14%
1.	2.9692	F2	1.1504	0.1130	5%	1.2204	0.0553	10%
2.	1.2898	30%	0.9530	0.0209	10%	0.8480	0.0268	6%
3.	0.8324	12%	0.7120	0.0075	4%	0.6746	0.0134	3%
4.	0.6130	7%	0.5566	0.0035	2%	0.5411	0.0079	2%
6.	0.4395	5%	0.4064	0.0021	1%	0.3995	0.0060	1%
8.	0.3387	4%	0.3122	0.0016	1%	0.3079	0.0060	1%
10.	0.2808	5%	0.2517	0.0018	1%	0.2492	0.0074	1%

F3.1 MEANS FACTOR OF 3.1

Table 8 (cont.)

IRON
ENERGY ABSORPTION BUILDUP
POINT ISOTROPIC SOURCE
20 MFP FIT

E(MEV)	MAXIMUM		A2	MAXIMUM		C	D	MAXIMUM
	A1	ERROR		B	ERROR			
0.5	4.3555	F2	1.6324	0.1692	3%	1.7887	0.0550	7%
1.	2.5718	F1.7	1.2621	0.0814	8%	1.2192	0.0466	8%
2.	1.2302	31%	0.8308	0.0248	5%	0.7868	0.0280	4%
3.	0.8780	25%	0.6100	0.0167	4%	0.5847	0.0255	4%
4.	0.7098	27%	0.4233	0.0178	2%	0.4494	0.0281	2%
6.	0.5267	31%	0.2857	0.0150	1%	0.2975	0.0353	3%
8.	0.4121	33%	0.1805	0.0144	2%	0.2076	0.0420	2%
10.	0.3742	40%	0.1034	0.0168	6%	0.1565	0.0528	1%

TIN
ENERGY ABSORPTION BUILDUP
POINT ISOTROPIC SOURCE
20 MFP FIT

E(MEV)	MAXIMUM		A2	MAXIMUM		C	D	MAXIMUM
	A1	ERROR		B	ERROR			
0.5	1.0731	8%	1.0838	-.0007	6%	1.1873	-.0069	4%
1.	1.3409	16%	1.1163	0.0140	4%	1.0819	0.0134	3%
2.	1.1007	26%	0.8284	0.0169	7%	0.7490	0.0245	4%
3.	0.8999	40%	0.5545	0.0215	8%	0.4909	0.0380	9%
4.	0.7997	F1.58	0.3073	0.0306	6%	0.3352	0.0534	8%
6.	0.7685	F1.84	-.0552	0.0512	25%	0.1931	0.0820	2%
8.	0.7247	F2.2	-.2351	0.0597	F2	0.1237	0.1030	2%
10.	0.6837	F2.4	-.3169	0.0622	F2.2	0.0930	0.1148	4%

F3.1 MEANS FACTOR OF 3.1

Table 8 (cont.)

LEAD
ENERGY ABSORPTION BUILDUP
POINT ISOTROPIC SOURCE
2D MFP FIT

E(MEV)	MAXIMUM ERROR		A2	B	MAXIMUM ERROR		C	D	MAXIMUM ERROR	
	A1									
0.5	0.1925	23%	0.3156	-.0101	14%	0.4551	-.0753	10%		
1.	0.4592	20%	0.5870	-.0079	10%	0.7027	-.0278	7%		
2.	0.5424	3%	0.5183	0.0015	4%	0.5510	-.0014	3%		
3.	0.5268	25%	0.3131	0.0133	4%	0.3476	0.0251	2%		
4.	0.5398	F1.5	0.1325	0.0253	9%	0.2227	0.0532	1%		
5.1	0.6667	F2	-.0967	0.0474	20%	0.1646	0.0818	3%		
6.	0.7344	F2.5	-.2976	0.0641	F2	0.1167	0.1060	5%		
8.	0.7421	F3	-.4859	0.0763	F5	0.0781	0.1269	8%		
10.	0.6388	F3	-.4804	0.0696	F10	0.0588	0.1327	15%		

Table 9. Comparison of Average Percentage Deviation Using
Berger and Taylor Dose Formulas

Medium	Mean Percentage Deviation			
	20 MFP Range		7 MFP Range	
	Berger*	Taylor	Berger**	Taylor
Water	4.0	3.6	1.2	3.7
Aluminum	2.5	2.8	0.7	2.5
Iron	2.1	2.5	0.5	2.5
Tin	1.3	1.9	0.2	1.7
Tungsten	1.7	1.6	0.3	1.2
Lead	2.3	0.8	0.7	0.5
Uranium	1.6	0.8	0.4	0.5
Ordinary concrete	3.2	2.9	2.0	4.0
Ferrophos. concrete	3.2	2.6	1.4	3.3
Magnetite concrete	2.9	4.2	0.9	4.8
Barytes concrete	2.6	3.4	0.6	3.7

*20-MFP parameters used.

**7-MFP parameters used.

PART II - Application of Buildup Factors for Distributed Sources in Plane Geometry

Plane Isotropic Source Kernel Using Berger Formula

As an example of an integration making use of the Berger form, the kernel for the dose rate from an isotropic, monoenergetic, plane source of strength 1 photon/cm²-sec is

$$\Gamma(z) = K(E) \int_{\rho=0}^{\infty} \frac{e^{-\mu R}}{4\pi R^2} B(\mu R) 2\pi\rho d\rho , \quad (10)$$

where

ρ = distance to source point on plane from perpendicular to plane from detector,

z = distance of detector from plane,

$$R = \rho^2 + z^2 ,$$

$K(E)$ = flux-to-dose factor at energy E

Changing variables and replacing $B(\mu R)$ with the Berger formula yields

$$\Gamma(z) = \frac{K(E)}{2} \int_z^{\infty} e^{-\mu R} (1 + C\mu R e^{D\mu R}) \frac{dR}{R} . \quad (11)$$

Then

$$\Gamma(z) = \frac{K(E)}{2} \left[E_1(\mu z) + \frac{C}{1-D} e^{-(1-D)\mu z} \right] , \quad (12)$$

where

$$E_n(x) = x^{n-1} \int_x^{\infty} e^{-y} y^{-n} dy ,$$

or, in terms of a plane buildup factor,

$$B(\mu z) = 1 + \frac{C}{1-D} \frac{e^{-(1-D)\mu z}}{E_1(\mu z)} . \quad (13)$$

Integration of Plane Kernel with Exponential Source Distribution

Often a large fraction of the radiation dose behind reactor and shelter shields is the secondary gamma-ray dose due to neutron capture. If the spacial behavior of the neutron flux is fairly well known, the gamma-ray dose may be calculated by integrating the dose kernel over the source volume. In a manner similar to that of the previous section and with the geometry shown in Fig. 39, the dose rate at t due to a distributed monoenergetic isotropic source $S(x)$ between $a \leq t$ and b is given by

$$\Gamma(t, a, b) = K(E) \int_a^b S(x) dx \int_0^\infty \frac{e^{-\mu R}}{4\pi R^2} B(\mu R) 2\pi\rho d\rho \quad (14)$$

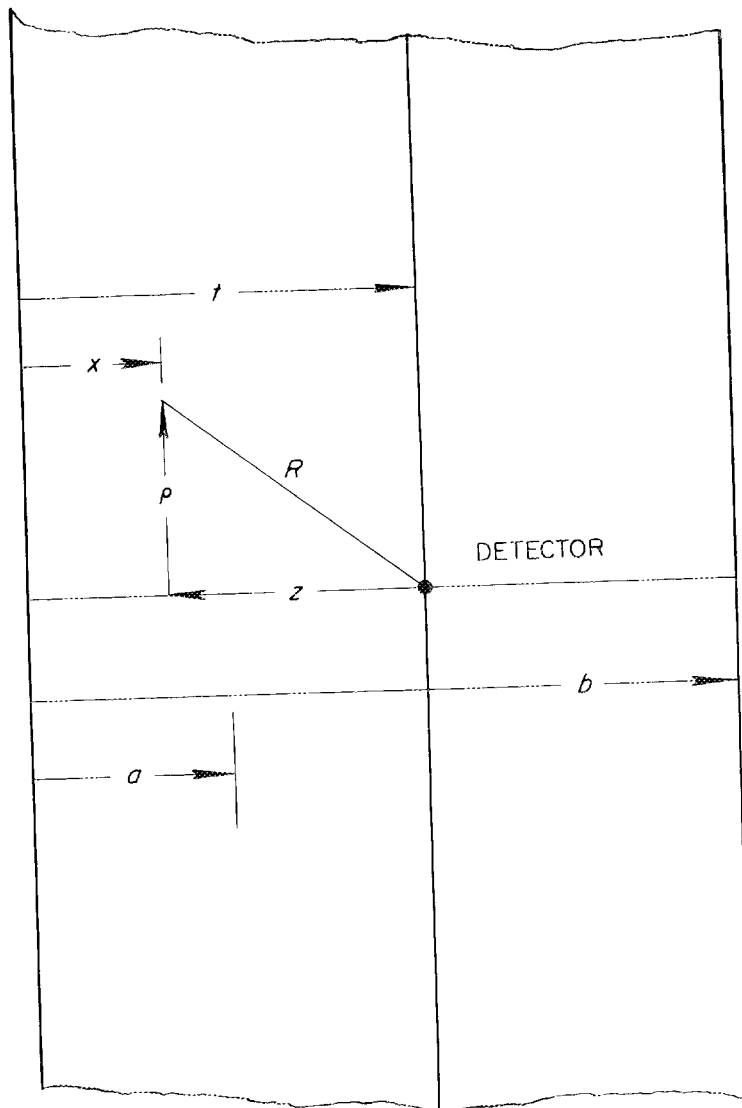
$$= \frac{K(E)}{2} \int_a^b S(x) dx \int_{|t-x|}^\infty \frac{e^{-\mu R}}{R} B(\mu R) dR \quad (15)$$

$$= \frac{K(E)}{2} \int_a^t S(x) dx \int_{t-x}^\infty \frac{e^{-\mu R}}{R} B(\mu R) dR \\ + \frac{K(E)}{2} \int_t^b S(x) dx \int_{|x-t|}^\infty \frac{e^{-\mu R}}{R} B(\mu R) dR . \quad (16)$$

Let $z = |t - x|$. Then

ORNL-DWG 65-11933

Fig. 39.
GEOMETRY OF INTEGRATION OVER EXPONENTIAL
SOURCE DISTRIBUTION



$$\begin{aligned} \Gamma(t, a, b) = & \frac{K(E)}{2} \int_0^{t-a} s(t-z) dz \int_z^\infty \frac{e^{-\mu R}}{R} B(\mu R) dR \\ & + \frac{K(E)}{2} \int_0^{b-t} s(t+z) dz \int_{|z|}^\infty \frac{e^{-\mu R}}{R} B(\mu R) dR . \quad (17) \end{aligned}$$

Often the neutron flux and consequently the secondary gamma-ray source may be represented by an exponential over a certain range. This can be part of a piece-wise integration. Let

$$s(x) = S_0 e^{-\alpha \mu x},$$

where α is the reciprocal of the product of the gamma-ray absorption coefficient and the neutron relaxation length.

Then

$$\begin{aligned} \Gamma(t, a, b) = & \frac{K(E)S_0}{2} e^{-\alpha \mu t} \left\{ \int_0^{t-a} e^{\alpha \mu z} dz \int_{\mu z}^\infty \frac{e^{-y}}{y} B(y) dy \right. \\ & \left. + \int_0^{b-t} e^{-\alpha \mu z} dz \int_{|\mu z|}^\infty \frac{e^{-y}}{y} B(y) dy \right\} . \quad (18) \end{aligned}$$

Uncollided Dose Rate

Using the Berger form for the buildup factor, the integration breaks into two parts: the uncollided and scattered terms. The uncollided term from Eq. (18) is:

$$\Gamma_o(t, a, b) = \frac{K(E) S_o e^{-\alpha \mu t}}{2\mu} \left\{ \begin{array}{l} \int_0^{\mu(t-a)} e^{\alpha y} E_1(y) dy \\ + \int_0^{\mu(b-t)} e^{-\alpha y} E_1(|y|) dy \end{array} \right\} . \quad (19)$$

In many cases of shield design the detector is at the edge of the shield; that is, $b \leq t$. In this case Eq. 19 becomes upon integration by parts:

$$\Gamma_o(t, a, b) = \frac{K(E) S_o e^{-\alpha \mu t}}{2\alpha \mu} \left[e^{\alpha y} E_1(y) \Big|_{\mu(t-b)}^{\mu(t-a)} + \int_{\mu(t-b)}^{\mu(t-a)} e^{\alpha y} \frac{e^{-y}}{y} dy \right] \quad (20)$$

$$= \frac{K(E) S_o e^{-\alpha \mu t}}{2\alpha \mu} \left[e^{\alpha \mu(t-a)} E_1(\mu[t-a]) - E_1([1-\alpha] \mu[t-a]) + E_1([1-\alpha] \mu[t-b]) - e^{\alpha \mu(t-b)} E_1(\mu[t-b]) \right] . \quad (21)$$

If $\alpha > 1$ the argument of the E_1 function is negative, in which case the values may be determined from graphs such as those in Blizzard¹⁷ or Rockwell⁷ or from tables of the E_i function, noting

$$E_i(x) = -E_1(-x) = - \int_{-x}^{\infty} \frac{e^{-y}}{y} dy . \quad (22)$$

There are some special cases in which arguments of the exponential integral are zero. These cases result in indeterminates which may be evaluated as follows.

Case I

$$b = t, \alpha \neq 1; a = 0, \alpha \neq 0.$$

$$\text{Let } y = t - b$$

$$\begin{aligned} & \lim_{y \rightarrow 0} \left\{ E_1((1-\alpha)\mu y) - e^{\alpha\mu y} E_1(\mu y) \right\} \\ &= - \lim_{y \rightarrow 0} \left\{ \ln |\gamma(1-\alpha)\mu y| - \ln |\gamma\mu y| \right\}, \text{ where } \ln \gamma = \text{Euler's constant} \\ &= 0.577215665 \dots, \\ &= -\ln |[1-\alpha]|, \end{aligned} \quad (23)$$

since

$$E_1(x) = \sum_{n=1}^{\infty} (-1)^{n-1} \frac{x^n}{n \cdot n!} - \ln|\gamma x|.$$

Thus

$$\Gamma_o(t, o, t) = \frac{K(E)S_o}{2\mu} \left[E_1(\mu t) - e^{-\alpha\mu t} \left(E_1((1-\alpha)\mu t) + \ln|1-\alpha| \right) \right]. \quad (24)$$

Case II

$$b = t, \alpha = 0, a = 0.$$

$$\Gamma_o(t, o, t) = \frac{K(E)S_o}{2\mu} \int_0^{\mu t} E_1(y) dy = \frac{K(E)S_o}{2\mu} \left[1 - E_2(\mu t) \right]. \quad (25)$$

Case III

$$b = t, \alpha = 1, a = 0.$$

$$\text{Let } y = t - b.$$

$$\begin{aligned}
 & \lim_{\alpha \rightarrow 1} \left[E_1([1 - \alpha]\mu y) - E_1([1 - \alpha]\mu t) - e^{\alpha\mu y} E_1(\mu y) \right] \\
 &= - \lim_{y \rightarrow 0} \left\{ \ln |\gamma(1 - \alpha)\mu y| - \ln |\gamma(1 - \alpha)\mu t| - \ln |\gamma\mu y| \right\} \\
 &= \lim_{y \rightarrow 0} \frac{|\gamma(1 - \alpha)\mu t \gamma y|}{|\gamma(1 - \alpha)y|} = \ln \gamma + \ln \mu t , \tag{26}
 \end{aligned}$$

and

$$\Gamma_o(t, o, t) = \frac{K(E)S_o}{2\mu} \left[E_1(\mu t) + e^{-\mu t} (\ln \gamma + \ln \mu t) \right] . \tag{27}$$

Case IV

$b < t, \alpha = 1, a = 0$.

$$\begin{aligned}
 & \lim_{\alpha \rightarrow 1} \left[E_1([1 - \alpha]\mu[t - b]) - E_1[1 - \alpha]\mu t \right] \\
 &= - \lim_{\alpha \rightarrow 1} \left\{ \ln |\gamma(1 - \alpha)\mu(t - b)| - \ln |\gamma[1 - \alpha]\mu t| \right\} \\
 &= \ln \frac{t}{t-b} , \tag{28}
 \end{aligned}$$

and

$$\Gamma_o(t, o, t) = \frac{K(E)S_o}{2\mu} \left[E_1(\mu t) - e^{-\mu b} E_1(\mu[t-b]) + e^{-\mu t} \ln \frac{t}{t-b} \right] . \tag{29}$$

If the detector is located within the shield, it remains only to evaluate the second term of Eq. 19. We consider the case for $b \rightarrow \infty$.

$$\int_0^\infty e^{-\alpha y} E_1(y) dy = \frac{1}{\alpha} \left[-e^{-\alpha y} E_1(y) \right]_{y=0}^\infty + \int_0^\infty e^{-\alpha y} \frac{e^{-y}}{y} dy \quad (30)$$

$$= \lim_{y \rightarrow 0} \frac{1}{\alpha} \left\{ E_1(y) - E_1([1 + \alpha]y) \right\} \\ = \frac{1}{\alpha} \ln|1 + \alpha| \quad . \quad (31)$$

The result for sources beyond t is then

$$\Gamma_o(t, t, \infty) = K(E) S_o \frac{e^{-\alpha_o t}}{2\mu\alpha} \ln|1 + \alpha| \quad . \quad (32)$$

Either heating or dose rate may be computed by multiplying by the appropriate conversion factors. Adding Eqs. 24 and 32 gives the heating result probably first published by Enlund.¹⁸

Scattered Dose Rate

The Berger buildup term is evaluated as follows:

$$\Gamma_s(t, a, b) = \frac{K(E) S_o}{2} \int_a^b dx \int_{\rho=0}^{\infty} e^{-\alpha_o x} \frac{e^{-\mu R}}{R^2} C \mu R e^{D \mu R} \rho d\rho \quad (33)$$

where $\Gamma_s(t, a, b)$ = scattered dose rate. For the situation discussed in connection with Eq. 20 (detector at edge of slab), Eq. (33) may be evaluated as follows.

Let $z = t - x$. Then

$$\Gamma_s(t, a, b) = K(E)CS_0 \frac{e^{-\alpha\mu t}}{2} \int_{t-b}^{t-a} dz \int_z^{\infty} e^{\alpha\mu z} e^{-(1-D)\mu R} \mu dR \quad (34)$$

$$= \frac{K(E)CS_0 e^{-\alpha\mu t}}{2(1-D)} \int_{t-b}^{t-a} e^{\alpha\mu z} e^{-(1-D)\mu z} dz \quad (35)$$

$$= K(E)S_0 \frac{e^{-\alpha\mu t}}{2} \frac{C}{1-D} \frac{1}{(1-D-\alpha)\mu} \left[e^{-(1-D-\alpha)\mu(t-b)} - e^{-(1-D-\alpha)\mu(t-a)} \right]. \quad (36)$$

For $\alpha + D = 1$,

$$\Gamma_s(t, a, b) = \frac{K(E)S_0}{2} e^{-\alpha\mu t} \frac{C(b-a)}{1-D} . \quad (37)$$

For the detector within the slab, the contribution from sources beyond t remains to be evaluated. Again we consider the case for $b \rightarrow \infty$:

$$\int_t^{\infty} e^{-\alpha\mu x} dx \int_x^{\infty} e^{-\mu R} C\mu R e^{D\mu R} \frac{dR}{R} = e^{-\alpha t} \frac{C}{1-D} \int_0^{\infty} e^{-(1-D+\alpha)\mu z} dz . \quad (38)$$

where $z = x + t$. The scattered contribution from sources beyond t is then

$$\Gamma_s(t, t, \infty) = \frac{K(E)CS_o e^{-\alpha\mu t}}{2(1 - D)} \int_0^\infty e^{-(1 - D + \alpha)\mu z} dz \quad (39)$$

$$= K(E) S_o \frac{e^{-\alpha\mu t}}{2(1 - D)} \frac{C}{(1 + \alpha - D)\mu} \quad . \quad (40)$$

This result is added to Eq. 36 for a detector within the slab.

Graphed Functions for Distributed Plane Sources

The uncollided photon flux solution for Case I (Eq. 24) may be written

$$\varphi_o(t) = \frac{S_o}{\mu} \underline{\psi}_o(\mu t, \alpha) , \quad (41)$$

where

$$\underline{\psi}_o(\mu t, \alpha) = \frac{1}{2\alpha} \left[E_1(\mu t) - e^{-\alpha\mu t} \left(E_1([1 - \alpha]\mu t) + \ln|1 - \alpha| \right) \right] . \quad (42)$$

This function is plotted in Fig. 40 for various values of α . The scattered flux solution for the case of $a = 0$, $b = t$ may be written

$$\varphi_s(t) = \frac{S_o}{\mu} \frac{C}{1 - D} e^{D\mu t} \underline{\psi}_s(\mu t, \alpha') \quad (43)$$

where

$$\Psi_1(\mu t, \alpha') = \frac{e^{-\alpha' \mu t}}{2} \frac{1 - e^{-\mu t(1 - \alpha')}}{1 - \alpha'} \quad (44)$$

where $\alpha' = \alpha + D$.

The $\Psi_1(\mu t, \alpha')$ function is shown in Fig. 41 for various values of α' . It is readily seen that the formulation may also be applied for a linear buildup factor by setting $D = 0$.

For sources of neutrons impinging on a semi-infinite medium with an interface net current J , the gamma-ray source may be written

$$S(x) = k J e^{-kx} \quad . \quad (45)$$

Then

$$\varphi_o(t) = \frac{J}{\mu} k \Psi_0(\mu t, \alpha) = J \alpha \Psi_0(\mu t, \alpha) \quad (46)$$

and

$$\varphi_s(t) = J \alpha \frac{C}{1 - D} e^{D \mu t} \Psi_1(\mu t, \alpha') \quad , \quad (47)$$

where $\alpha = k/\mu$.

The use of the Ψ functions is due to Claiborne¹⁹ who developed similar equations using polynomial buildup factors for the case of the detector within a slab which is of interest in a heating calculation. The polynomial buildup factor is

$$B(\mu R) = \sum_{n=0}^{\infty} \beta_n (\mu R)^n \quad . \quad (48)$$

The total flux is the sum

$$\varphi(\mu t) = \sum_n \varphi_n(\mu t) , \quad (49)$$

where

$$\varphi_n(\mu t) = \frac{S}{\mu} n! \beta_n \Psi_n(\mu t) . \quad (50)$$

For the semi-infinite medium,

$$\Psi_0(\mu t) = \frac{1}{2\alpha} \left[E_1(\mu t) - e^{-\alpha\mu t} \left\{ E_1((1-\alpha)\mu t - \ln|\frac{1+\alpha}{1-\alpha}|) \right\} \right] , \quad (51)$$

$$\Psi_1(\mu t) = \frac{e^{-\alpha\mu t}}{2} \left[\frac{1 - e^{-(1-\alpha)\mu t}}{1-\alpha} + \frac{1}{1+\alpha} \right] , \quad (52)$$

$$\Psi_2(\mu t) = \frac{4e^{-\alpha\mu t} - (1+\alpha)^2 (2-\alpha) e^{-\mu t} - (1+\alpha)^2 (1-\alpha)\mu t e^{-\mu t}}{4(1-\alpha)^2 (1+\alpha)^2} , \quad (53)$$

$$\begin{aligned} \Psi_3(\mu t) &= \frac{2}{3} \Psi_2 + \left[\frac{1}{(1-\alpha)^3} + \frac{1}{(1+\alpha)^3} \right] \frac{e^{-\alpha\mu t}}{6} \\ &\quad - \left[\frac{(\mu t)^2}{2(1-\alpha)} + \frac{\mu t}{(1-\alpha)^2} + \frac{1}{(1-\alpha)^3} \right] \frac{e^{-\mu t}}{6} . \end{aligned} \quad (54)$$

For $\alpha = 0$,

$$\Psi_0(\mu t) = 1 + \frac{\mu t}{2} E_1(\mu t) - \frac{e^{-\mu t}}{2} = 1 - \frac{1}{2} E_2(\mu t) . \quad (55)$$

For $\alpha = 1$,

$$\Psi_0(\mu t) = \frac{E_1(\mu t)}{2} + \frac{e^{-\mu t}}{2} \left[\ln 2 + \ln \gamma + \ln \mu t \right] , \quad (56)$$

$$\Psi_1(\mu t) = (\mu t + \frac{1}{2}) \frac{e^{-\mu t}}{2} , \quad (57)$$

$$\Psi_2(\mu t) = \left[\frac{(\mu t)^2}{2} + \mu t + \frac{3}{4} \right] \frac{e^{-\mu t}}{4} , \quad (58)$$

$$\Psi_3(\mu t) = \frac{2\Psi_2}{3} + \left[\frac{(\mu t)^3}{3} + \frac{1}{4} \right] \frac{e^{-\mu t}}{12} . \quad (59)$$

Claiborne's article (ref. 19) also gives the functions for slabs of finite thickness as well as averages over the slab thickness.

These Ψ functions for the semi-infinite medium are plotted in Figs. 42-45 for various values of α . The first two may be compared with Figs. 40-41 which were evaluated for slabs.

Fig. 40.

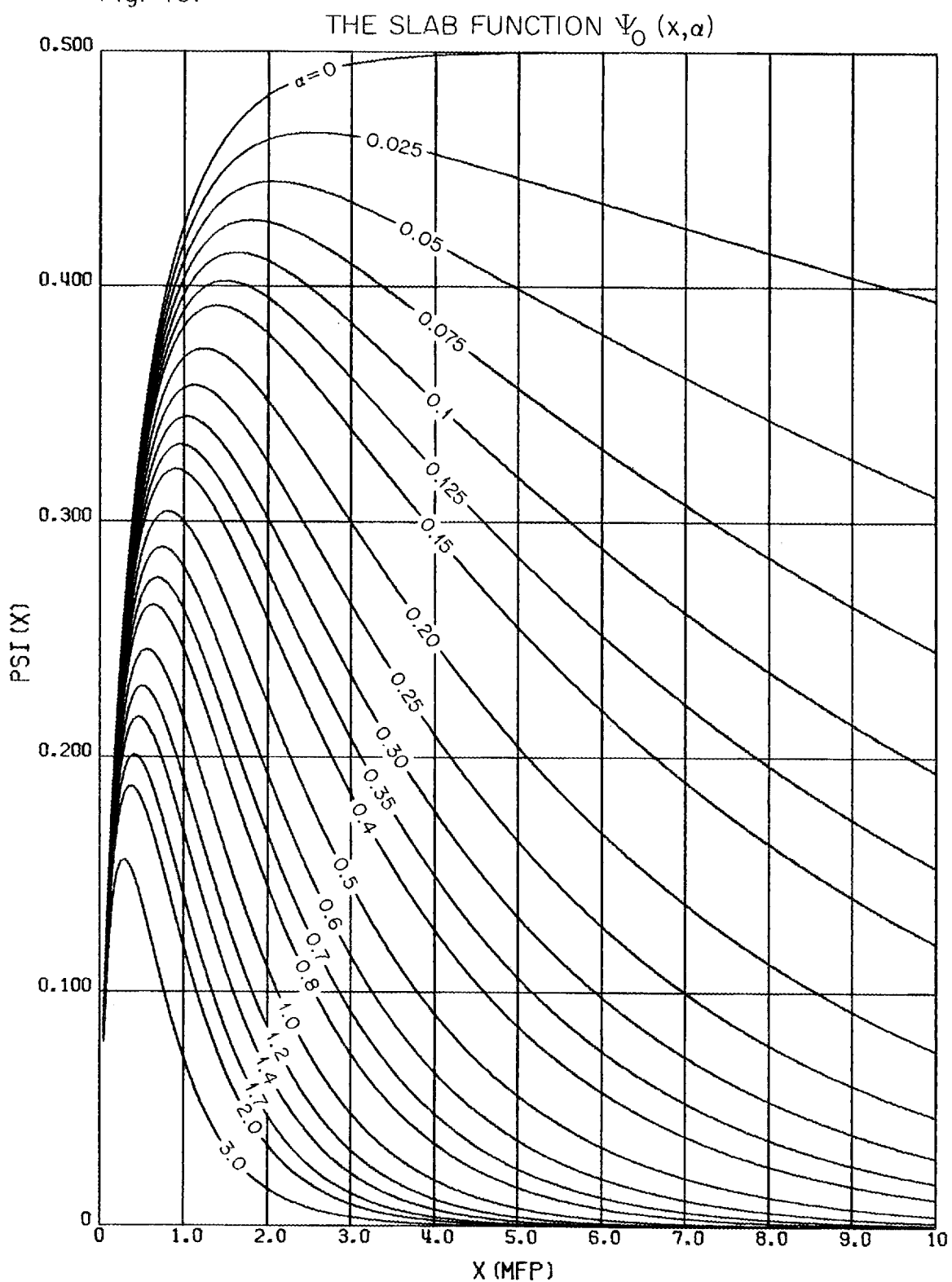


Fig. 41.

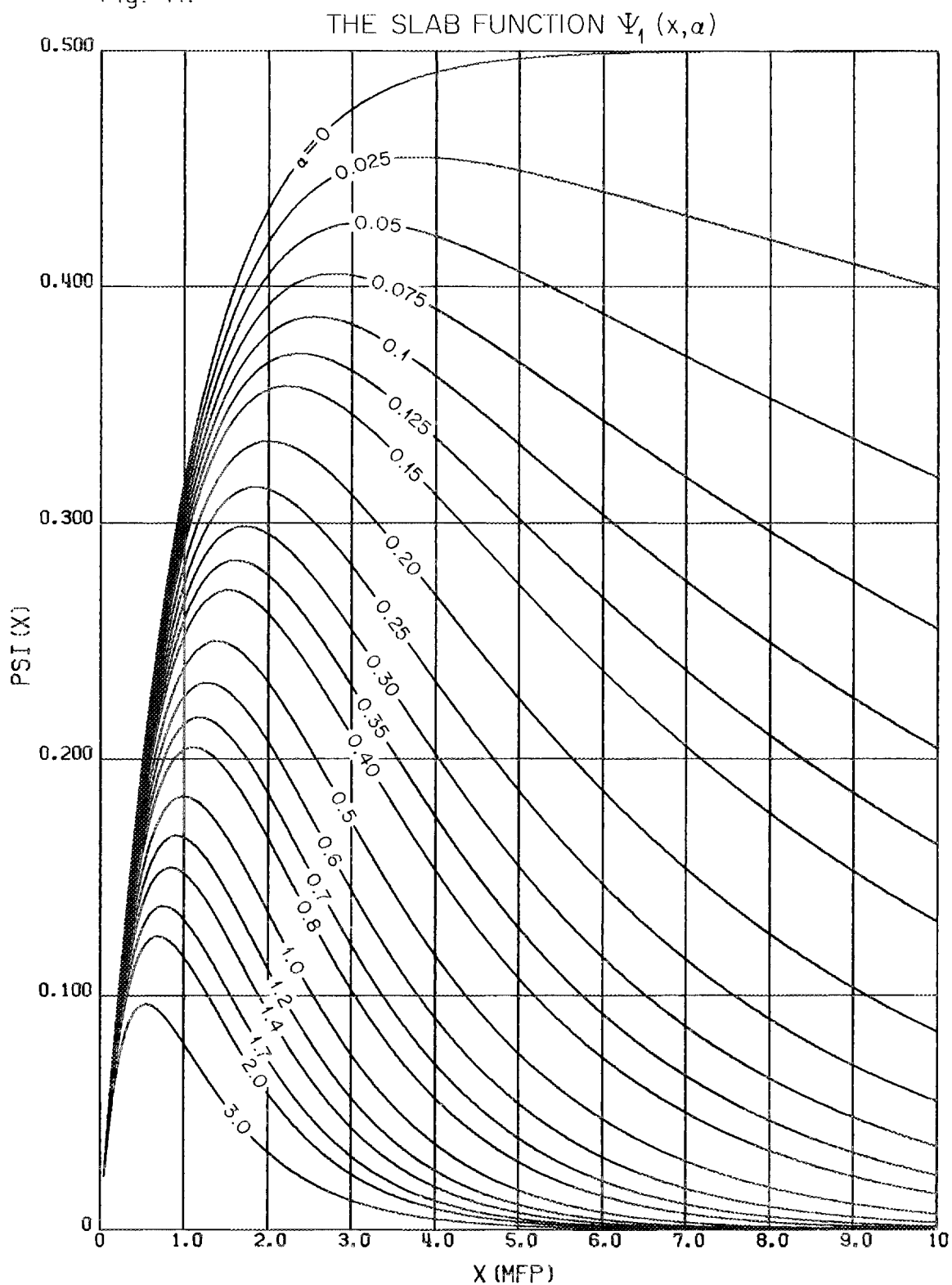


Fig. 42.

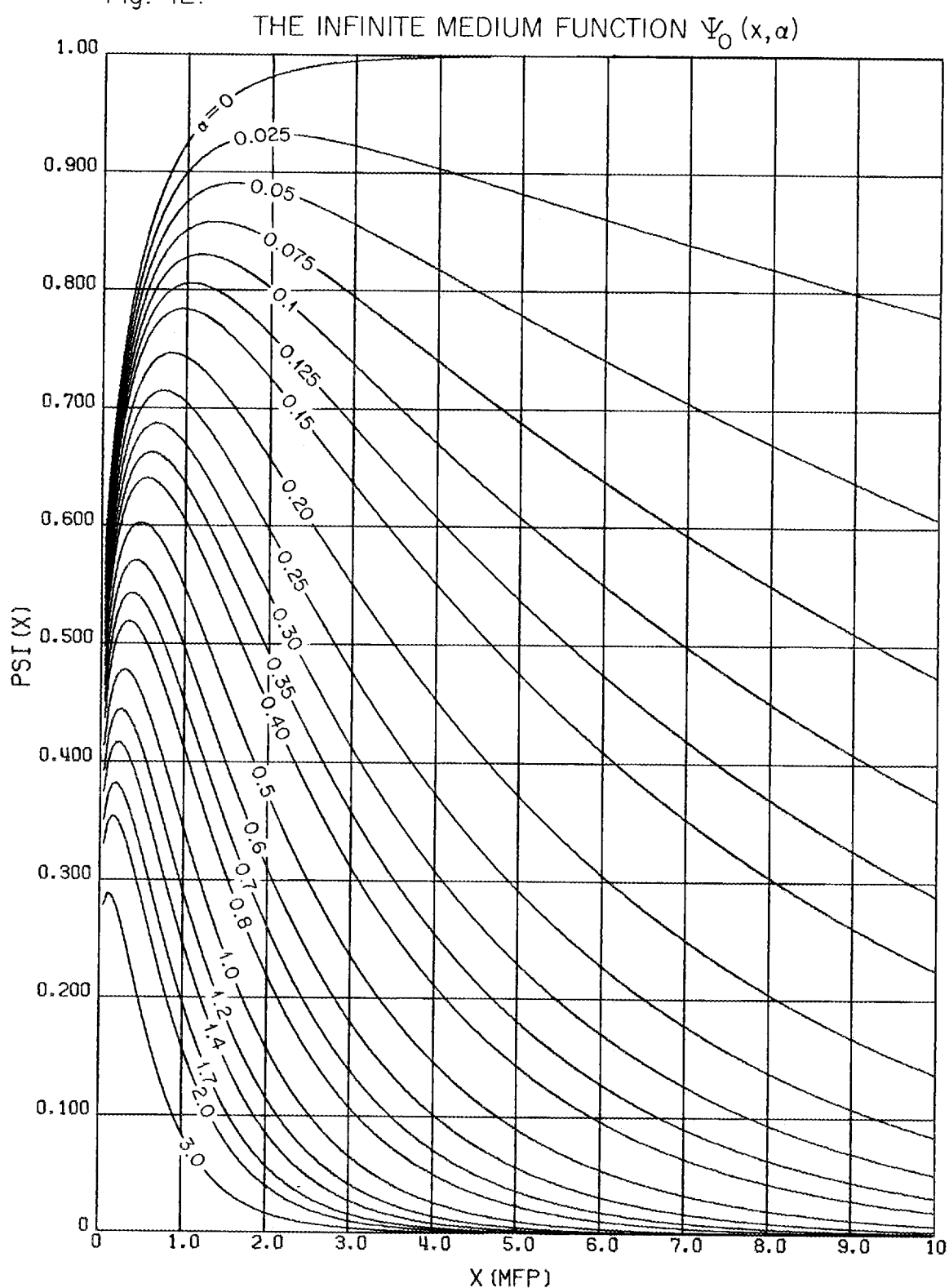


Fig. 43.

THE INFINITE MEDIUM FUNCTION $\Psi_1(x, \alpha)$

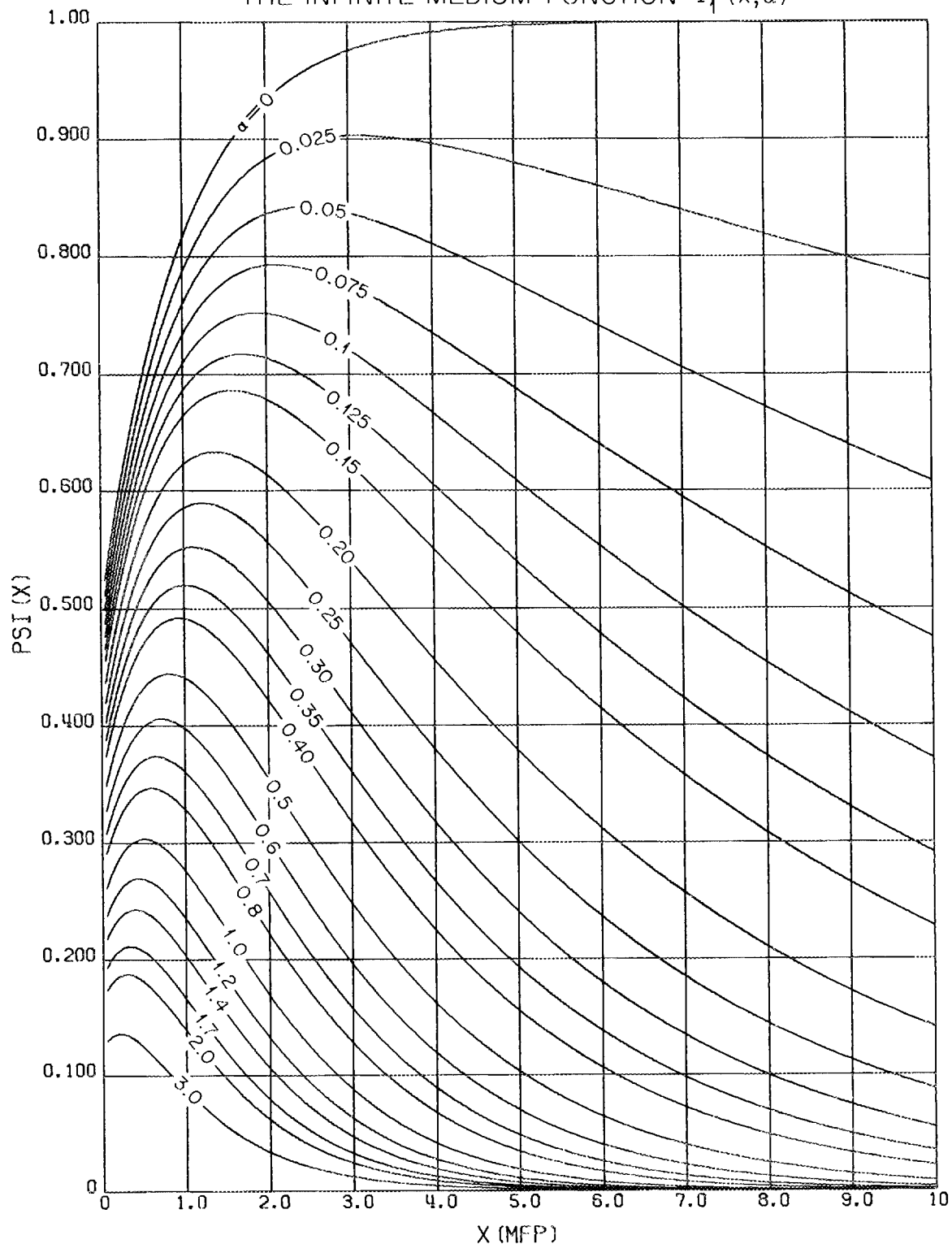


Fig. 44.

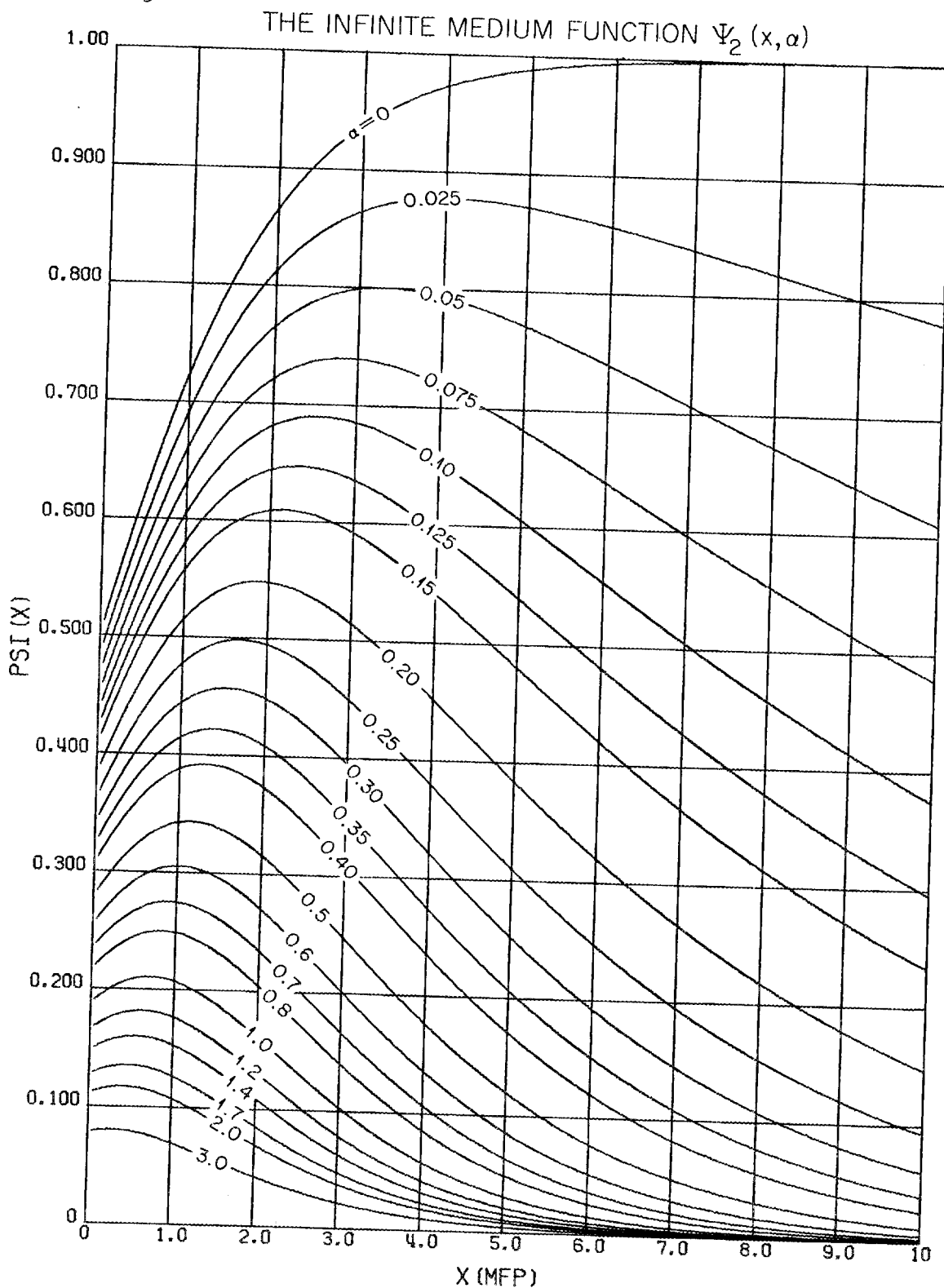
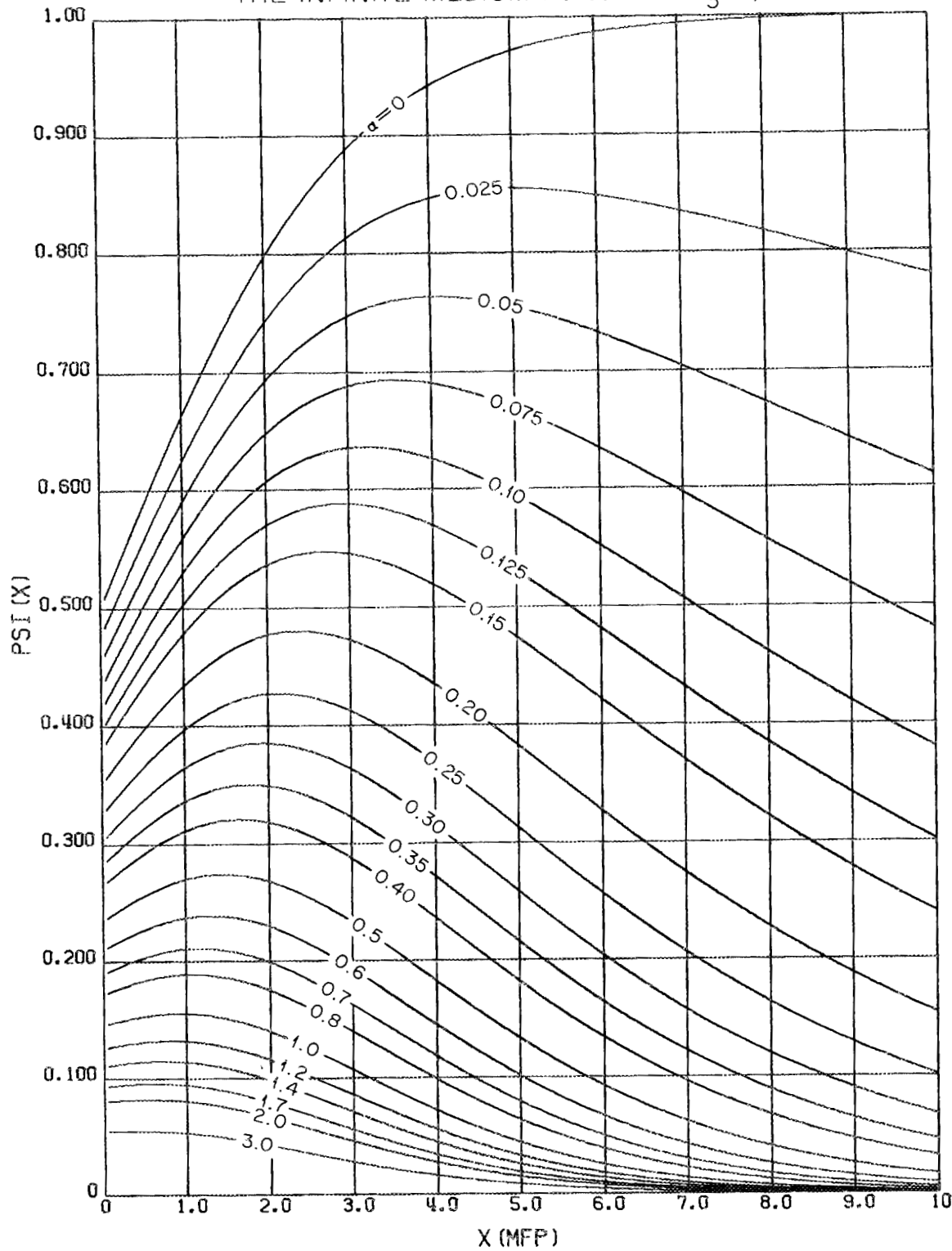


Fig. 45.

THE INFINITE MEDIUM FUNCTION $\Psi_3(x,\alpha)$



PART III - Application of Buildup Factors in Finite or Laminated Media

Although the scope of this report was determined to primarily include only the buildup factor functions for infinite homogeneous media, a short survey of work concerning finite or laminated media is included here.

Effect of Leakage

The effect of leakage from slabs is given by Berger^{20,21} as a correction factor on the scattered portion of the buildup factor. The results were obtained by Monte Carlo calculations.

Effect of Laminations

Empirical formulas based on Monte Carlo data have been given by Kalos²² for dose rate and by Bowman and Trubey^{23,24} for heating. These formulas prescribe how homogeneous medium buildup factors may be combined to yield values for laminated media.

Slant Penetration

Empirical formulas, again based on Monte Carlo data, have been given by Pieper and Beach²⁵ for calculating the effect of slant incidence. Similar, but more complicated, formulas are given by Rexroad and Schmoke²⁶ for calculating dose rate from fallout in a blockhouse.

Tabulated results from moments method calculations are given by Spencer and Lamkin^{27,28} and from Monte Carlo calculations by Burrell and Cribbs.²⁹

ACKNOWLEDGEMENTS

The author is grateful to E. E. Branstetter of the ORNL Mathematics Division for programming the least-squares code which produced the coefficients of Tables 5 - 8 and to H. C. Claiborne for many helpful discussions and for his equations prior to publication.

REFERENCES

1. H. Goldstein and J. E. Wilkins, Jr., Calculations of the Penetration of Gamma Rays, NYO-3075 (1954).
2. H. Goldstein, Fundamental Aspects of Reactor Shielding, p. 218, Addison-Wesley, Reading, Mass., 1959.
3. J. J. Taylor, Application of Gamma Ray Buildup Data to Shield Design, WAFD-RM-217 (1954).
4. G. L. Strobel, Nucl. Sci. Eng., 11(4), 450 (1961).
5. S. Buscaglione and R. Manzini, Sui Fattori Di Accumulazione: Coefficienti Della Formula Di J. J. Taylor, RT/FI(65)7 (1965) or the English translation Buildup Factors: Coefficients of the J. J. Taylor Eq., ORNL-tr-80 (Rev.) (1965).
6. R. L. Walker and M. Grotenhuis, A Survey of Shielding Constants for Concrete, ANL-6443 (1961).
7. T. Rockwell, ed., Reactor Shielding Design Manual, New York, McGraw-Hill Book Company, 1956.
8. A. Honig, Dose Buildup Factor for Concrete, ORNL-tr-502 translated from Kerntechnik, 6(9), 393-99 (1964).
9. M. A. Capo, Polynomial Approximation of Gamma Ray Buildup Factors for a Point Isotropic Source, APEX-510 (1958).
10. M. L. Tobias, D. R. Vondy, and M. P. Leitzke, Nightmare - An IBM-7090 Code for the Calculation of Gamma Heating in Cylindrical Geometry, ORNL-3198 (1962).
11. S. Buscaglione and R. Manzini, Sui Fattori Di Accumulazione Del Calcestruzzo: Coefficienti Della Rappresentazione Poliomiale, CEC-94 or the English Translation On the Buildup of Concrete: Coefficients of the Polynomial Representation, ORNL-tr-349 (1965).
12. M. J. Berger, Proceedings of Shielding Symposium held at the Naval Radiological Defense Laboratory, USNRDL Reviews and Lectures No. 29, p. 47 (1956).
13. A. B. Chilton, D. Holoviak, and L. K. Donovan, Determination of Parameter in an Empirical Function for Buildup Factors for Various Photon Energies, USNCEL-TN-389 (AD-249195) (1960).
14. A. Rudloff, The Use of Buildup Factors in Calculating Gamma Radiation from Plane Sources Behind Absorber of Finite Extension, Atomkernenergie, 9, 451 (1964).

15. A. B. Chilton, Two-Parameter Formula for Point Source Buildup Factors, Nucleonics, 23(8), 119-122 (August 1965).
16. J. H. Hubbell, A Power Series Buildup Factor Formulation. Application to Rectangular and Off-Axis Disk Source Problems, J. Res. NBS, 67c, 4, 291-306 (1963).
17. E. P. Blizzard and L. S. Abbott, editors, Reactor Handbook, Sec. Ed., Vol. III, Part B, Shielding, p. 148, Interscience, New York.
18. H. L. F. Enlund, Energy Absorption of Capture Gammas, ORNL CF-52-6-99 (Suppl. 1) (1952). See Also E. P. Blizzard and L. S. Abbott, editors, op. cit., p. 179.
19. H. C. Claiborne, private communication, also article in IAEA Engineering Compendium on Radiation Shielding (to be published).
20. Cited by Goldstein, H., Fundamental Aspects of Reactor Shielding, p. 212, Addison-Wesley, Reading, Mass., 1959.
21. M. J. Berger, and J. Doggett, Reflection and Transmission of Gamma Radiation by Barriers: Semianalytic Monte Carlo Calculations, J. Res. of NBS, 56(2), 89-98 (1956).
22. H. Goldstein, op. cit., p. 225-226.
23. E. P. Blizzard and L. S. Abbott, editors, Reactor Handbook, 2nd Ed., Vol. III, Part B, Shielding, p. 175-176, Interscience, New York, 1962.
24. L. A. Bowman and D. K. Trubey, Deposition of Gamma-Ray Heating in Stratified Lead and Water Slabs, ORNL CF-58-7-99 (1958).
25. A. G. Pieper and L. A. Beach, Stochastic Estimates of the Penetration of Gamma Rays through Slab Shields, NRL-5981 (1963).
26. R. E. Rexroad, M. A. Schmoke, and H. J. Tiller, Point-to-Point Kernel Analysis of an Experiment to Determine Wall Penetration of a Square-based Concrete Structure by Gamma Radiation, Nucl. Sci. Eng., 20(1) 66-79 (1964).
27. L. V. Spencer and J. C. Lamkin, Slant Penetration of Gamma-Rays in H_2O , NBS Report 5944 (1958).
28. L. V. Spencer and J. C. Lamkin, Slant Penetration of Gamma-Rays in Concrete, NBS Report 6591 (1959).
29. M. O. Burrell and D. L. Cribbs, A Monte Carlo Calculation of Gamma Ray Penetration through Iron Slabs, NR-82, Vol. II (1960).

Distribution

1. E. P. Blizzard
2. F. C. Maienschein
3. W. H. Jordan
4. Arthur Reetz, NASA Headquarters, Washington, D. C.
5. William Alfonte, DASA, Washington, D. C.
6. Phil Hemmig, Division of Reactor Dev. & Technology, USAEC
7. R. E. Bowman, DTIE
8. G. Dessauer (Consultant)
9. M. L. Goldberger (Consultant)
10. M. H. Kalos (Consultant)
11. L. V. Spencer (Consultant)
- 12-14. Laboratory Records Department
15. Laboratory Reacords, RC
16. ORNL Patent Office
- 17-18. Central Research Library
19. Document Reference Section
- 20-244. RSIC Distribution
- 245-694. Division of Technical Information Extension
695. Research and Development Division (ORO)